COVENTRY
POLYTECHNIC

Priory Street Coventry CV1 5FB Telephone 0203 24166

COVENTRY POLYTECHNIC

Faculty of Engineering

Department of Civil Engineering and Building

VENTILATION IN INDUSTRIAL BUILDINGS

FINAL REPORT

J R Waters

CONTENTS

1 INTRODUCTION

This is a report of the principal results and conclusions of a three year study of Ventilation in Industrial Buildings. The study was supported by SERC Research Grant GR/C/38425.

The overall aim of the project was to study ventilation mechanisms in large single cell buildings, especially those used for industrial activities. Since the ventilation problems of such buildings are due as much to the industrial activity as to the building itself, it was considered important to direct the project towards buildings in use. It was necessary therefore to develop a methodology which would provide measurements of whole building infiltration and broad patterns of internal air movement without causing undue disturbance to the building occupier. Three specific objectives were identified:

i) To design and construct a suitable tracer gas system for the measurement of infiltration and internal air movement;

ii) To conduct a programme of measurements in a small but representative number of buildings of suitable sizes.

iii) To develop a theory for ventilation and air movement in single cell buildings.

All three objectives have been substantially achieved. In particular, the measurement system has proved to be very successful, and this has allowed the gathering of a good range of data from five different buildings. The development of a suitable theoretical basis for the interpretation of measurements has proved to be much more difficult. Partial success has been achieved by a careful examination of existing multi-zone theory, and some progress has been made in extending and modifying the theory to the type of building which has been studied here. However, further work will be needed to bring these theoretical matters to a satisfactory conclusion.

The detailed results of this project are being published in journals and conference proceedings. Copies of these publications are appended to this report.

2 THE MEASUREMENT SYSTEM

The performance criteria and the design of the measurement system were derived from a pilot study carried out by Waters and Simons (1). The need to measure internal air movements imposes a limitation on the choice of tracer gas method. Methods which require some additional imposed stirring are likely to upset the internal air movements which are to be measured, and so the tracer decay method is to be preferred to the constant concentration method. Also, it is necessary to use tracer gases which are unlikely to be present in industrial atmospheres. By choosing a single rather than a multiple tracer system, and by optimising the detection for the chosen tracer, the problems of selecting an appropriate tracer are much reduced. Sulphur hexafluoride was chosen, and has been found to be wholly satisfactory. The system is therefore a tracer gas monitoring device, in which detection of the tracer is achieved by six independent custom built gas chromatograph units. The six independent units permit rapid sampling from at least six sample points, and the use of pulse modulated electron capture detectors within the chromatographs provides both high sensitivity and good linearity over a large range of tracer concentrations.

A comprehensive evaluation of the detector behaviour was carried out, allowing the performance to be optimised with respect to sulphur hexafluoride. The same evaluation and optimisation procedure could be carried out for alternative tracers if necessary, though sulphur hexafluoride has been entirely satisfactory in all the buildings which have been measured. Because the system uses six separate detector units, calibration is of particular importance. For this purpose a special calibration rig was built, based on the accurate dilution of a standard sulphur hexafluoride in air mixture. Details of the design, evaluation and optimisation are given by Lawrance (2), and a description of the calibration and operation procedures is given by Waters, Lawrance and Jones (3).

In practice, the system is operated from a micro-computer, which provides all control and data collection functions. The whole system, complete with calibration gases, is mounted in a small covered trailer which serves as a mobile laboratory, and which can be stationed immediately outside, or even inside, the building being tested.

3 MEASUREMENT METHODOLOGY

The theoretical basis of the methodology which has been adopted is that the single large volume enclosed by a single cell building can be notionally subdivided, or discretised by imaginary boundaries into a large number of small volumes, or zones. Although the boundaries between these zones are hypothetical, in practice many buildings contain partitions, screens or furniture which give physical reality to some of the boundaries. If each zone is small enough, the distribution of contaminants, including the tracer gas, within the zone will be sufficiently uniform for the air within the zone to be considered as well mixed. The system is then identical to the usual multizone model of air flow within a building, and the interzone flow rates are a measure of the magnitude and direction of air movement within the complete volume.

A detailed theoretical evaluation of multizone theory has been carried out (reference 4) with a view to determining the best seeding strategy for determining the flows in a multizone model using a single tracer in the decay mode. This showed that the best strategy is to seed a single zone, and that this zone should be the zone associated with the smallest component of the dominant eigenvalues in the solution of the multizone equations. As a rule of thumb, this zone is likely to be the one receiving the largest inflow of fresh air, and is therefore likely to be the most exposed zone on the windward side of the building. It was also found that certain flow patterns may give rise to solutions which contain repeated eigenvalues, or lead to ill-conditioning or even linear dependency in any attempted solution for the inter-zone flows. Seeding strategy, therefore, had also to take account of these difficulties.

The actual measurement procedure is conventional. The trailer is parked either within the building, or immediately outside, so that it is only necessary to run tubing from the trailer to the sample points. The position of the sample points is chosen according to building geometry and the extent of internal obstructions. In open buildings with few obstructions, the building is divided into imaginary zones of approximately equal volume, with a sample point at the centre of each zone.

Where internal obstructions are significant, sample points are placed to represent the spaces that obstructions delineate. However, in occupied buildings, it is often necessary to displace the sample point from the desired position to avoid interference with building activities. The sampling heads themselves consist of a small cylindrical manifold from which radiate nine 1 cm lengths of copper tubing, in the manner of the spokes of a wheel. At each sample point, therefore, air is collected from nine equally spaced points around the circumference of a 2 m circle. This provides some spatial integration of the sample collection within each zone.

Before each experimental run, an SF_6/air mixture of known concentration is injected into all six gas analyser units simultaneously. The carrier gas flow rate to each unit is then adjusted to ensure that the SF_6 peak retention times are approximately equal; this is necessary for satisfactory measurement of the SF_6 peak. The SF peaks due to the calibration mixture are then measured, so that the responses of the six units can be normalised with respect to each other.

As a result of the theoretical study described above the normal seeding strategy is to inject pure SF_6 into a single zone on the windward side of the building, with stirring during the injection process to ensure mixing within that zone. The SF_6 injection equipment is kept separate from the measurement system to avoid contamination. The tracer decay is then followed for between 1 and 2 hours, with sampling at 1 minute intervals.

4 MEASUREMENT PROGRAMME

The main problem in devising a measurement programme was finding and gaining access to suitable buildings. Co-operation for this was obtained from four organisations, namely Warwick County Council Education Department, Courtaulds Engineering Limited, Coventry Airport Authority, and British Gas West Midlands Region. This help is gratefull acknowledged. Altogether a total of 58 sets of measurements were obtained, distributed approximately equally between the following five buildings:-

1. Abbey School Sports Hall, Kenilworth — Volume 4220 m^3
2. Courtaulds Engineering Workshop, Coventry — Volume 14370 m^3
3. Courtaulds Pattern Making Shop, Coventry — Volume 6420 m^3
4. Hangar 5, Coventry Airport — Volume 31300 m^3
5. British Gas Maintenance Depot, Birmingham — Volume 31020 m^3

Except for the Sports Hall, all the buildings were in use during the measurements; in Hangar 5 all measurements were taken with the aircraft doors closed. In all cases, six sampling points were used, which were positioned to represent equal volumes, except where internal obstructions were significant, in which case they were positioned to represent the spaces that the obstructions created. All the buildings were naturally ventilated, but Courtaulds Pattern Making Shop and British Gas Maintenance Depot had fume extract systems at strategic positions. Also, the British Gas building had an experimental mechanical ventilation and heat recovery system which was switched off for all but three of the measurement sets.

5 ANALYSIS OF RESULTS

Results for each measurement set were processed in two ways:-

1. Readings for all six sample points were averaged to give a single overall average tracer concentration for the whole building. The decay of the average concentration was used to obtain the fresh air infiltration rate of the whole building.

2. Using multizone theory, a constrained least squares technique was used to determine the complete set of interzone flow rates. The fresh air infiltration rate of the whole building was found by summing the flows between individual zones and the outside.

For both methods of analysis, the data set for each run is split into sections, and each section analysed separately. These sections are:

1. the first third of the data in the time series
2. the second third
3. the last third
4. the first two thirds

5. the last two thirds
6. the whole data set.

Thus for each method of analysis there were six sets of results for each run. Further details of the method of analysis are given in references 3, 4 and 5, and the results are presented in references 3, 5, 6 and 7.

Results for the whole building infiltration rate obtained from the averaged tracer concentration gave values generally between 1 and 4 air changes per hour. The values obtained from the different sections of the same data set were in reasonable agreement and showed variations which were consistent with the theory. However the interzone air flows obtained by means of the multizone analysis often showed substantial changes in value when different sections of a data set were analysed. This lack of consistency was most pronounced when the whole building infiltration rates obtained by the two separate methods of analysis were markedly different. Nevertheless, there were some data sets where there was reasonable consistency between the whole building infiltration rates calculated by the two methods, and between the interzone flows calculated from the different sub-sets of the measurement set.

6 CONCLUSIONS AND DEVELOPMENTS

The first conclusion is that the measurement system was entirely satisfactory. Apart from some problems during the development phase due to the pulse-modulation amplifiers, the equipment performed extremely well, giving a high degree of confidence in the measured value of tracer concentration. Although all the reported measurements were conducted in tracer decay mode, some trial measurements were carried out using constant injection, and it is intended to include additional components to enable the constant concentration to be used.

The results for fresh air infiltration rate computed from the averaged data appear to be sufficiently consistent to be considered reliable, and show that it is comparatively easy to obtain reasonable values for buildings in the size range considered without recourse to elaborate technique or analysis.

The results for interzone flows were always plausible, but this was due to the imposition of constraints on the least squares solution technique. Sometimes, these flows were consistent with the fresh air infiltration rate found from the averaged data, but often they were not. In the absence of separate independent measurement of the flows it is, therefore, difficult to know the level of error in these flows. Three possible explanations for the lack of consistency have been identified. These are:-

1. The size of the hypothetical zones was too large to give adequate discretisation of the internal volume of these buildings. The choice of six channels for the measurement system was dictated partly by experience from the preceding pilot study and partly by available resources. Thus, in the larger buildings, each zone was large enough for there to be spatial variations within it.

2. The 2 m diameter sampling head used in each zone was small in relation to the size of each zone, and therefore may not have given a reasonable measure of the average tracer concentration in that zone.

3. Because artificial mixing of the air in these buildings has been deliberately avoided, the normal multizone model is not strictly applicable, even with discretisation into small zones.

Each of these problems can be overcome to some degree. The first two could be ameliorated by increasing the number of zones, either by adding extra channels to the equipment, or by multiplexing the existing channels. At the same time, the sampling arrangement could be altered to give a more representative value of the concentration in each zone. Unfortunately, both of these possible courses of action would increase the disturbance caused to the building occupier.

The third problem has been approached by reconsidering the air flow model of the building. Instead of considering the air volume as an assembly of perfectly mixed zones, it is more realistic to consider it as a combination of pockets of good mixing (or zones) linked by volumes in which the air flow is predominantly in one direction.

These latter approximate to ducts. An alternative model is therefore, an assembly of perfectly mixed zones linked by ducts in which the flow is uni-directional. The solution of this alternative model is much more difficult. Nevertheless a solution has been obtained for the case of two zones linked by two ducts (reference 8). The most significant feature of the solution is that the decay curves can exhibit a type of oscillatory behaviour which has often been observed in our measured decay curves. It would be very interesting to solve a model of six zones connected by uni-directional flow ducts, but this has not yet been achieved.

7 REFERENCES

1. J R Waters and M W Simons, Ventilation in Industrial Buildings. Final Report, SERC project GR/B/64604, Coventry Lanchester Polytechnic, May 1983.

2. G V Lawrance, Ventilation and Air Movement in Industrial Buildings. Interim Report No CB/85/0001, Coventry Lanchester Polytechnic, September 1985.

3. J R Waters, G V Lawrance and N Jones, A tracer gas decay system for monitoring air infiltration and air movement in large single cell buildings. Symposium on Design and Protocol for Monitoring Indoor Air Quality, ASTM, Cincinnati, April 1987.

4. J R Waters and M W Simons, The Evaluation of Contaminant Concentrations and Air Flows in a Multi-zone Model of a Building. Building and Environment.

5. G V Lawrance and J R Waters, Measurements of Infiltration and Air Movement in Five Large Single Cell Buildings. 8th AIVC Conference, Uberlingen, September 1987.

6. J R Waters and G V Lawrance, Ventilation and Air Movement Measurements at Duddeston Mill Maintenance Depot, Birmingham. Report No CB/85/0002, Coventry Lanchester Polytechnic, January 1987.

7. M W Simons and J R Waters, The Measurement of Ventilation and Air Movement in Factory Buildings. ICBEM '87, Lausanne, September 1987.

8. J R Waters, The Effect of Time Lags in a Two-zone Air Movement Model. BSER & T.

VENTILATION IN INDUSTRIAL BUILDINGS

FINAL REPORT

J R Waters

SERC Research Grant
Project GR/C/38425

June 1987

VENTILATION AND AIR MOVEMENT IN INDUSTRIAL BUILDINGS

Interim Report

G.V. LAWRANCE BSc

Report No. CB/85/0001

September 1985

C O N T E N T S

1 INTRODUCTION

Energy conservation in Winter requires ventilation rates to be kept to a minimum, whereas health and safety requires them to be maintained at acceptable levels. The conflict between these two requirements is becoming more difficult to resolve not only due to a greater desire to save energy but also because of more stringent standards regarding air borne contaminant levels. This is particularly true for large single cell buildings in which industrial processes are performed.

Consequently this project has been set up to measure ventilation and air movement within large single cell buildings. Its aims form three basic sections, namely the construction of suitable measurement equipment, the measurement of representative buildings and the development of a theoretical model to enable interpretation and prediction. In this the first stage of the project the specific aims have been to design and construct a tracer gas measurement system using the experience gained in a pilot study conducted by Waters and Simons (1), and to begin to examine the mechanisms which govern tracer gas distribution.

This report details the design and performance criteria, describes the system that was built and discusses the factors which affect its performance. It also examines, from a theoretical point of view, the effects of molecular diffusion on tracer gas distribution.

2 DESIGN and PERFORMANCE CRITERIA

a) General

Waters' and Simons' pilot study (1) and Simons' multizone model (2) form the experimental and theoretical base from which the design and performance criteria for this measurement system have been drawn. This was particularly the case in determining that the method of evaluating ventilation and air movement rates in large single cell buildings should be based on multizone tracer decay measurements.

Given the method the basic requirement of the measurement system was that it be capable of detecting, on a quantative basis, the tracer gas or gases being used. Initially this was to be restricted to one specific gas, namely sulphur hexafluoride (SF_6). However the possibility of using alternative or additional tracer gases had to be borne in mind.

Further general requirements were that the system be automated, portable and flexible. Automation would provide control, data collection and possibly some on site data processing. Portability would allow "on site" measurements and required that the system's weight, robustness and reliability be considered. Flexibility would allow changes and modifications to be made more easily in the development stages.

b) Tracer Gas Analysis

Quantitative analysis of sulphur hexafluoride was to be performed using a gas chromatograph and a pulse modulated electron capture detector.

b) Tracer Gas Analysis

Electron capture was chosen because of the sensitivity of sulphur hexafluoride to this detection method. For example the AI505 SF_6 Chromatograph/Detector used in the pilot study provided a practical operating range for concentrations between 7 and 350 parts per billion and a resolution better than 1 part per billion. Using the more modern pulse modulated version of the detector should, according to Swan (3), provide greater sensitivity and resolution. (The reasons for this are discussed in section 3). In practice the optimum sensitivity will be determined by signal noise and injected sample volume. However consistency and repeatability of the analysis will be more important. The requirement will be that the detector remains calibrated over the whole range of operating concentrations for test periods of upto twenty four hours duration.

The function of the gas chromatograph will be to separate sulphur hexafluoride from the injected air sample. This will be necessary because of the electron capturing species present in air. Although these are in general seven or more orders of magnitude less reactive than sulphur hexafluoride they will be present in relatively high concentrations. For example oxygen, which is believed to be the most reactive, is present at approximately one part in five. Chromatographic separation however is a batch process and as such will impose a time interval on data collection. In the pilot study a minimum analysis cycle time of one minute was achieved. The requirement for the chromatograph in this measurement system was to produce the required level of sulphur hexafluoride separation within a nominal cycle time of one minute. Reductions in this time and hence increased data collection rates were to be left to future developments.

c) Multizone Measurements

Multizone measurements were to be performed by six gas analyser units running in parallel. Each was to be capable of being operated independently of the main system.

In the pilot study multizone measurements were made using a single gas analyser, an AI505 SF_6 Chromatograph/Detector, and sequentially sampling six zones. Given an analysis cycle time of one minute this produced staggered data at six minute intervals. Employing six gas analyser units would allow simultaneous sampling of six zones with a one minute time interval. This would represent a major improvement as calculating interzonal flows from the data using Simons' model (2) demands that the interval between data points be as small as practically possible, particularly as rates of change of concentration are required for the solution.

Simons' model also shows sampling rate to be important from another aspect of the analytical solution. Solving for interzonal flows requires that the data be collected before "dynamic equilibrium" is established. This can be regarded as where the rates of decay in each zone became very similar. Experience has shown that typically this condition is reached after about thirty minutes. Consequently sufficient data for solution needs to be collected within that relatively short initial period.

One major disadvantage of using six gas analyser units is the standard of calibration that will be required. Using a single analyser for all zones

c) Multizone Measurements

ensures that the correlation between concentration data in each zone is correct. However using individual analysers the zone concentration correlation will require corrections to be made when accounting for differences in the response of each gas analyser. Thus each gas analyser unit will have to be accurately calibrated over the whole range of expected tracer gas concentrations, and again from the pilot study experience this could be up to three or four orders of magnitude.

3 PULSE MODULATED ELECTRON CAPTURE

a) Electron Capture Principles

A comprehensive treatment of electron capture principles and the three modes of operation has been given by Swan (3). However it is useful to present a brief summary of the major points here.

Electron capture is based on the principle that the conductivity of gases in an ionisation chamber undergoes large changes with the presence of contaminants. If that contaminant is electrophilic, and halogenated compounds are highly electrophilic, the change in conductivity can be very large. Thus an electron capture detector consists of an ionisation chamber containing a β-ray source through which a stream of inert gas, typically argon, is passed.

The β-rays cause ionisation of the gas

$$Ar + \beta\text{-ray} \rightleftharpoons Ar^{+} + e^{-}$$

and the liberated electrons in the applied potential allow a current flow to be established. This current flow is known as the standing current.

Now if an electrophilic compound is introduced into the chamber the compound and the free electrons react either dissociatively or non-dissociatively

$$e^{-} + AB \rightleftharpoons A^{o} + B^{-}$$

or

$$e^{-} + AB \rightleftharpoons AB^{-}$$

respectively. In either case the resulting charge carrier is much less mobile than the free electron and a drop in standing current results.

b) Modes of Operation

Electron capture detectors can be operated in any of three modes DC, Pulse and Pulse Modulated. DC was the first to be developed and is the simplest mode of operation. In this mode a constant current, equal to the standing current, is maintained by varying the applied potential. Contaminent concentration is then measured by the change in this potential. However because an applied potential is always present anomolous responses due to detector contamination are greatly accentuated. This results in the detector being inaccurate and unreliable.

The pulsed mode of operation was developed to overcome these problems by applying fixed potential pulses of 0.5 to 1 μ second duration every 50 to 500 μ seconds. This keeps the anomolous responses to an undetectable level and increases the sensitivity of the detector. However measuring contaminant concentration by the change in current significantly limits the detectors linearity.

To overcome this limited linearity the pulse modulated mode of operation was developed. This returns to constant current operation of the detector. In this case a constant average current is maintained not by increasing the potential but by increasing the pulse frequency. Consequently the sensitivity of the pulsed mode is preserved and linearity over a range of four orders of magnitude is reportedly achieved.

4 VENTILATION AND AIR MOVEMENT MEASUREMENT SYSTEM

a) General Description

The Ventilation and Air Movement Measurement System (VAMMS) consists of (see figure 4.1) a Hewlett Packard HP85 microcomputer, a Hewlett Packard HP-IB interface bus, a Hewlett Packard Data Acquisition and Control Unit (DACU), a Power and Control Unit (PCU) and six Gas Analyser Units (GAU).

The most important components in this system are the Gas Analyser Units. They contain the chromatograph columns and electron capture detectors, which when used together provide the essential quantitative analysis of tracer gas concentration. All the other components serve only to provide control and data collection functions. Control is provided by HP85 software which sends instructions via the HP-IB to the DACU. In turn the DACU controls relays in the PCU which actuate the flush/inject and sample/calibrate operations in each of the GAU's.

Data generated by each GAU, is fed to the DACU data bus by the PCU after any requisite processing. The DACU selectively collects this data at times controlled by HP85 software.

b) Computer Control

Computer control of the ventilation and air movement measurement system is achieved by a real time program (see figure 4.2). Its function is to control sample injection, output data collection, data processing and storage for future analysis. All of these operations are performed for each Gas Analyser Unit simultaneously and constitute one system cycle.

The real time aspect of the program is realised by the use of three timed interrupts, related to specific chromatograph events, in a one minute cycle. The first interrupt initialises the cycle by collecting base line data and actuating sample injection. The second and third interrupts implement data collection at times corresponding to the output of chromatograph peaks (see figure 4.3). After each interrupt operation the HP85 computer returns to the processing and storage of the data generated in the previous cycle.

This method of programming allows the efficient use of computer time which is important when one considers that data processing and storage takes approximately 50 seconds of the one minute cycle.

c) Power and Control Unit

The function of this unit is to serve as a distribution interface providing each of the six Gas Analyser Units with the four Input/Output connections they require. Two of these supply carrier and calibration gases the other two act as a data transfer bus and a control bus (Figure 4.4).

Both the carrier and calibration gases supplied from conventional gas cylinders, are distributed to each GAU via six port manifolds. The carrier gas, however, is first dried and then passed through an oxygen trap.

Each GAU data transfer bus carries three outputs to the PCU. Two are voltage signals from the electron capture amplifier, the third is a resistance signal from a thermistor which measures the air temperature at the sampling point.

The PCU directs the first voltage signal (0-10v) to the DACU data bus and the second signal (0-1v) to a chart recorder output via a channel selector switch. Thermistor resistance is measured by a thermistor amplifier which produces a temperature calibrated 0-100mV signal. This is also directed to the DACU data bus.

The control bus provides each GAU with a 240V ac supply, a 24V ac supply and four relay actuated control lines. Two of these are devoted to sample injection and two to sample/calibrate mode switching. The relays which operate on 24V ac are themselves switched by the DACU.

d) Gas Analyser Unit

Each gas analyser unit can be considered as containing two systems, (see figure 4.5). One of these is devoted to analysis and consists of a carrier gas flow control valve, a gas chromatograph, an electron capture detector and its associated amplifier, and a detector output flow meter. The second system is devoted to sample collection. This consists of a dust filter, a pump, a solenoid bypass valve for calibration gas input, and a combined flow control valve and meter.

Both systems pass through the six port sample injection valve to which the sample loop is connected. In the flush position the valve allows air sample or calibration gas to pass through the sample loop. Rotating the valve into the inject position injects the contents of the sample loop into the carrier gas stream. The sample is then carried on to the chromatograph column where the tracer gas is separated. These separated components then pass through the detector where the electron capturing components are measured.

Pulse modulated electron capture detectors (Pye Unicam) were employed as this method of detection, particularly for sulphur hexafluoride, provided many advantages, (sections (2) and (3)). The gas chromatograph employed was specifically designed and developed to meet the performance requirements detailed in section (2). Commercially available gas chromatographs would have been unnecessarily sophisticated and expensive given these requirements.

Designing the gas chromatograph by the application of chromatography theory would have been, because of the number of variables involved, extremely

difficult. In fact the gas chromatograph was based on the design employed by the AI505 SF_6 Chromatograph/Detector (1). This consisted of an alumina (Al_2O_3) column and argon carrier gas (suitable for use in electron capture detectors), and operated at ambient temperature.

Using this basic design and experience gained from evaluations of performance under different operating conditions (section 6) an ambient temperature gas chromatograph was developed to meet the performance criteria. This chromatograph employed a 1.5m x 3.5mm chromatography grade alumina (F20, 100-120 BS Mesh) column and high purity (ie low oxygen content) argon carrier gas.

5 TRACER GAS DIFFUSION

a) Introduction

Interpretation of tracer gas decay or build up as the result of ventilation and air movement generally assumes the contribution from molecular diffusion to be insignificant. However the validity of this assumption cannot be determined without quantitative assessment. Its contribution in situations where the bulk air movement is low or non-existant, as in stratification, could be highly significant. In all cases the need for a quantitative treatment of tracer gas diffusion was clear.

b) Diffusion Coefficients

In the steady state the diffusion process may be described by Fick's equation

$$F = - D \frac{dc}{dx} \qquad \ldots\ldots \quad 5.1$$

where F is the rate of diffusion of the diffusing molecule in air
D is the diffusion coefficient
C is the concentration at x
x is the space co-ordinate

The diffusion coefficient may be obtained experimentally by measuring F, the rate of diffusion, and $\frac{dc}{dx}$, the concentration gradient, and substituting in Fick's equation. However, it may also be derived from a theoretical examination of the diffusion process. For example Skelland (4) has shown that the diffusion coefficient D_{AB}, for the diffusion of a gaseous molecule A in a gaseous medium B, may be expressed as

$$D_{AB} = \frac{0.0018583\ T^{3/2}}{P\ (\sigma_{AB})^2\ \Omega_{AB}} \sqrt{\frac{1}{M_A} + \frac{1}{M_B}} \qquad \ldots\ldots \quad 5.2$$

where

T = temperature (K)
P = pressure (atms)
M = molecular weight
σ_{AB} = Leonard-Jones force constant (attractive and repulsive forces)
Ω_{AB} = collision integral (molecular size effects)

Values of σ_{AB} and Ω_{AB} calculated for specific components (ie A and B) from the tables of data also given by Skelland (4).

The diffusion coefficients for a variety of gases in air have been calculated in this way and are given in table (5.1).

Table 5.1 : Diffusion Coefficients for Various Gases in Air

Temp K / Gas	273	283	293	313
Air	17.5×10^{-6}	18.6×10^{-6}	19.8×10^{-6}	22.2×10^{-6}
N_2O	13.2×10^{-6}	14.1×10^{-6}	15.0×10^{-6}	16.9×10^{-6}
He	59.7×10^{-6}	63.8×10^{-6}	67.2×10^{-6}	75.2×10^{-6}
SF_6	8.2×10^{-6}	8.8×10^{-6}	9.3×10^{-6}	10.5×10^{-6}

D_{AB} M^2/sec from equation 5.2

c) Radial Diffusion

The problem to be considered is the diffusion of gas from an initially high concentration, at a fixed point in space, into the volume of air surrounding that point. Given this the most convenient form of the time dependant diffusion equation is, in spherical co-ordinates:

$$\frac{\partial C}{\partial t} = \frac{1}{r^2}\left[\frac{\partial}{\partial r}\left(Dr^2\frac{\partial C}{\partial r}\right) + \frac{1}{\sin\theta}\frac{\partial}{\partial \theta}\left(D\sin\theta\frac{\partial C}{\partial \theta}\right) + \frac{D}{\sin^2\theta}\frac{\partial^2 C}{\partial \phi^2}\right] \quad \ldots \quad 5.3$$

where C = concentration
r = radius
t = time
D = diffusion coefficient

This may be idealised as follows. At the time zero, consider the diffusing gas to be entirely contained within a sphere of radius r centred at the

origin of the co-ordinate system, and let the concentration within the sphere be uniform. Assuming that the diffusing gas and the diffusing medium are stationery (ie there are no air currents) transfer is by pure diffusion. As the problem is radially symetric the diffusion equation (5.3) simplifies to:

$$\frac{\partial C}{\partial t} = D\left(\frac{\partial^2 C}{\partial r^2} + \frac{2}{r}\frac{\partial C}{\partial r}\right) \qquad \ldots 4.$$

and the boundary conditions may be written as:

$$\text{for } r = 0 \text{ to } a \quad \text{then } C_r = C_o$$
$$\text{for } r > a \quad \text{then } C_r = 0$$

where C_o is the uniform concentration within the sphere at time zero

C_r is the concentration at radius r and time t.

A solution of equation (5.4), with these boundary conditions, has been obtained by Crank (5) in the following form:

$$\frac{C_o}{C_o} = \tfrac{1}{2}\left[\operatorname{erf}\left(\frac{a-r}{2\sqrt{Dt}}\right) + \operatorname{erf}\left(\frac{a+r}{2\sqrt{Dt}}\right)\right] - \frac{1}{r}\sqrt{\frac{Dt}{\pi}}\left[\exp\left(-\frac{(a-r)^2}{4Dt}\right) - \exp\left(-\frac{(a+r)^2}{4Dt}\right)\right] \qquad \ldots 5.$$

where erf ( ) is the error function.

The time dependant concentration at the origin of the space co-ordinate system, C_{ro} (ie r = o) can be approximated by considering equation (5.5) as $r \to o$. Thus:

$$\frac{C_{ro}}{C_o} = \operatorname{erf}\left(\frac{a}{2\sqrt{Dt}}\right) - \left[\frac{1}{r}\sqrt{\frac{Dt}{\pi}}\left[\exp\left(\frac{-a^2}{4Dt} + \frac{2ar}{4Dt} + \frac{r^2}{4Dt}\right) - \exp\left(\frac{-a^2}{4Dt} - \frac{2ar}{4Dt} - \frac{r^2}{4Dt}\right)\right]\right]_{r=o} \qquad \ldots 6.$$

The r^2 terms become insignificant and the exponentials containing r can be approximated:

$$\frac{C_{ro}}{C_o} = \operatorname{erf}\left(\frac{a}{2\sqrt{Dt}}\right) - \left[\frac{1}{r}\sqrt{\frac{Dt}{\pi}}\left[\exp\left(\frac{-a^2}{4Dt}\right)\left(1+\frac{2ar}{4Dt} - 1 + \frac{2ar}{4Dt}\right)\right]\right]_{r=o} \qquad \ldots 7.$$

Reducing gives

$$\frac{C_{ro}}{C_o} \simeq \operatorname{erf}\left(\frac{a}{2\sqrt{Dt}}\right) - \frac{a}{\sqrt{\pi Dt}}\left(\exp\left(\frac{-a^2}{4Dt}\right)\right) \qquad \ldots 5.9$$

However equation (5.9) was not used in any of the subsequent calculations of

C_{ro}/C_o. In fact, as an aid to program simplicity, C_{ro}/C_o was calculated by defining ro as $r_o = 1 \times 10^{-10}$ and evaluating equation (5.5). Also for all the subsequent calculations the values of three variables were fixed, these were:

$D = 8.2 \times 10^{-6}\ m^2\ s^{-1}$; the diffusion coefficient of SF_6 in air at 273K

$a = 0.1m$; the initial (t=o) radius of the gassphere

$C_o = 1$; the uniform concentration in the initial sphere

d) Diffusion of Sulphur Hexafluoride

In considering the diffusion of sulphur hexafluoride the first step was to examine the distribution of concentration in time and space. Using equation (5.5) time contours of concentration ratio (C_r/C_o) against radius (r) were calculated and plotted. Figure (5.1) shows a series of these contours over a period of 600 secs. As can be seen the concentration within and close to the boundary of the initial sphere changes signifcantly. At distances of three times the initial radius and beyond changes in concentration are small by comparison. For example, given an initial sphere of 0.1 metres radius with an initial concentration of 1, the concentration after 10 minutes at 0.5 metres distance will have only reached 10^{-9}, (10 volume parts per billion).

Whilst illustrating the slowness of the diffusion process the above treatment did not provide a quantitative assessment of its contribution to mixing. To provide this it was necessary to define a diffusion mixing index.

Perfect mixing will have occurred when, assuming infinite space, the concentration at zero radius equalls the concentration at all other points in space. The time taken to reach this condition would be infinite and the concentration would be zero. However, from this it can be seen that an estimate of the degree at mixing at time t can be obtained for a sphere of radius r by comparing the concentrations at r and at zero radius; C_r and C_{ro} respectively. Thus the diffusion mixing index is defined as the ratio of these concentrations where:

$$\frac{C_r}{C_{ro}} = 1, \quad \text{perfect mixing}$$

$$0 < \frac{C_r}{C_{ro}} < 1, \quad \text{non-perfect mixing}$$

$$\frac{C_r}{C_{ro}} = \frac{C_r}{C_o}\,\frac{C_o}{C_{ro}} \qquad \ldots 5.10$$

Both C_r/C_o and C_o/C_{ro} are obtained from equation (5.5)

Diffusion mixing index contours were then plotted on a radius against logtime graph. (Fig 5.2). This gave the quantitative assessment required. For example after 1000 seconds a 0.95 degree of mixing would be established within a sphere of 0.043 metres radius (initial sphere radius of 0.1 metres) and a 0.5 degree of mixing within a 0.16 metre sphere.

e) Diffusion Mixing

It has been shown that from an inital sphere of 0.1 metres radius the diffusion of tracer gas will be insignificant within a measurement time frame of 20 to 30 minutes. The contribution of diffusion to mixing under these same conditions, analogous to the injection of tracer gas at the outset of tracer decay measurements, has also been shown to be insignifcant. However the analysis has not as yet been sufficiently developed to allow valid assessments of other conditions, stratification in particular.

6 EVALUATION OF SYSTEM PERFORMANCE

a) Introduction

Optimal performance from both the gas chromatograph and pulse modulated electron capture detector was an essential pre-requisite for the successful operation of the ventilation and air movement measurement system. Most of the development work to date has therefore been concerned with meeting their performance criteria. However determing the operating parameters which gave this required a pragmatic approach. This was because of both the number of operating parameters and their interdependence.

Chromatograph and detector performance was evaluated by reference to five output parameters. These were peak resolution (oxygen and sulpher hexafluoride), tracer gas peak height, tracer gas peak width, peak retention times, and base line response. Again interdependence between some of these parameters existed. For example, tracer gas peak width, if large, would produce overlap with the oxygen peak and hence reduce peak resolution.

Fixing some of the operating parameters of the chromatograph (temperature, column material and carrier gas) and detector (temperature) did simplify to some extent the process of optimizing performance. However this left detector current, column dimensions, carrier gas flow rate and sample loop volume still to be determined. Whilst these parameters are dealt with separately in the following paragraphs it must be realised that it was not always possible to determine their final values in isolation.

b) Electron Capture Detector (ECD) Current

Two sets of experiments to evaluate the effects of detector current on the performance of the pulse modulated ECD have been conducted. One studied the effect on tracer gas peak height, for a fixed concentration of sulphur hexafluoride, the other the effect on base line response. Collectively they illustrated both the need for and the method of obtaining an optimum current setting.

Both the peak height, given a fixed concentration of sulphur, hexafluoride (fig 6.1), and the base line response (fig 6.2) were shown to increase with increased detector current (arbitrary units). This represented an increase in sensitivity, in the first case to sulphur hexafluoride and in the second

to the carrier gas and the contaminants it contained. However as the detector has a saturation level which is relatively independent of current, the increase in base line response also represented a decrease in operating range. The optimum detector current is determined, as recommended by the manufacturer, from measurement of the "runaway current". This is defined as the lowest current to give a base line response from the amplifier output which is 50% or greater of its full scale output, the optimum current setting (arbitary units) being one half of this.

c) Column Dimensions

Experiments conducted to determine the optimum column dimensions (section 4d) were performed using a carrier gas flow rate of 60 $cm^3 min^{-1}$. This was the optimum flow rate given both the need to minimise carrier gas usage and to exceed the minimum ECD flow rate of 50 $cm^3 min^{-1}$. Initially four columns were examined, 0.67m x 5.0mm, 0.5m x 5.0mm, 0.33m x 5.0mm and 1.0m x 3.5mm.

Of the two column dimensions, length and diameter, the former was found to have the most significant effect on the output parameters. Decreasing column length decreased peak resolution, tracer gas peak width and peak retention times but increased peak height. Base line response was not affected. Decreasing the column diameter increased peak resolution by reducing peak width but had comparatively little effect on the remaining output parameters.

Thus, from the point of view of minimising peak width and retention times the column length was required to be as small as possible whilst ensuring complete resolution of the sulphur hexafluoride peak. The optimum column diameter would have been the smallest which maintained the column's capacity to perform the separation. However from a practical view point this was limited to 3.5mm. In fact this was the internal diameter of the nylon tubing used to pipe each Gas Analyser Unit.

d) Carrier Gas Flow Rate

Although the optimum flow rate of 60 $cm^3 min^{-1}$ was determined by other factors, it was still necessary to investigate the effect of carrier gas flow on output parameters. Consequently a number of experiments were performed in which a range of flow rates, 30 to 120 $cm^3 min^{-1}$, were studied.

In all cases increasing the carrier gas flow rate reduced the output parameter; base line response (fig 6.3), peak resolution, peak width, peak height (fig 6.4), and peak retention time (fig 6.5). With exception of base line response and peak height these reductions were consistent with the time dependent processes occurring in the chromatograph column. The reductions in base line response and peak height, (in conjunction with a reduction in peak width) were more difficult to interpret. If, as believed, this was not a feature of chromatograph performance then ECD performance must also have been a function of time dependent processes. However there was insufficient experimental data to indicate what mechanisms were responsible for this behaviour.

e) Sample Loop Volume

Sample loop volume was found to be a flexible input parameter in that it could be adjusted, within limits, to determine the range of sulphur hexafluoride concentrations over which the gas analyser operated. In this case

the loop volume was adjusted to give an operating range similar to that of the AI505 SF_6 Chromatograph/Detector, which, employing a sample loop of 0.5 ml volume, operated at a maximum concentration limit of c.a. 350 parts per billion. However the gas analyser units in this system, employing pulse modulated electron capture detectors, only required sample loop volumes of 0.08ml to give maximum concentrations of c.a. 400 parts per billion.

The limits to sample loop volume were determined by the dimensions, and physical properties and chemical properties of the chromatograph column. For example using a large sample loop volume, 0.5ml compared to 0.08ml, produced an "oxygen" peak with so large a peak width that the sulphur hexafluoride peak was completely overlapped. Whilst this could have been corrected for by increasing the column length and diameter the resulting peak retention time would have been increased beyond the one minute cycle time.

7 CONCLUSIONS

The design and construction of the ventilation and air movement measurement system have for the most part been successfully completed. The problems that remain are related to calibration and operation of the system. Whilst this may represent an equally large volume of work to that of the design and construction all the evidence to date supports an eventual successful measurement system.

8 REFERENCES

1 WATERS J.R. and SIMONS M.W. "Ventilation in Industrial Buildings" Final Report, SERC project GR/B/64604 Coventry (Lanchester) Polytechnic, May 1983

2 SIMONS M.W. "An Investigation of the Air Infiltration Characteristics of Industrial Buildings" Dept. of Mathematics, Coventry (Lanchester) Polytechnic, May 1984

3 SWAN D.F.K. "Three Selective Detectors", Published by Pye Unicam.

4 SKELLAND A.H.P. "Diffusional Mass Transfer", Ch 3, P 50, John Wiley and Sons

5 CRANK J. "The Mathematics of Diffusion, Ch 2, P 15, 2nd ed. Oxford University Press

VENTILATION & AIR MOVEMENT MEASUREMENT SYSTEM

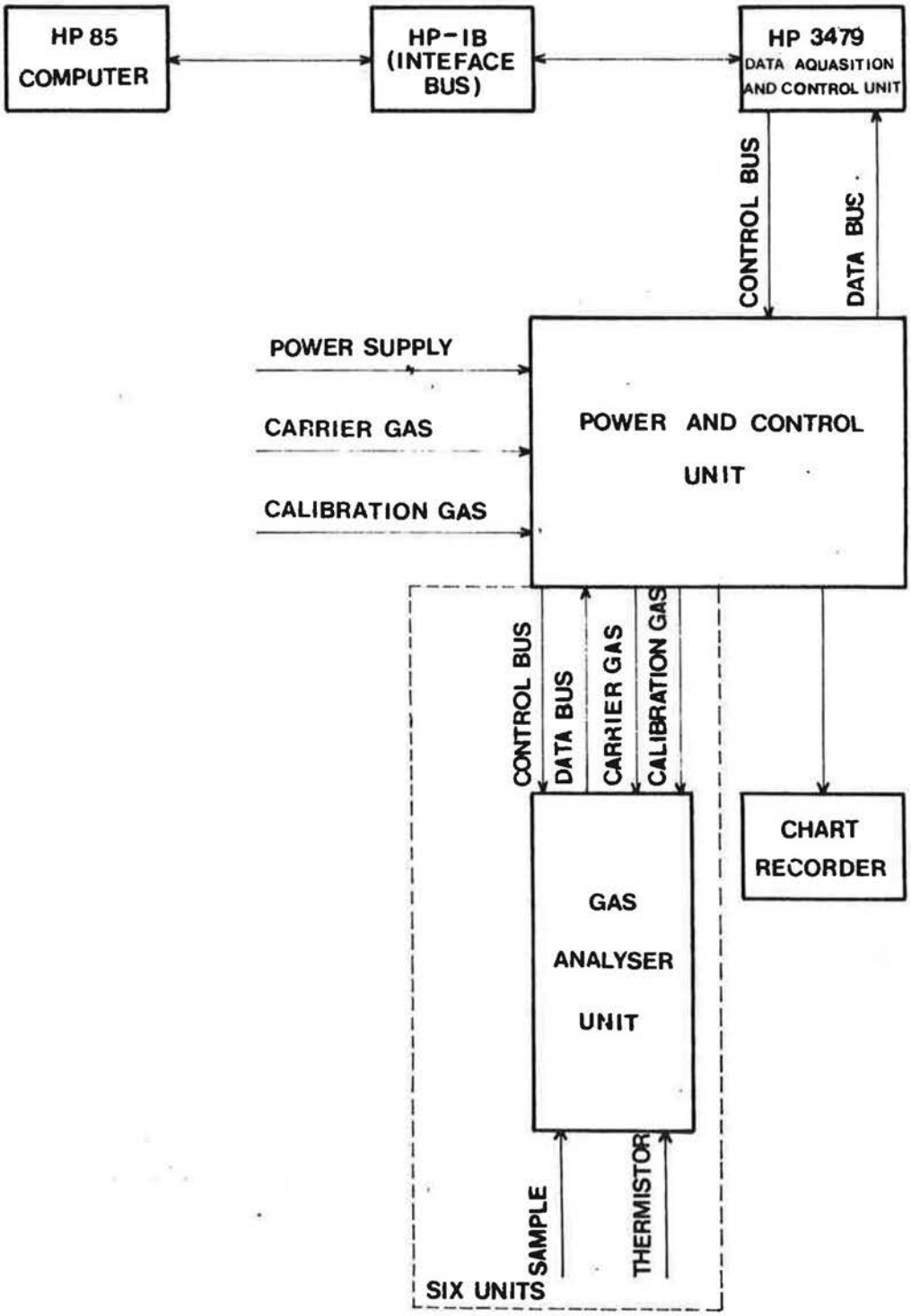

FIG. 4·1 **Block diagram showing the component parts of the Ventilation and Air Movement Measurement System**

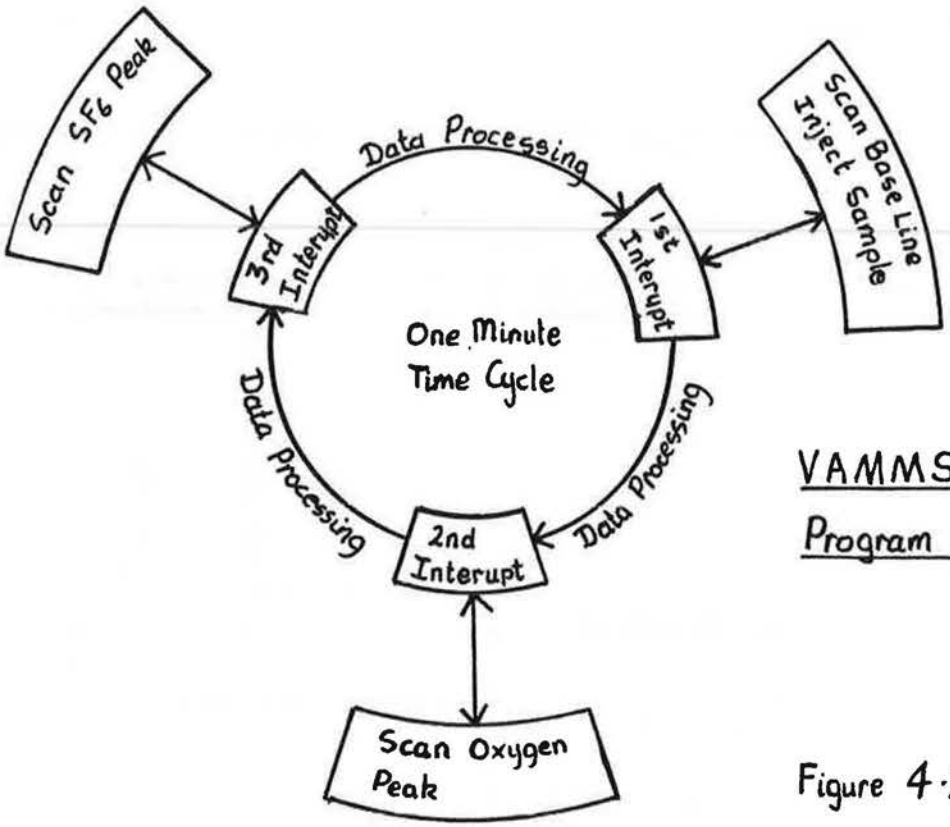

VAMMS Real Time Program Flow Chart.

Figure 4·2

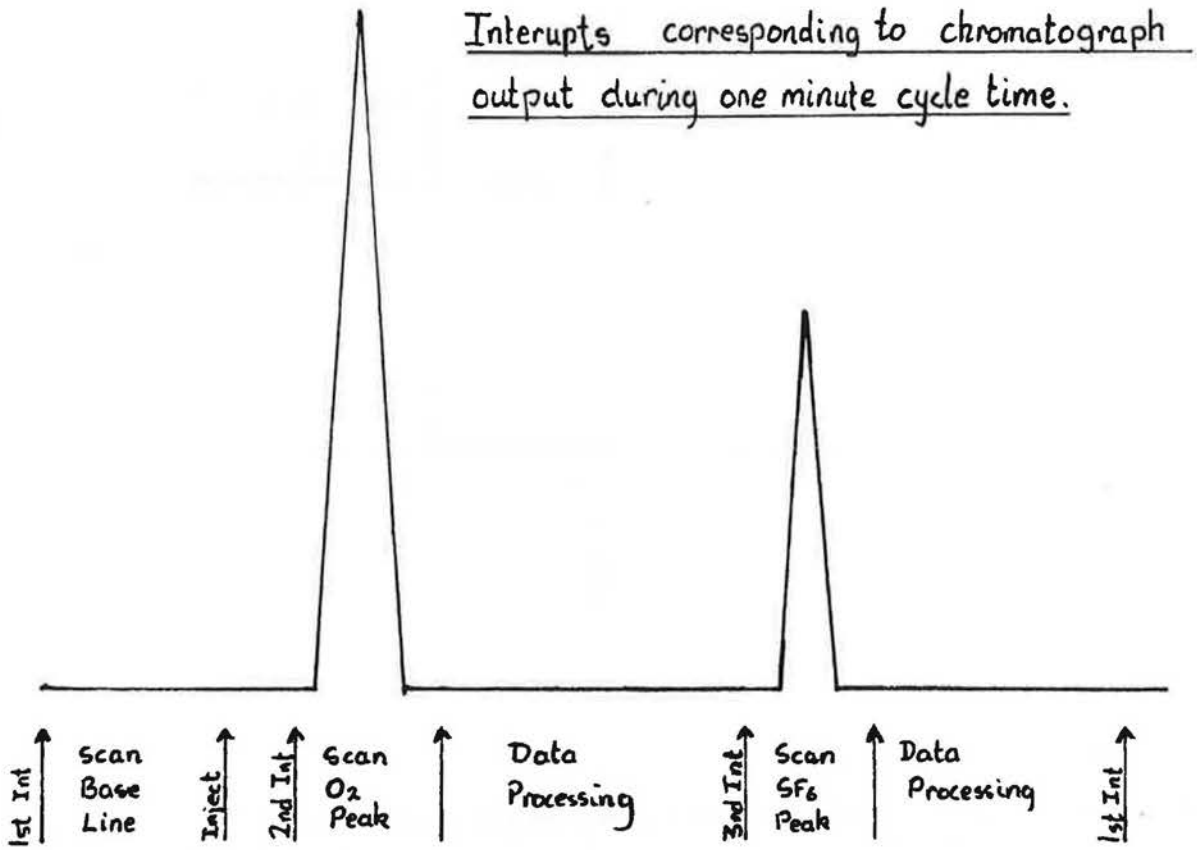

Figure 4·3

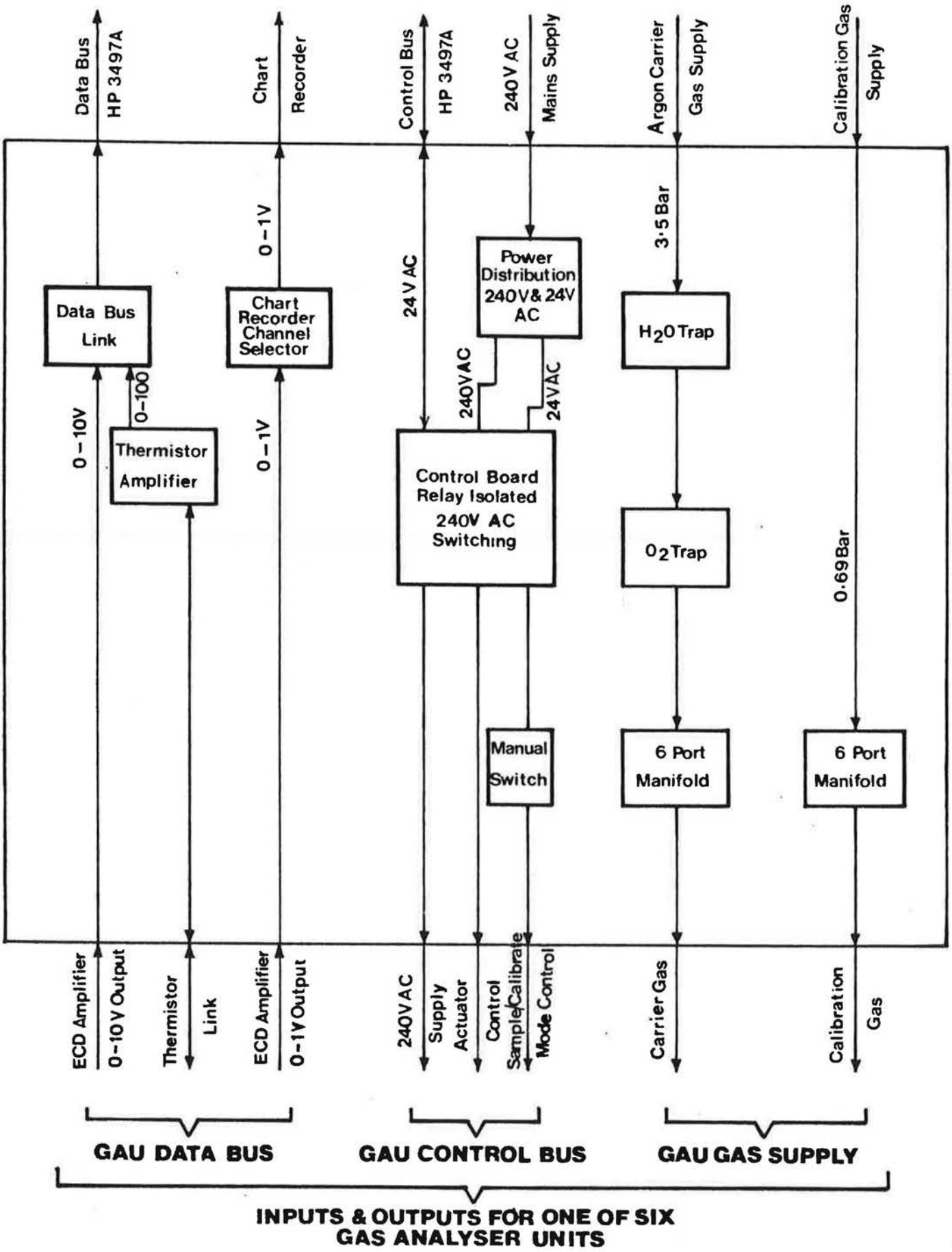
POWER & CONTROL UNIT
Data Bus
HP 3497A
Chart
Recorder
Control Bus
HP 3497A
240V AC
Mains Supply
Argon Carrier
Gas Supply
Calibration Gas
Supply
Data Bus Link
Chart Recorder Channel Selector
Power Distribution 240V & 24V AC
H_2O Trap
O_2 Trap
Thermistor Amplifier
Control Board Relay Isolated 240V AC Switching
Manual Switch
6 Port Manifold
6 Port Manifold
0 – 10V
0 – 100
0 – 1V
24 V AC
240V AC
24V AC
3·5 Bar
0·69 Bar
ECD Amplifier
0 – 10 V Output
Thermistor
Link
ECD Amplifier
0 – 1V Output
240V AC
Supply
Actuator
Control
Sample/Calibrate
Mode Control
Carrier Gas
Calibration
Gas
GAU DATA BUS
GAU CONTROL BUS
GAU GAS SUPPLY
INPUTS & OUTPUTS FOR ONE OF SIX GAS ANALYSER UNITS

Figure 4·4

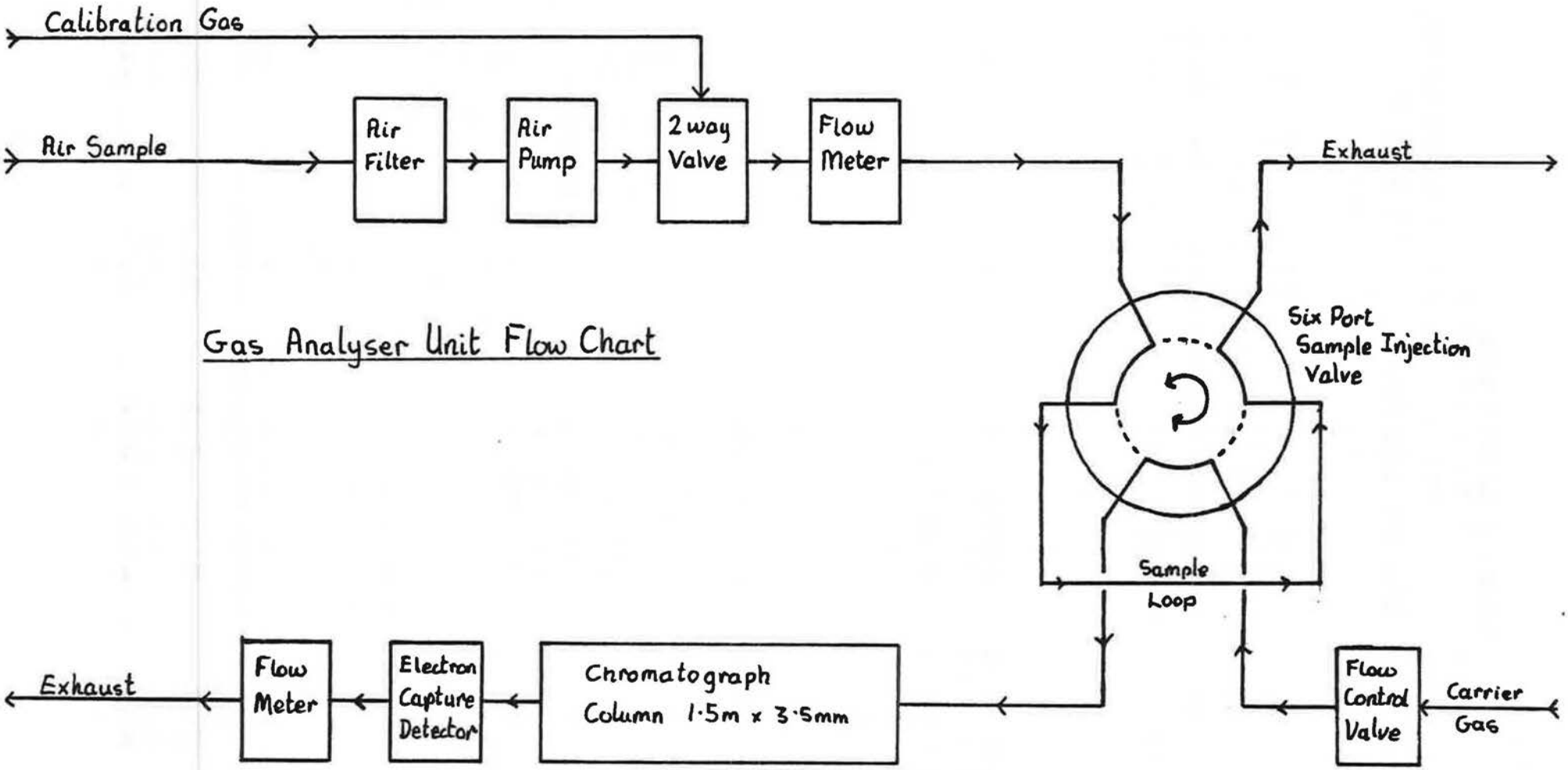

Gas Analyser Unit Flow Chart

Figure 4·5

[8] Grot, R.A. and Persily, A.K., "Measured Air Infiltration and Ventilation Rates in Eight Large Office Buildings", Measured Air Leakage of Buildings, ASTM STP 904, H.R. Trechsel and P.L. Lagus, American Society for Testing and Materials, Philadelphia, 1986, pp. 151- 183.

[9] Perera, M.D.A.E.S., Walker, R.R. and Trim, M.J.B., "Measurements of Intercell Airflows in Large Buildings Using Multiple Tracer Gases", Energy Savings in Buildings. Proceedings of the International Seminar, The Hague, Netherlands, Nov. 1983, H. Ehringer and U. Zito, Eds., Reidel, Dordrecht, 1984, pp. 476-483.

[10] Fisk, W.J., Binenboym, J., Kaboli, H., Grimsrud, D.T., Robb, A.W. and Weber, B.J., "A Multi-Tracer System for Measuring Ventilation Rates and Ventilation Efficiencies in Large Mechanically Ventilated Buildings", in Proceedings, 6th AIC Conference, Netherlands, Sept. 1985, Air Infiltration and Ventilation Centre, Bracknell, Berks, United Kingdom.

[11] Swan, D.F.K., "Three Selective Detectors", Pye Unicam Limited, Cambridge, United Kingdom.

[12] Lovelock, J.E., "Electron Absorption Detectors and Techniques for Use in Quantitive and Qualitative Analysis by Gas Chromatography", Analytical Chemistry, Vol. 35, 1963, pp. 474-481.

[13] Lanczos, C., "Applied Analysis", Pitman, London, 1957, p. 316.

[14] Penman, J.M. and Rashid, A.A.M., "Experimental Determination of Air-flow in a Naturally Ventilated Room Using Metabolic Carbon Dioxide", Building and Environment, Vol. 17, 1982, pp. 252-256.

[15] Lawson, C.L. and Hanson, R.J., "Solving Least Squares Problems", Prentice-Hall, Englewood Cliffs, N.J., 1974.

[16] Walker, R.R., "Interpretation and Error Analysis of Multi-tracer Gas Measurements to Determine Air Movement in a House", Paper S.3, in Proceedings, 6th AIC Conference, Netherlands, Sept. 1985, Air Infiltration and Ventilation Centre, Bracknell, Berks, United Kingdom.

[17] Waters, J.R., "The Effect of Time Lags in a Two Zone Air Movement Model", BSER&T, Vol. 8, 1987, pp. 43-46.

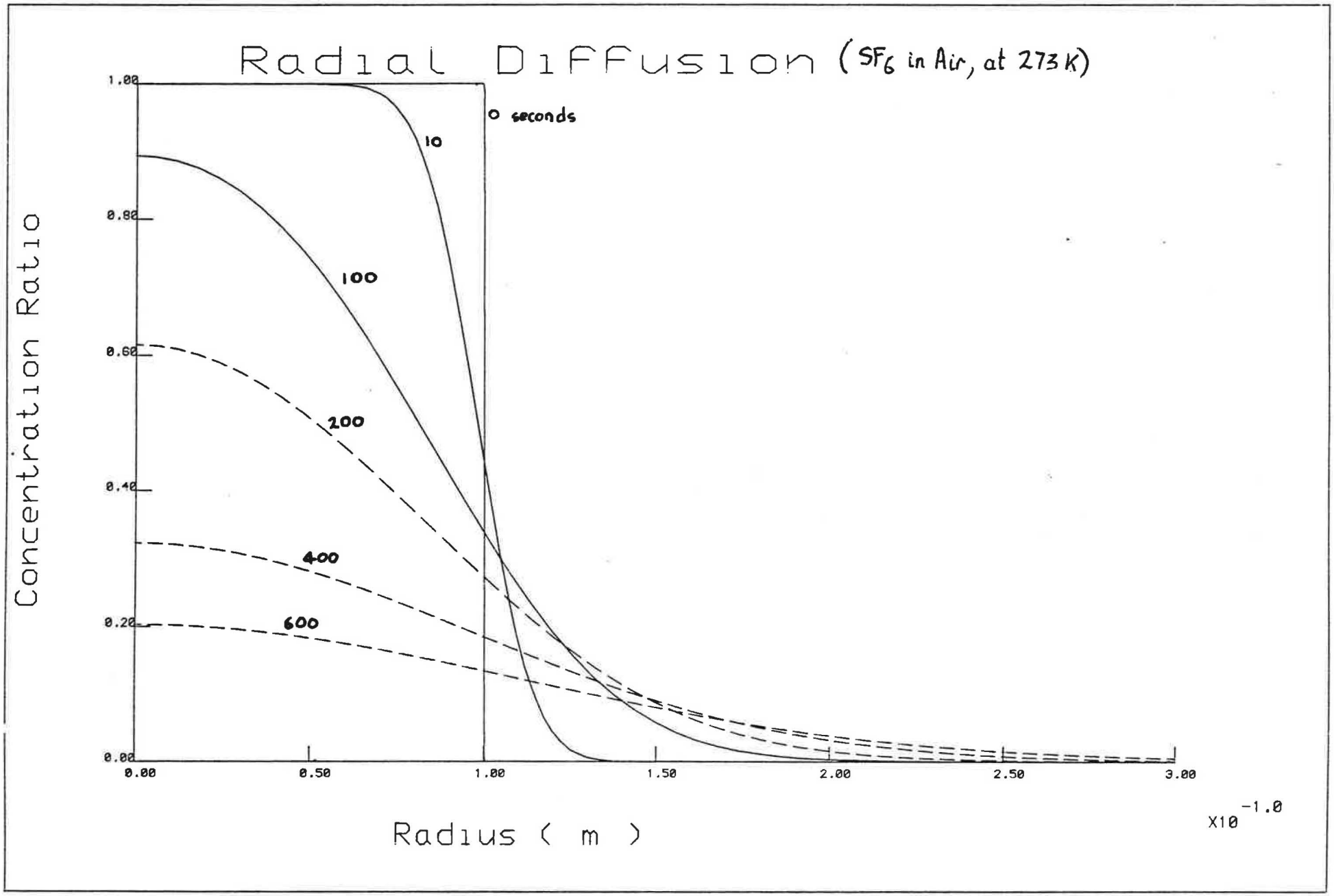
Radial Diffusion (SF_6 in Air, at 273 K)
Concentration Ratio
1.00
0.80
0.60
0.40
0.20
0.00
0 seconds
10
100
200
400
600
0.00
0.50
1.00
1.50
2.00
2.50
3.00
Radius (m)
X10^-1.0

Fig 5-1

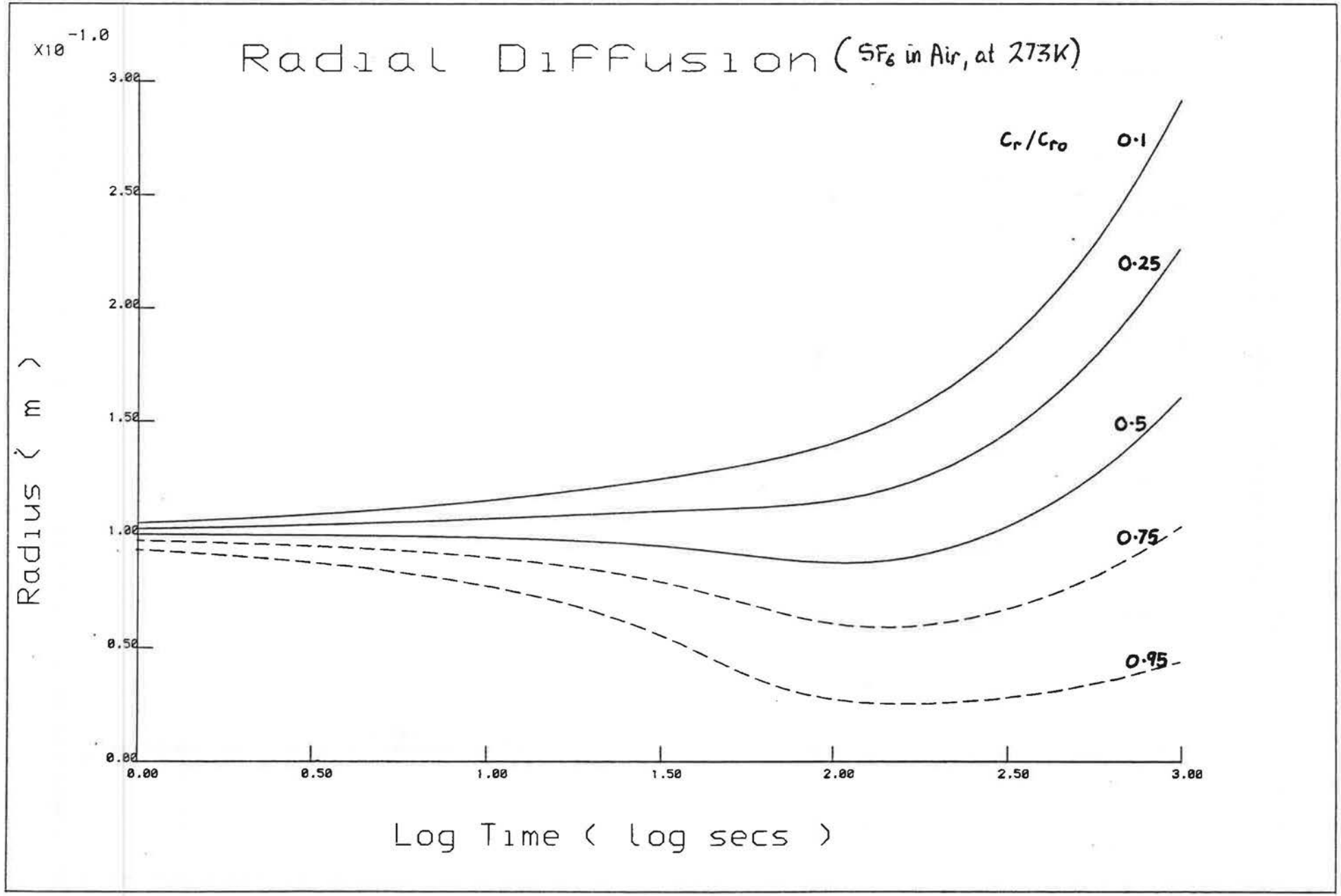
Radial Diffusion (SF_6 in Air, at 273K)
X10 -1.0
Radius (m)
3.00
2.50
2.00
1.50
1.00
0.50
0.00
0.00
0.50
1.00
1.50
2.00
2.50
3.00
Log Time (log secs)
C_r/C_{ro}
0·1
0·25
0·5
0·75
0·95

Figure 5-2

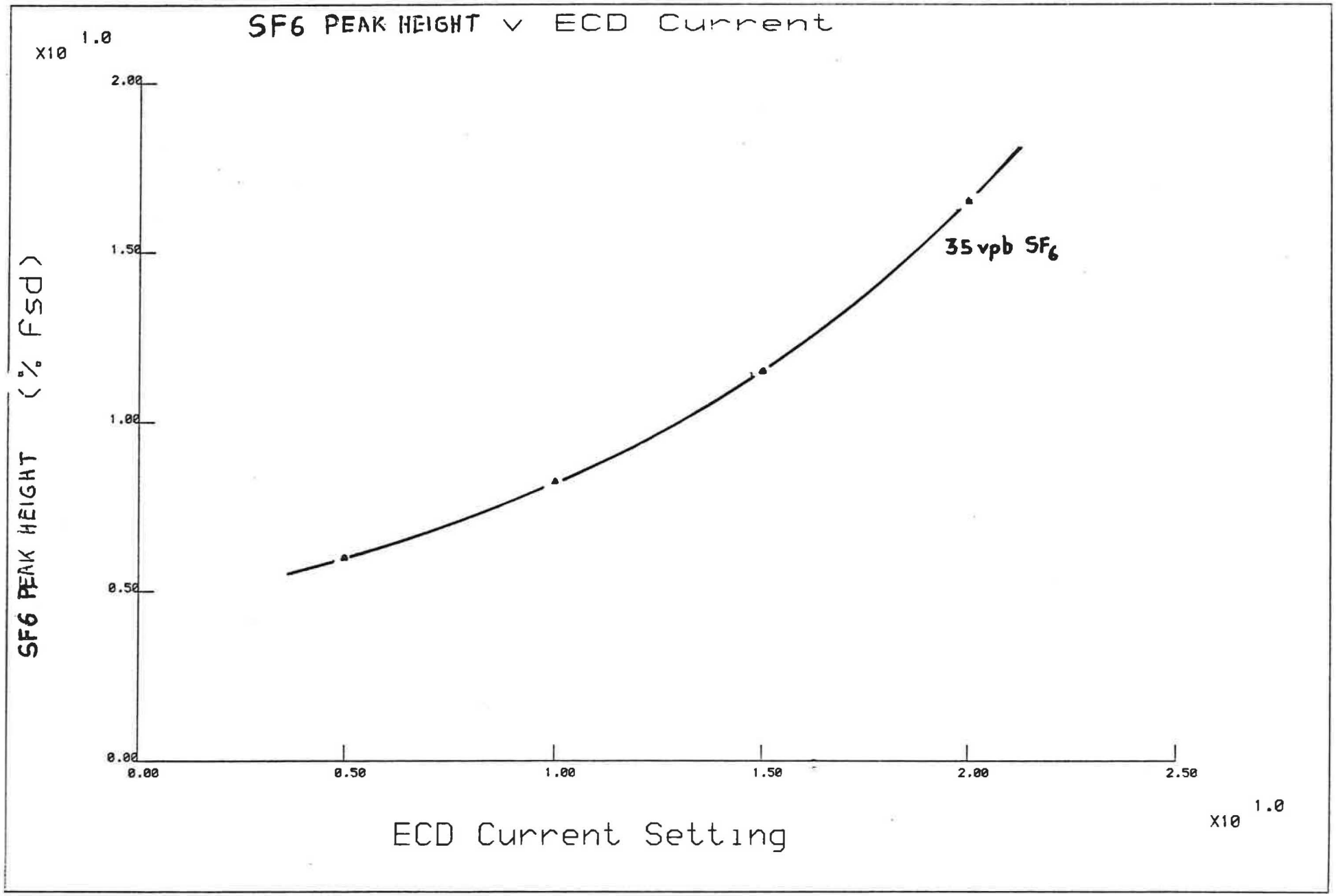
SF6 PEAK HEIGHT v ECD Current
X10 1.0
2.00
1.50
1.00
0.50
0.00
SF6 PEAK HEIGHT (% Fsd)
35 vpb SF6
0.00
0.50
1.00
1.50
2.00
2.50
X10 1.0
ECD Current Setting

Fig 6-1

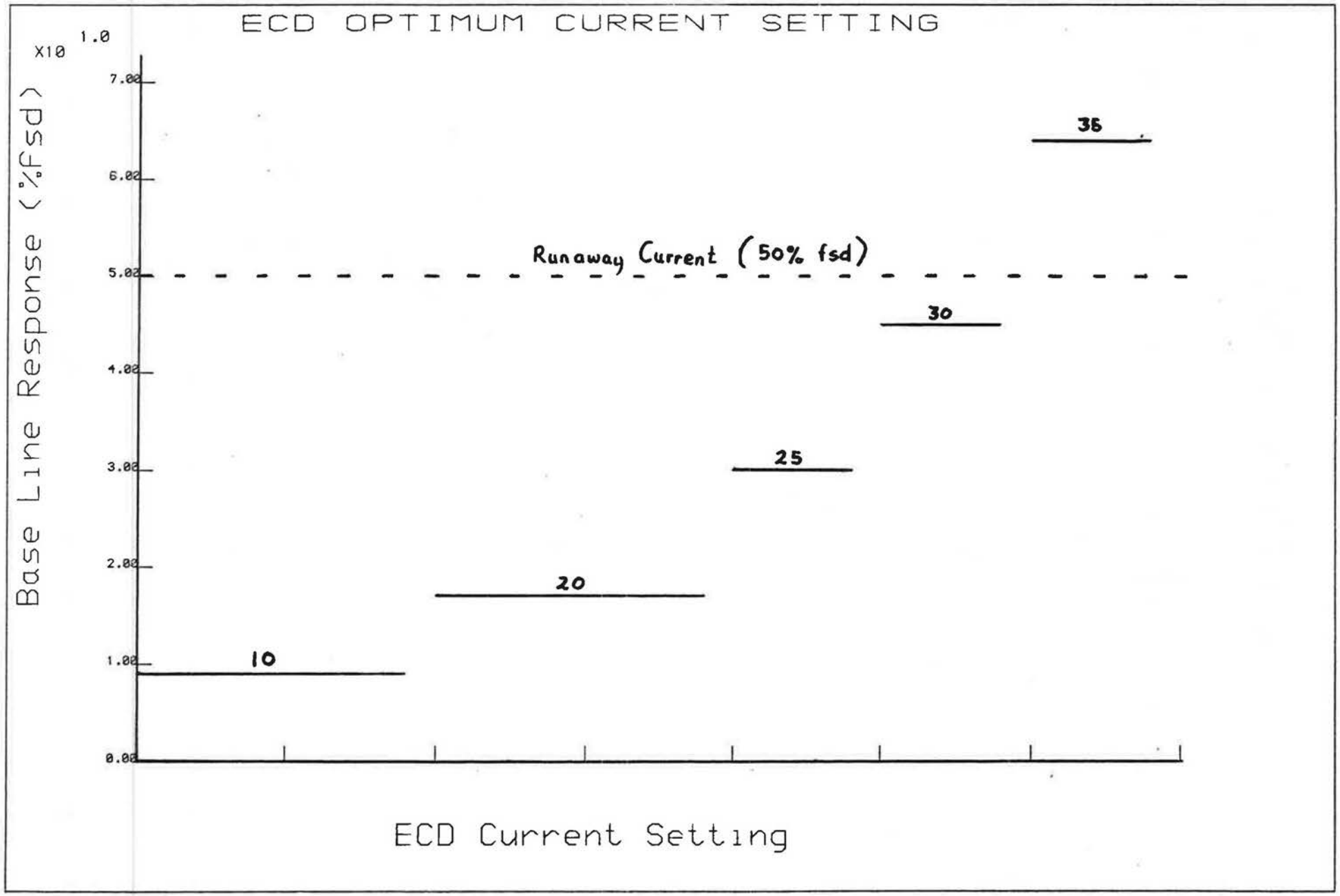
ECD OPTIMUM CURRENT SETTING
X10 1.0
Base Line Response (%Fsd)
7.00
6.00
5.00
4.00
3.00
2.00
1.00
0.00
Runaway Current (50% fsd)
35
30
25
20
10
ECD Current Setting

Fig 6-2

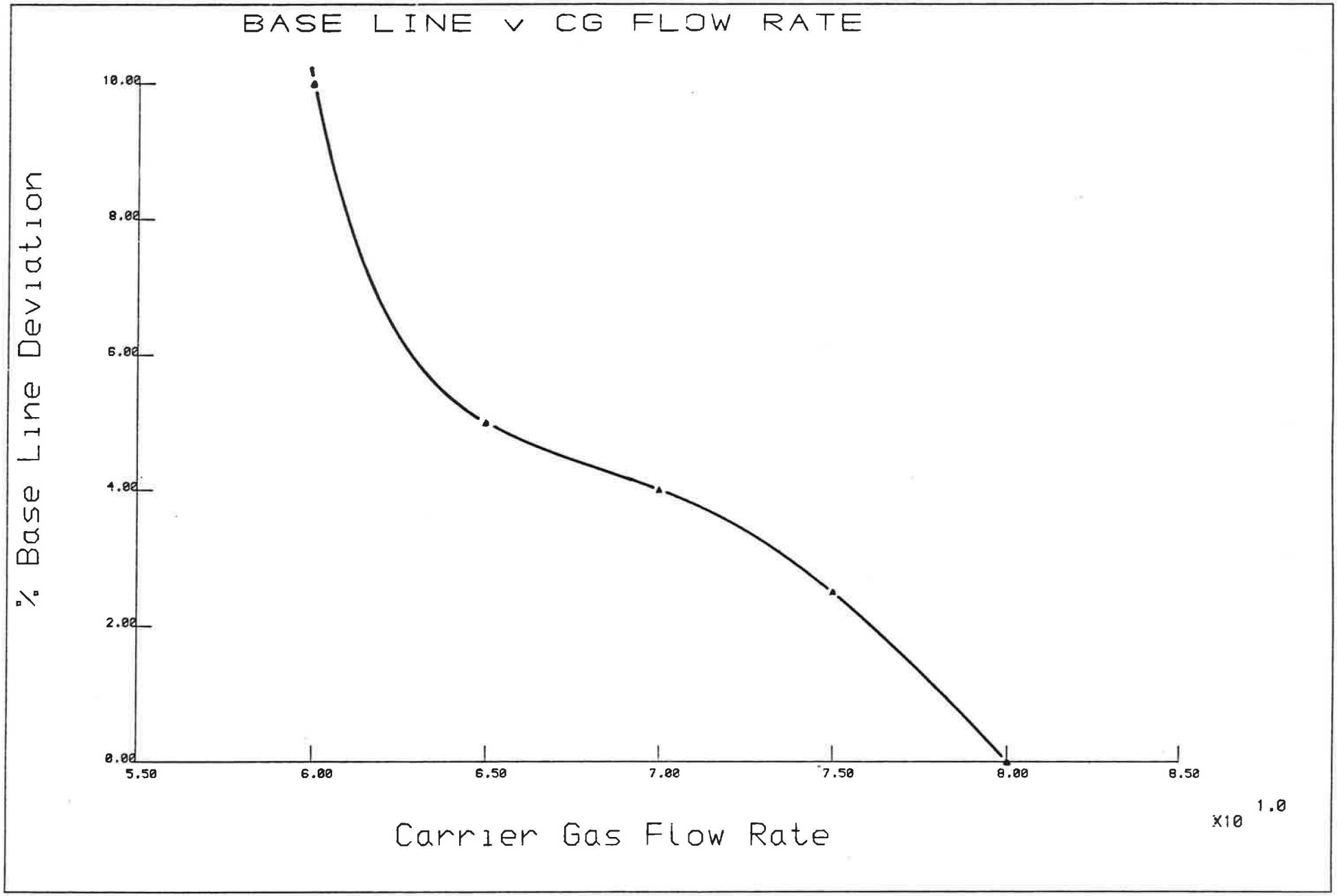
BASE LINE v CG FLOW RATE
% Base Line Deviation
10.00
8.00
6.00
4.00
2.00
0.00
5.50
6.00
6.50
7.00
7.50
8.00
8.50
X10 1.0
Carrier Gas Flow Rate

Fig 6-3

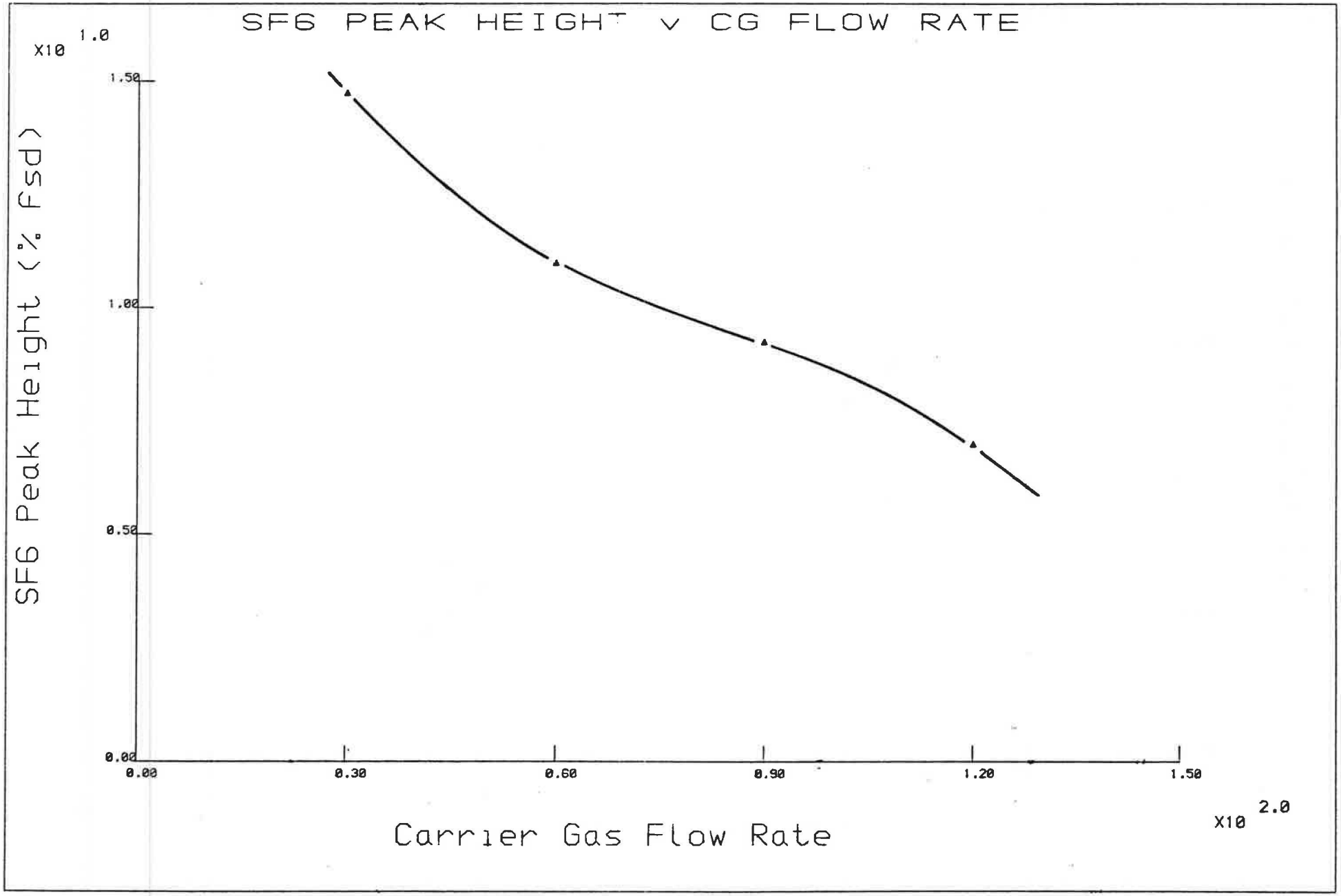
SF6 PEAK HEIGHT v CG FLOW RATE
X10 1.0
1.50
1.00
0.50
0.00
SF6 Peak Height (% Fsd)
0.00
0.30
0.60
0.90
1.20
1.50
X10 2.0
Carrier Gas Flow Rate

Fig 6-4

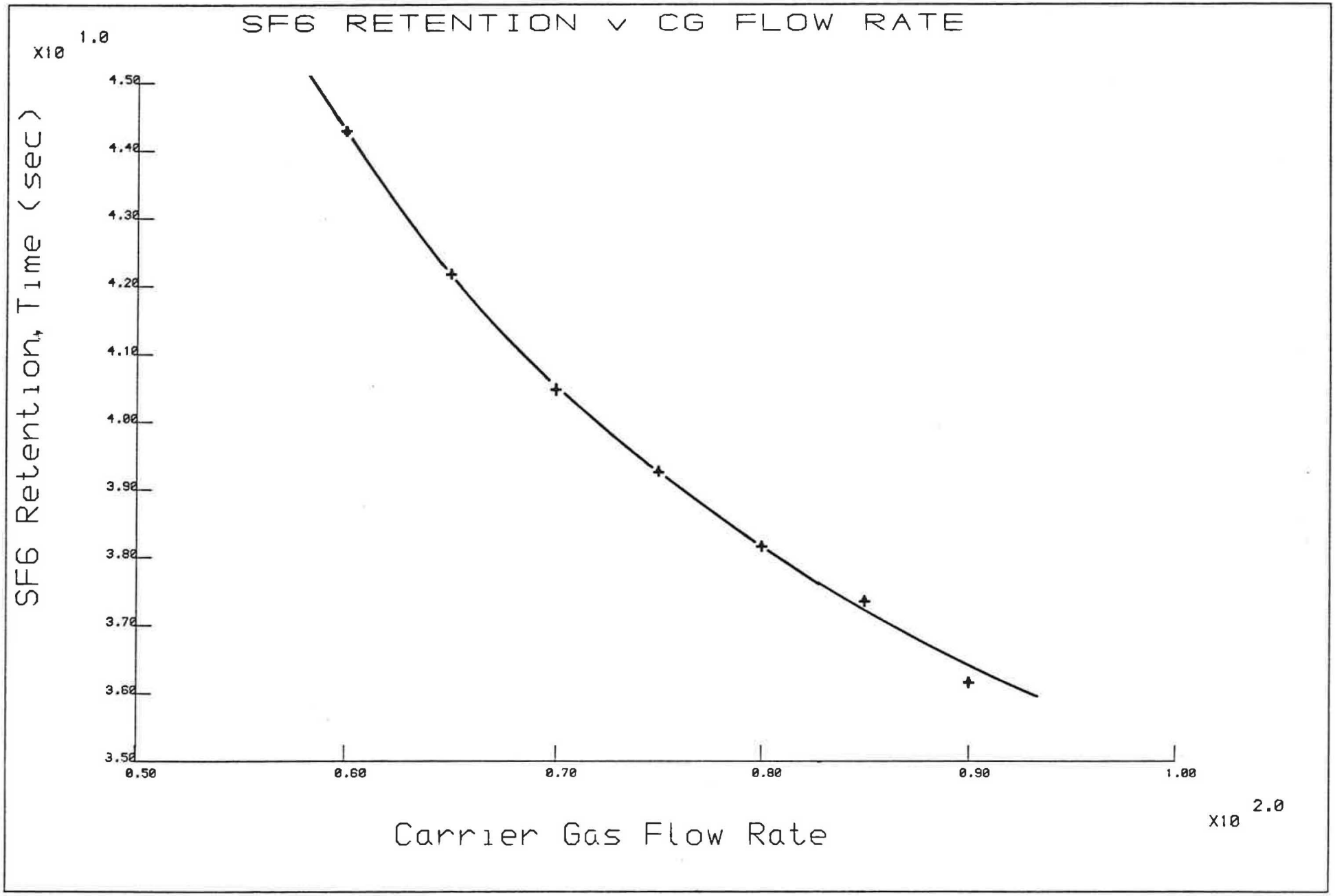
SF6 RETENTION v CG FLOW RATE
X10 1.0
SF6 Retention, Time (sec)
4.50
4.40
4.30
4.20
4.10
4.00
3.90
3.80
3.70
3.60
3.50
0.50
0.60
0.70
0.80
0.90
1.00
X10 2.0
Carrier Gas Flow Rate

Fig 6-5

A TRACER GAS DECAY SYSTEM FOR MONITORING AIR INFILTRATION AND AIR MOVEMENT IN LARGE SINGLE CELL BUILDINGS

J.R. WATERS, G.V. LAWRANCE and N. JONES

Symposium on Design and Protocol
For Monitoring Indoor Air Quality
American Society for Testing and Materials
Cincinnati
April 1987

A Tracer Gas Decay System for Monitoring Air Infiltration and Air Movement in Large Single Cell Buildings

John R. Waters, Graham V. Lawrance and Neville Jones

Introduction

Buildings such as factories, sports halls and aircraft hangars which are not divided internally into distinct rooms may be regarded as large single cell buildings. The measurement of air infiltration in such buildings by a tracer gas method does not present any particular difficulty provided the air in the building can be stirred sufficiently to maintain a uniform distribution of the tracer throughout the measurement period. Using sulphur hexafluoride (SF_6), Ashley and Lagus [1] have successfully used the tracer decay method to measure infiltration rates of aircraft hangers up to 96000 m^3 internal volume. Waters and Simons [2] have also used the tracer decay method, with SF_6 and nitrous oxide (N_2O), to measure air infiltration in several industrial units around 3000 m^3 internal volume. Etheridge, Jones and O'Sullivan [3] have used the constant concentration method, with both SF_6 and N_2O, in two small factory units of 810 m^3 and 1300 m^3 internal volume. However, the maintenance of a uniform tracer distribution requires artificial stirring and this gives rise to several objections. From a practical viewpoint the fan power required may be very high and, even in unoccupied buildings, it may be difficult to avoid completely stagnation points and volumes of poorly mixed air. In addition the installation of mixing fans and the high air velocities in their vicinity could cause unacceptable disturbances to people and processes within the building. Perhaps of more importance, however, is the fact that industrial buildings often have a wide variation in the size of openings around their perimeter, especially given the need for large

industrial doors. In addition they frequently have localised extraction systems associated with specific processes or pieces of machinery. Both factors give rise to strong spatial variations in the effective infiltration rate which must be taken into account if infiltration related phenomena such as heat transfer and contaminant distribution are to be analysed adequately. Artificial stirring destroys these spatial variations.

Potter et al [4] considered this problem and concluded that artificial stirring should be avoided. To account for the spatial variations in the space they designed a multi-point tracer decay system, using Infra-Red Gas Analysers (IRGA) with which they monitored three buildings, the largest being around 4000 m^3 in volume. The tracer gas used was not reported. Their measured infiltration rates appear to be for the whole building and to be taken from the average slope of the long term decay curve. Waters and Simons [5] have shown that this is likely to give errors when air within the monitored space is imperfectly mixed. Furthermore, Waters and Simons [2], in their preliminary study, suggested that by avoiding artificial stirring and combining multi-point sampling with non-uniform initial tracer distribution it should be possible to obtain data on internal air flows. Their equipment, however, was insufficient to follow this through.

This paper describes the specification, design and commissioning of a multi-point tracer gas system for monitoring air infiltration and internal air movements in large single cell industrial buildings. Examples of the operation of the system are given together with the method of treating the results.

Specification

The overall requirement was for a system which would measure infiltration and air movement in industrial buildings during normal conditions of use, for the purpose of providing data on heat transfer and contaminant distribution. This precludes the use of artificial mixing and leads immediately to the need for multi-point sampling.

The problem of multi-point sampling in a single cell may be regarded as one in which the large, continuous volume of air is subdivided, or discretised, into a number of smaller volumes, or zones, with hypothetical (ie. physically non-existent) boundaries between them. Each zone would then have a sampling point within it. This approach has been used by Potter et al [4], and Waters and Simons [2] and has been discussed by Dewsbury [6]. In principle, the discretisation process can be continued until each zone is sufficiently small for it to be assumed that the air within it is always fully mixed. Multizone theory can then be applied to analyse the results and identify infiltration and air movement throughout the building. In practice, the number of zones is limited by the number of sampling points which the instrumentation can accommodate, and by the difficulties of placing sampling points in convenient positions. Ashley and Lagus used five sampling points, Potter used nine, and Waters and Simons used six. The system described here was therefore designed around a basic configuration of six channels with the capability of multiplexing so that the number of sampling points could be increased in multiples of six.

From these initial considerations, it was concluded that:

1. at any time, the tracer concentration may show large spatial variations and so the detection system must have low cross-talk between channels.

2. at any sampling point, tracer concentration may vary rapidly with time and so the system must have a fast response, and be able to monitor continuously or at least with a short sampling interval.

3. because of 1 and 2, the range of tracer concentration in an experimental run may be large, and so the detection system must be capable of operating with known calibration over a large range.

4. because the buildings are large, tracer concentration may sometimes be very low, necessitating good sensitivity to the chosen tracer. Operating with low tracer concentrations also minimises concern by the buildings occupants to any dangers related to the particular tracer gas.

In addition a system which had the capability of measuring, analysing and computing results in one site visit was preferred. This would allow the occupants to have immediate feedback on the performance of their building.

For infiltration measurements in large buildings, most workers have preferred to use SF_6 as the tracer, detected by a gas chromatograph using an electron capture detector (ECD). This combination allows very low concentrations of tracer to be used. Ashley and Lagus used SF_6 , Waters and Simons used both SF_6 and N_2O, although they concluded that SF_6 was preferable, and in large office buildings SF_6 has been used successfully by, for example, Grot [7] and Grot and Persily [8]. Some workers have used multiple tracers in order to increase the amount of data available for analysis. Perera, Walker and Trim [9] used SF_6, N_2O and carbon dioxide (CO_2), detected by IRGA's, and Fisk et al [10] have described a multiple tracer system employing SF_6 and five halocarbons, and a gas chromatograph.

In large buildings, therefore, SF_6 gas chromatographs have been found to be highly suitable. However, in industrial buildings which are in use particular care has to be taken to select a tracer which is not present in the building atmosphere. SF_6 is a comparatively rare constituent, but oxides of nitrogen and carbon, and halocarbons are relatively common. A decision was made, therefore, to use SF_6 as the tracer and to design an electron capture gas chromatograph system which was selectively sensitive to it, thus reducing interference due to other electrophilic contaminants in the air.

However, the use of an ECD chromatograph precludes continuous monitoring. For air movement studies in factories, Waters and Simons [2] suggested that tracer concentrations should be measured at least at one minute intervals at all sample points. This cannot be achieved by a single detector switched through six channels, and so it was considered necessary to have six independent detector systems, one for each channel.

Gas Analyser Unit and System Design

ECD Amplifier

An electron capture cell can be operated in direct current mode (DC), pulse mode, or pulse modulated mode. The relative merits of these modes have been described by Swan [11]. In the DC mode a constant current through the detector cell is maintained by a variable applied potential. The presence of an electrophilic contaminant reduces the effective conductivity of the gas stream in the cell, the compensatory increase in voltage being a measure of contaminant concentration. However, because the applied potential is always present anomalous responses due to detector

contamination are greatly accentuated, causing the detector to be inaccurate and unreliable.

The pulse mode of operation was developed by Lovelock [12] to overcome these problems. Fixed potential pulses, typically between 0.5 and 1.0 μs duration at intervals of 50 to 500 μs are applied. This reduces the anomalous responses to levels which are normally undetectable, and also increases sensitivity. The change in the cell conductivity is measured as a change in the average current. Unfortunately, the output is linear with respect to contaminant concentration over a restricted range only, making calibration difficult over a large range. To overcome the lack of linearity the pulse modulated mode operates with a constant average current. Fixed potential pulses are applied and a constant average current is obtained by varying the pulse frequency. It is found that the sensitivity of the pulse mode is preserved and that an essentially linear response is obtained. Swan claims that a linear response range of up to 10^4 is achievable, although he does not give details of the conditions required for this. From these considerations the pulse modulated mode of ECD operation was selected.

Chromatograph

The ECD cell, the pulse modulated ECD amplifier, and the sample injection valves were purchased commercially. It was decided to use alumina as the column material and high purity argon as the carrier gas. It was also decided to operate the detector and column at an elevated temperature (nominally 35°C), to reduce the risk of column contamination by condensation and to stabilise detector sensitivity.

System Optimisation

A single channel prototype was constructed in order that the components and parameters could be optimised in experimental design exercises. The components and parameters examined were:

1. ECD current
2. Column dimensions
3. Carrier gas flow rate
4. Sample loop volume

These were evaluated by reference to five output parameters:

1. peak resolution (oxygen and SF_6)
2. peak retention time
3. SF_6 peak height
4. SF_6 peak width
5. base line response

The objectives were to achieve, firstly, minimum peak retention times in order to keep the cycle time and hence sampling interval short, secondly narrow well defined SF_6 peaks, and thirdly good separation of the oxygen and SF_6 peaks (resolution).

ECD Current

Using a mixture of 35×10^{-12} volume parts SF_6 in air, the effects of different average current settings on SF_6 peak height and base-line response were found, as shown in figure 1. The increase of both output parameters with detector current represents an increase in sensitivity, in the first case to SF_6 and in the second to the carrier gas and the contaminants it contained. However, as the detector has a saturation level which is relatively independent of current, the increase in base line response also represents a decrease in operating range. Thus the current

setting must be chosen to give the best compromise between range and sensitivity. Our initial choice has been found to be satisfactory in all subsequent measurements.

Column Dimensions

Of the two column dimensions, length and diameter, the former was found to have the more significant effect on the output parameters. Shortening the column decreased peak resolution, tracer gas peak width and peak retention times but increased peak height. Base line response was not affected. Reducing the column diameter increased peak resolution by reducing peak width but had little effect on the remaining output parameters.

Thus in order to minimise peak width and retention times the column was required to be as short as possible whilst ensuring complete resolution of the SF_6 peak. The optimum column diameter would be the smallest which maintained the column's capacity to perform the separation. From these investigations, a column 1 m long and 3.5 mm diameter was chosen.

Carrier Gas Flow Rate

The effect of flow rates between 30 and 120 cm^3/min was investigated. In all cases, increasing the carrier flow rate reduced all five output parameters, indicating that it is preferable to operate at a low rate. Of particular interest is the effect on peak height and base line response, as shown in figure 2. Both curves have a minimum gradient in the region of 65 cm^3/min, indicating a point of maximum stability with respect to flow rate fluctuations. Because of this, and because a minimum rate of

50 cm^3/min was needed to provide satisfactory purging of the cell, carrier flow rates were kept within the range 55 to 75 cm^3/min.

Sample Loop Volume

It was found that sample loop volume could be adjusted over a reasonable range independently of the other design parameters. With the ECD current, column dimensions and carrier gas flow rates set as above a sample loop volume of 0.08 cm^3 gave maximum output for a sample containing approximately 400 x 10^{-12} volume parts SF_6 in air. This was considered to provide ample sensitivity.

Performance

The completed detector system operated above initial target specifications. Clear, sharp SF_6 peaks were obtained with retention times (measured from injection) of about 20 seconds, with no detectable "tail" or memory. Thus the target cycle time of one minute between successive samples was easily met, with the possibility of going to shorter intervals if desired.

Six Channel Design

Each of the six independent Gas Analyser Units (GAU) was assembled as shown in figure 3 and incorporated in the complete system as shown in figure 4. In operation the computer operates all six sample injection valves simultaneously at one minute intervals, and then scans the amplifier outputs to measure the base lines and SF_6 peaks. Several methods of measuring the SF_6 peak have been tried, including peak height and various measures of peak area. Generally it has been found that peak area gives

more consistent results although the algorithm for measuring peak height is much simpler and quicker to operate. The software includes subroutines for initialisation and calibration, but currently data is stored on floppy disc and transferred to a mainframe computer for analysis.

Calibration

With six independent gas analyser units, calibration is particularly important to ensure compatability of results between channels. Initially, calibration was attempted by means of a range of commercially available SF_6/air mixtures. However, below about 200×10^{-12} volume parts SF_6 in air, it was found that the supplier was unable to specify the SF_6 concentration with sufficient accuracy. Now when using the tracer decay method, the absolute accuracy of the measurement of tracer concentration is not important if the relative precision over the measurement range can be established. Therefore, calibration was carried out by means of a single mixture of SF_6 in air which was carefully diluted to lower concentration, as shown in figure 5. Air and the SF_6/air mixture were fed through fine control valves into capillary tubes before mixing and entering the gas analyser unit. The control valves were adjusted to give a suitable delivery flow for Q_d whilst at the same time maintaining zero pressure difference (as registered by the micromanometer) between the capillary tube inlets. The radii and lengths of the capillaries, r_s, l_s, r_a, l_a were chosen so that (i) the flow in the capillaries was laminar, and (ii) the pressure difference P_1-P_2 was large enough to swamp any error in the setting of the micromanometer. The pressure drop across both capillaries must be the same, and so, from elementary pipe flow theory,

$$Q_s = k\alpha_s(P_1 - P_2) \qquad Q_a = k\alpha_a(P_1 - P_2)$$

$$Q_d = Q_s + Q_a = k(P_1 - P_2)(\alpha_s + \alpha_a)$$

where k is a constant, $\alpha_s = \frac{r_s^4}{l_s}$ and $\alpha_a = \frac{r_a^4}{l_a}$.

Also if C_s and C_d are the tracer concentrations in the original mixture and the diluted mixture respectively, then

$$C_d = C_s \frac{Q_s}{Q_d} = C_s \frac{\alpha_s}{\alpha_s + \alpha_a} = C_s\left(1 + \frac{\alpha_a}{\alpha_s}\right)^{-1}$$

A range of values for the dilution ratio $\left(1 + \frac{\alpha_a}{\alpha_s}\right)^{-1}$ can be obtained by choosing capillary tubes of appropriate length and radius. However, in order to allow for end effects and variations in tube radius, the ratios $\frac{\alpha_a}{\alpha_s}$ were determined experimentally. This may be done very simply by allowing a container of compressed air to discharge to atmosphere through each tube in turn. The gauge pressure in the container decays exponentially, with a decay constant β which is proportional to α. Measurements over a pressure range which encompassed the pressure difference used in the calibration apparatus showed that β could be obtained with regression coefficients better than 0.999. Thus the effective ratio $\frac{\alpha_a}{\alpha_s}$ for each pair of capillary tubes was found from the measured ratio of $\frac{\beta_a}{\beta_s}$, with an estimated maximum error of about 0.2%.

The calibration measurements showed that the response of each gas analyser unit could be fitted to an equation of the form

$$R = lC^m e^{nt}$$

where R is the chosen measure of the SF_6 peak (peak height or peak area), C is the concentration of SF_6 in air, t is the retention time of the SF_6 peak, and l, m, n are regression coefficients. The exponential term, which

allows for variations in carrier gas flow rate, uses retention time as the variable because it can be measured more easily and more accurately than the carrier flow rate on which it depends. The coefficient m was in all cases close to unity, showing that the response to SF_6 was essentially linear.

Operation and Analysis

Setting Up

The complete system is mounted in a covered trailer, and except for a 240 VAC power supply, is self-contained. On site, the trailer is parked either within the building, or immediately outside, so that it is only necessary to run tubing from the trailer to the sample points. The position of the sample points is chosen according to building geometry and the extent of internal obstructions. In open buildings with few obstructions, the building is divided into imaginary zones of approximately equal volume, with a sample point at the centre of each zone. Where internal obstructions are significant, sample points are placed to represent the spaces that obstructions delineate. However, in occupied buildings, it is often necessary to displace the sample point from the desired position to avoid interference with building activities. The sampling heads themselves consist of a small cylindrical manifold from which radiate nine 1 m lengths of copper tubing, in the manner of the spokes of a wheel. At each sample point, therefore, air is collected from nine equally spaced points around the circumference of a 2 m circle. This provides some spatial integration of the sample collection within each zone.

Site Calibration

Before each experimental run, an SF_6/air reference mixture of known concentration is injected into all six gas analyser units simultaneously. The carrier gas flow rate to each unit is then adjusted to ensure that the SF_6 peak retention times are approximately equal; this is necessary for satisfactory measurement of the SF_6 peak. The SF_6 peaks due to the reference mixture are then measured, so that the responses of the six units can be normalised with respect to each other.

Tracer Injection Strategy

The degree of success with which interzone flow rates can be extracted from measurements of tracer decay depends on the initial distribution of the tracer. In the case of a single tracer, Waters and Simons [5] have shown that the best strategy is to seed a single zone. Ideally, this should be the zone associated with the smallest component of the dominant eigenvector in the solution of the multizone flow equations for the building. However, this solution can only be obtained if the interzone flows are already known. Fortunately, it is almost as satisfactory to seed any single zone, provided that in the subsequent measurements it is possible to detect tracer gas in all zones in the system. The strategy which has been adopted, therefore, is to inject pure SF_6 into a single zone on the windward side of the building, with stirring during the injection process to ensure mixing within that zone. The SF_6 injection equipment is kept separate from the measurement system to avoid contamination. The tracer decay is then followed for between 1 and 2 hours, with sampling at 1 minute intervals.

Data Analysis

The raw data is first subjected to calibration corrections, and then, using a simple fourth difference technique (Lanczos [13]), smoothed values of tracer concentration and its time derivative are obtained. Results for each run are then processed in two ways:

1. Readings for all six sample points are averaged to give a single overall average tracer concentration for the whole building. Where the sample points represent zones of unequal size, the average is volume weighted. The decay of this average concentration is fitted using a standard least squares technique to a simple exponential law, the decay constant being taken as the fresh air infiltration rate of the whole building.
2. Using multizone theory, a constrained least squares technique is used to determine the complete set of interzone flow rates. The fresh air infiltration rate of the whole building is found by summing the flows between individual zones and the outside.

For both methods of analysis, the data set for each run is split into sections, and each section analysed separately. These sections are:

1. the first third of the data in the time series
2. the second third
3. the last third
4. the first two thirds
5. the last two thirds
6. the whole data set.

Thus for each method of analysis there are six sets of results for each run. In addition, as an indication of the effect of the constraints, the multizone solution is obtained from the full data set with reduced constraints and also with all constraints removed.

In the case of the averaged data, it may be expected that the decay over the first third of the data set will be faster than that due to fresh air infiltration. This is because the short term transients of the multizone solution will govern the decay. The infiltration rate from this section of the data will therefore be too large. On the other hand, the decay over the last third will be slower, because the long term, dominant decay constant will govern the decay, and this always leads to an infiltration rate which is too small. Thus, upper and lower bounds on the whole building infiltration rate can be found.

In solving for the interzone flow rates it is necessary to use a constrained least squares method in order to prevent negative flows (which are physically impossible) appearing in the solution. Penman and Rashid [14] used the non-negative least squares method employed by Lawson and Hanson [15]. However, additional constraints in the form of upper and lower bounds for flows associated with the seeded zone can be derived from examination of the tracer distribution immediately following injection. These have been incorporated by means of the method known as least squares with inequality constraints, also described by Lawson and Hanson. The complete solution procedure is therefore (i) set to zero all flows which, due to building geometry, cannot exist, (ii) set the constraint that all flows must be non-negative, (iii) from examination of the early tracer distribution establish upper and lower bounds for the flows from the seeded zone, and (iv) apply the method of least squares with inequality constraints.

Results

Measurements have been carried out in the folllowing five buildings:

1. Abbey School Sports Hall, Kenilworth, Volume 4220 m^3
2. Courtaulds Engineering Workshop, Coventry, Volume 14370 m^3
3. Courtaulds Pattern Making Shop, Coventry, Volume 6420 m^3
4. Hanger 5, Coventry Airport, Volume 31300 m^3
5. British Gas Maintenance Depot, Birmingham, Volume 31020 m^3

Except for the Sports Hall, all the buildings were occupied and in use during the measurements; in hanger 5 all measurements were taken with the aircraft doors closed. In all cases six sampling points were used, which were positioned to represent equal volumes except where internal obstructions were significant, in which case they were positioned to represent the spaces that the obstructions created. In all buildings the ceiling height was much smaller than the overall length or breadth, and so it was considered preferable to measure horizontal rather than vertical air movement. Therefore, the six sample points were positioned in a horizontal plane approximately half way between floor and ceiling. Thus each imaginary zone extended from floor to ceiling, so that measured flows between each zone and the outside include flow through the roof as well as the external wall. Tables 1 through 5 show details of a typical measurement from each of the five buildings, with the computed interzone flows and whole building infiltration rates. The nomenclature F_{mn} indicates the flow rate from zone m to zone n in cubic metres per second.

When the whole building infiltration rate is calculated from the average of the six sample points, the highest rate is obtained from the first third of the data, and the lowest rate from the last third of the data as expected. Assuming these represent over estimates and underestimates, and assuming also that the value obtained from the whole

data set is the best estimate, the whole building infiltration rate can be expressed in air change per hour (ACH) within limits:

Building 1 infiltration rate = $4.15^{+1.41}_{-0.32}$ ACH

Building 2 infiltration rate = $2.58^{+1.78}_{-0.39}$ ACH

Building 3 infiltration rate = $2.03^{+0.64}_{-0.08}$ ACH

Building 4 infiltration rate = $3.84^{+1.40}_{-0.26}$ ACH

Building 5 infiltration rate = $3.17^{+1.02}_{-0.21}$ ACH

It can be seen that the uncertainty on the positive side of the best estimate is between 4 and 8 times the uncertainty on the negative side. This is typical of all the measurements that have been made. Expressed as a percentage of the best estimate, the uncertainties vary between about 10% to 50% on the positive side, and between 2% and 20% on the negative side. Thus, although the main reason for using a non-uniform initial distribution of tracer gas is to investigate internal air movement, it is possible to use the tracer measurements in a relatively unsophisticated manner to obtain whole building infiltration data.

If the data sets were free from experimental error, and if the assumptions of multizone theory were actually realised in these buildings, then the infiltration rates calculated from interzone flows would be the same whichever section of the data set was used in the analysis. Neither condition is true, and the results show that the infiltration rates found in this way often show marked variations between different sections of the

same data set, and often differ markedly from the infiltration rates found from the averaged data. This indicates that the errors in the individual flow rates are probably quite large, and that the interzone flow values shown for these buildings should be treated with caution. Walker [16] has examined errors by considering suitable norms of the appropriate matrices, but this leads only to upper bounds for the errors in the computed flow rates, and does not lead to an estimate of the error in each individual flow. Also Waters and Simons [5] have noted that there are several circumstances in which the equations for the interzone flows will be ill-conditioned. Nevertheless, the most likely cause of the discrepancies is that in all of these buildings each sampling point represents too large a volume. Inspite of this, in many data sets, the discrepancies in the whole building infiltration rates are not excessive, the results for building 5 being an example. In such cases, the computed interzone flow rates may be a good indication of the air movements within the building.

Future Developments

Work to improve the consistency of the results, especially the interzone flow rates, is being pursued both experimentally and theoretically. Two experimental improvements are to be investigated, the first the effect of using more sampling points, and the second the use of sample heads which collect over a larger radius than the present 2 m. Theoretically, developments of the multizone model are being explored. One possible improvement concerns the assumption that the flow of air between zones is instantaneous, whereas in practice, especially in large open buildings, there may be a significant time lag. Waters [17] has analysed a two zone model with time lags, and found that in such a case the tracer decay curves appear to have an oscillation imposed upon them whose frequency depends on the magnitude of the time lags. This type of

oscillation has been observed in the decay curves for some of the buildings. Figure 6, which is a set of measured decay curves for building 4, is an example.

Conclusion

The work reported here represents the present position in an on-going project on large single-cell buildings. The results so far indicate that good estimates of the overall infiltration rate of the whole building can be obtained. However, although it is possible to use multizone theory to obtain results which give an indication of air movement within the building, further work is necessary before the measured internal air movement values can be considered reliable.

Acknowledgements

The project of which this work forms a part is part-funded by the Science and Engineering Research Council and by the National Advisory Board for Further and Higher Education of the United Kingdom. The authors would also like to thank British Gas Plc, Courtaulds Engineering Plc, Coventry Airports Authority, and Warwickshire Education Committee for making their buildings available for measurement.

References

[1] Ashley, J.L. and Lagus, P.L., "Air Infiltration Measurements in Large Military Aircraft Hangars", Measured Air Leakage of Buildings, ASTM STP 904, H.R. Trechsel and P.L. Lagus, Eds., American Society for Testing and Materials, Philadelphia, 1986, pp. 120-134.

[2] Waters, J.R. and Simons, M.W., "The Measurement of Air Infiltration in Large Single-Cell Industrial Buildings", Measured Air Leakage of Buildings, ASTM STP 904, H.R. Trechsel and P.L. Lagus, Eds., American Society for Testing and Materials, Philadelphia, 1986, pp. 106-119.

[3] Etheridge, D.W., Jones, P.L. and O'Sullivan, P.E., "Ventilation of Factories", in Proceedings, 6th AIC Conference, Netherlands, Sept. 1985, Air Infiltration and Ventilation Centre, Bracknell, Berks, United Kingdom.

[4] Potter, I.N., Dewsbury, J. and Jones, T.J., "The Measurement of Air Infiltration Rates in Large Enclosures and Buildings", in Proceedings, 4th AIC Conference, Elm, Switzerland, Sept. 1983, Air Infiltration and Ventilation Centre, Bracknell, Berks, United Kingdom.

[5] Waters, J.R. and Simons, M.W., "The Evaluation of Contaminant Concentrations and Air Flows in a Multizone Model of a Building", Building and Environment, Vol. 22, 1987, pp. 305-315.

[6] Dewsbury, J., "Use of a Single Tracer Gas for Measurement of Ventilation Rates in a Large Enclosure", in Proceedings, 6th AIC Conference, Netherlands, Sept. 1985, Air Infiltration and Ventilation Centre, Bracknell, Berks, United Kingdom.

[7] Grot, R.A., "The Air Infiltration and Ventilation Rates in Two Large Commercial Buildings", Proceedings, 2nd ASHRAE/DOE Conference on the Thermal Performance of the Exterior Envelopes of Buildings, ASHRAE SP 38, Atlanta, GA, 1983.

Table 1
Measured infiltration rates and interzone flows, Building 1

Date: 22.08.85 Wind Speed: 5.7 m/s Seeded Zone: 5

Constraints: (i) $0.43 \leqslant F_{05} + F_{35} + F_{65} \leqslant 4.48$, $F_{53} \leqslant 3.97$, $F_{56} \leqslant 4.25$
(ii) All $F \geqslant 0.00$

Data Subset Used	Computation Constraints Used	Infiltration Rate in Air Changes per Hour	
		From Interzone Flows	From Averaged Data
1st Third	(i) and (ii)	0.72	5.56
2nd Third	(i) and (ii)	0.83	4.25
3rd Third	(i) and (ii)	0.48	3.83
1st Two Thirds	(i) and (ii)	0.63	4.60
Last Two Thirds	(i) and (ii)	2.13	3.97
All	(i) and (ii)	1.09	4.15
All	(ii) only	1.09	. ..
All	none	3.12	. ..

Interzone Flows for All Data, Fully Constrained, m/s

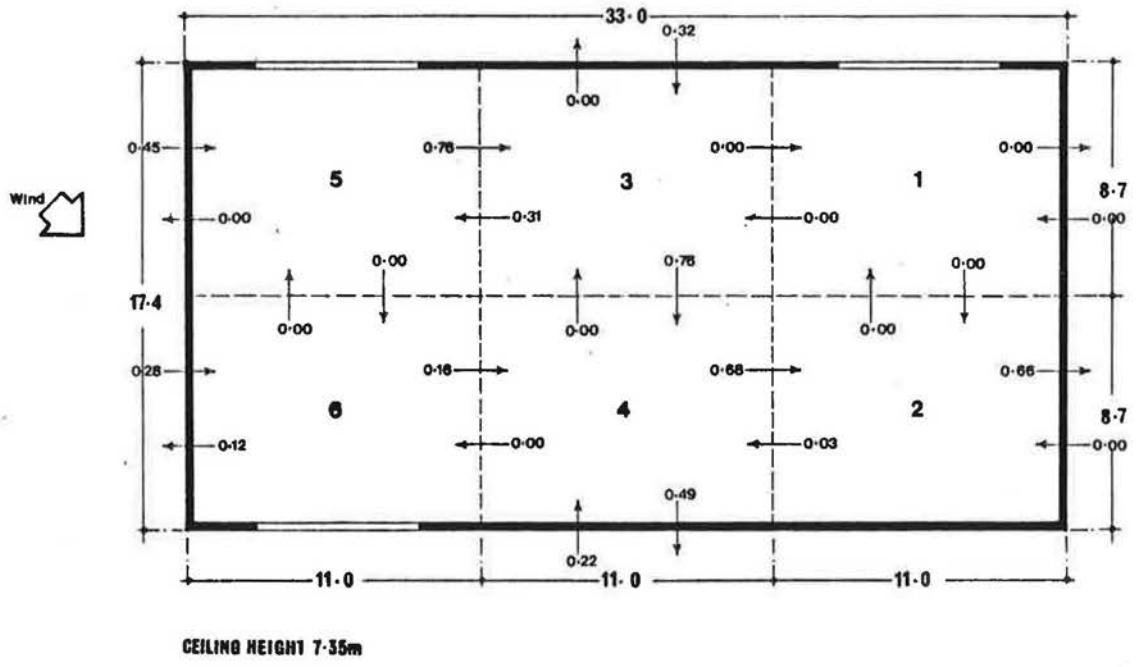

CEILING HEIGHT 7·35m

Table 2
Measured infiltration rates and interzone flows, Building 2

Date: 05.12.85 Wind Speed: 2.6 m/s Seeded Zone: 3

Constraints: (i) $3.9 \leqslant F_{03} + F_{23} + F_{53} \leqslant 19.1$, $F_{32} \leqslant 2.16$, $F_{35} \leqslant 15.2$
(ii) All $F \geqslant 0.00$

Data Subset Used	Computation Constraints Used	Infiltration Rate in Air Changes per Hour	
		From Interzone Flows	From Averaged Data
1st Third	(i) and (ii)	1.43	4.36
2nd Third	(i) and (ii)	0.88	2.85
3rd Third	(i) and (ii)	1.78	2.19
1st Two Thirds	(i) and (ii)	2.65	3.21
Last Two Thirds	(i) and (ii)	0.75	2.40
All	(i) and (ii)	2.60	2.58
All	(ii) only	2.05	. ..
All	none	0.61	. ..

Interzone Flows for All Data, Fully Constrained, m/s

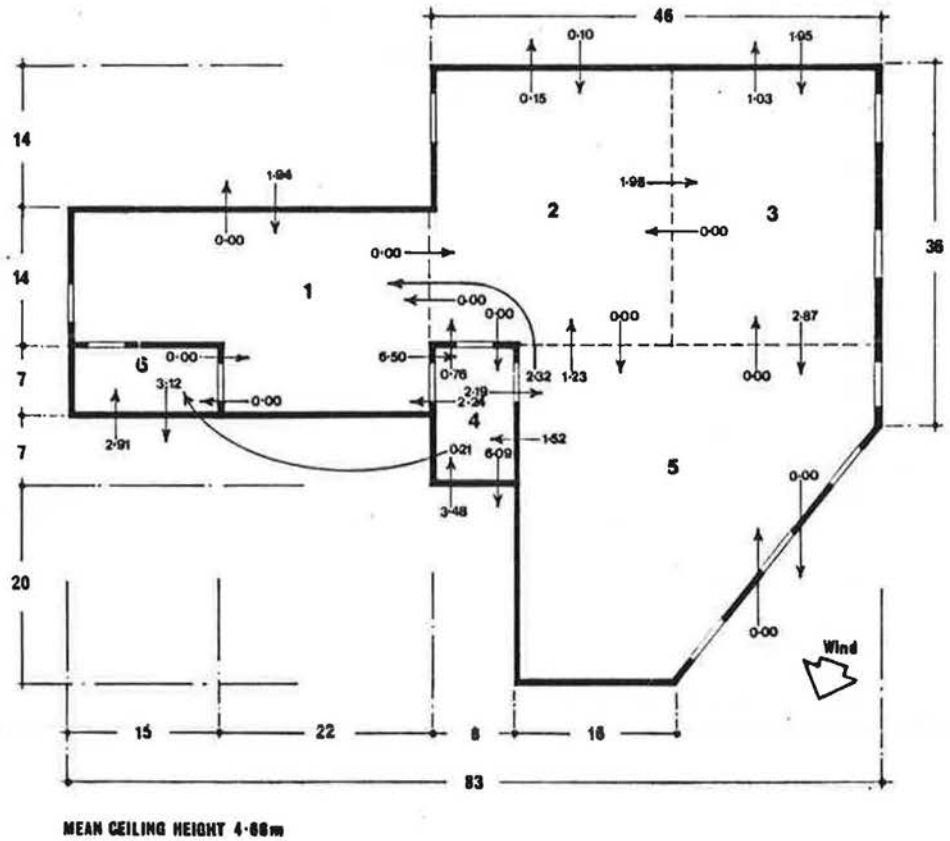

MEAN CEILING HEIGHT 4·66m

Table 3
Measured infiltration rates and interzone flows, Building 3

Date: 22.08.85 Wind Speed: 8.2 m/s Seeded Zone: 6

Constraints: (i) $3.15 \leqslant F_{06} + F_{16} + F_{26} + F_{36} + F_{46} + F_{56} \leqslant 5.58$, $F_{61} \leqslant 1.45$
$F_{62} \leqslant 6.13$, $F_{63} \leqslant 4.40$, $F_{64} \leqslant 0.78$, $F_{65} \leqslant 0.65$
(ii) All $F \geqslant 0.00$

Data Subset Used	Computation Constraints Used	Infiltration Rate in Air Changes per Hour	
		From Interzone Flows	From Averaged Data
1st Third	(i) and (ii)	3.10	2.64
2nd Third	(i) and (ii)	1.26	2.09
3rd Third	(i) and (ii)	1.43	1.95
1st Two Thirds	(i) and (ii)	1.29	2.19
Last Two Thirds	(i) and (ii)	3.47	1.99
All	(i) and (ii)	0.88	2.03
All	(ii) only	0.98	. ..
All	none	1.66	. ..

Interzone Flows for All Data, Fully Constrained, m/s

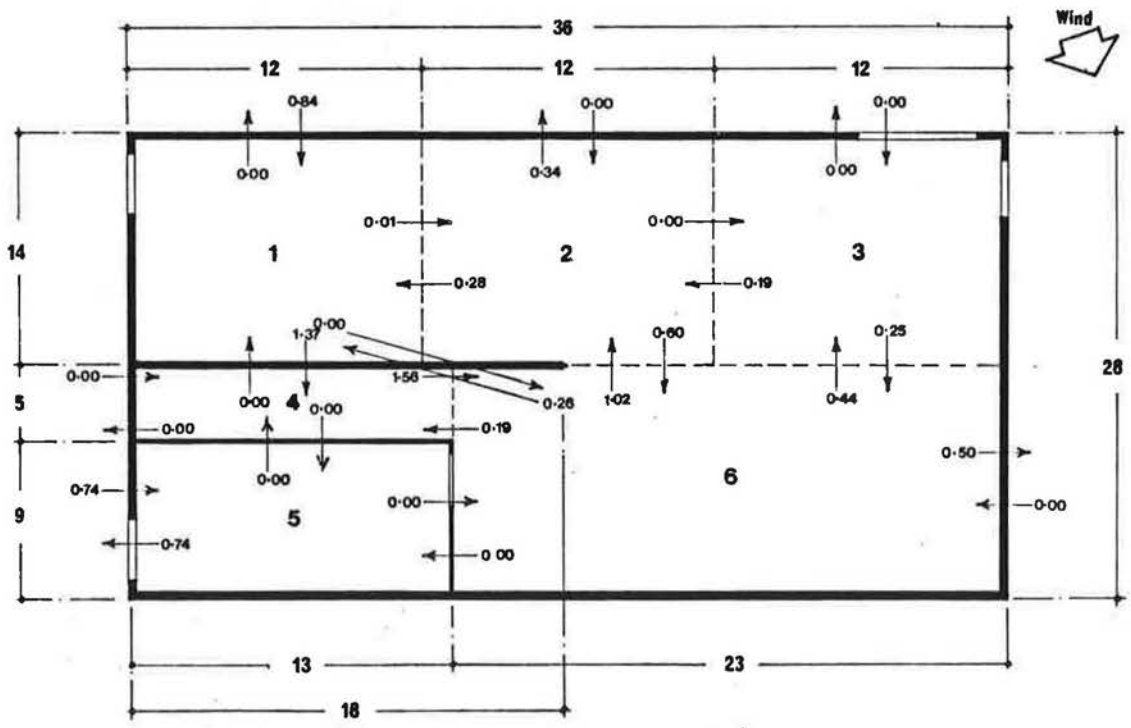

MEAN CEILING HEIGHT 6·37m

Table 4
Measured infiltration rates and interzone flows, Building 4

Date: 08.11.85 Wind Speed: 4.1 m/s Seeded Zone: 1

Constraints: (i) $22.5 \leqslant F_{01} + F_{21} + F_{41} \leqslant 50.0$, $F_{12} \leqslant 15.4$, $F_{14} \leqslant 32.8$
(ii) All $F \geqslant 0.00$

Data Subset Used	Computation Constraints Used	Infiltration Rate in Air Changes per Hour	
		From Interzone Flows	From Averaged Data
1st Third	(i) and (ii)	1.95	5.24
2nd Third	(i) and (ii)	1.58	4.12
3rd Third	(i) and (ii)	2.60	3.58
1st Two Thirds	(i) and (ii)	2.47	4.33
Last Two Thirds	(i) and (ii)	5.62	3.74
All	(i) and (ii)	3.14	3.84
All	(ii) only	3.87	. ..
All	none	1.87	. ..

Interzone Flows for All Data, Fully Constrained, m/s

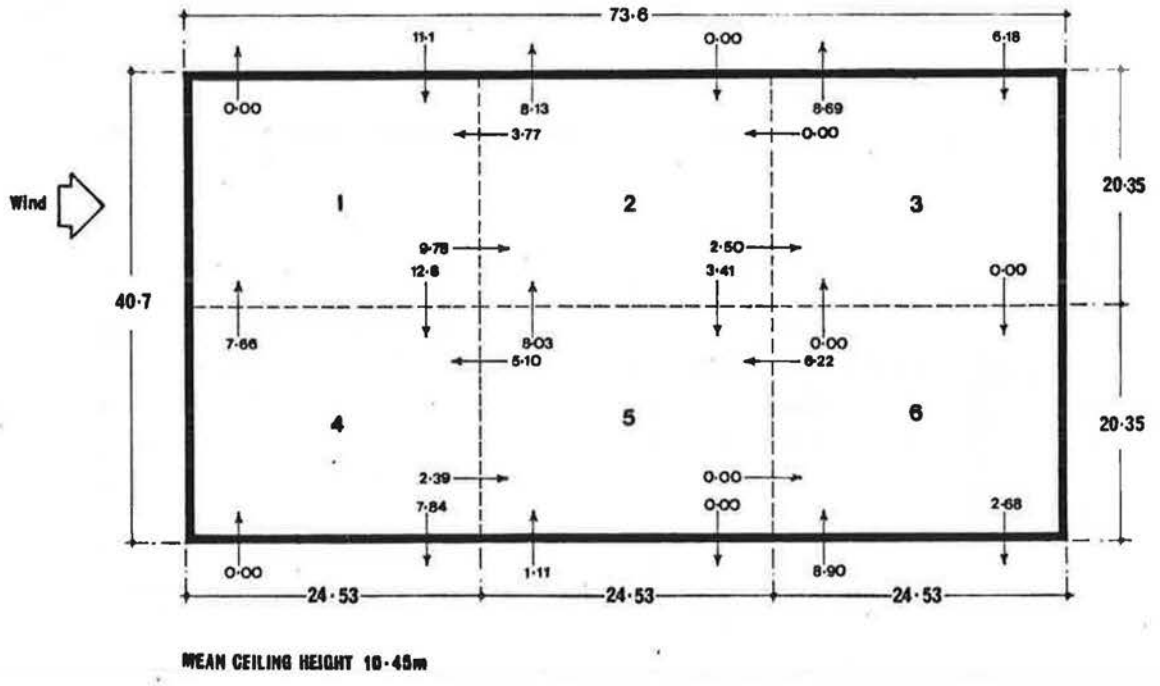

Table 5
Measured infiltration rates and interzone flows, Building 4

Date: 17.09.86 Wind Speed: 2.6 m/s Seeded Zone: 3

Constraints: (i) $14.2 \leqslant F_{03} + F_{23} + F_{63} \leqslant 54.6$, $F_{32} \leqslant 6.4$, $F_{36} \leqslant 12.2$
(ii) All $F \geqslant 0.00$

Data Subset Used	Computation Constraints Used	Infiltration Rate in Air Changes per Hour	
		From Interzone Flows	From Averaged Data
1st Third	(i) and (ii)	1.40	4.29
2nd Third	(i) and (ii)	4.04	3.26
3rd Third	(i) and (ii)	4.33	2.96
1st Two Thirds	(i) and (ii)	2.98	3.50
Last Two Thirds	(i) and (ii)	4.94	3.06
All	(i) and (ii)	3.76	3.17
All	(ii) only	3.02	. ..
All	none	0.30	. ..

Interzone Flows for All Data, Fully Constrained, m/s

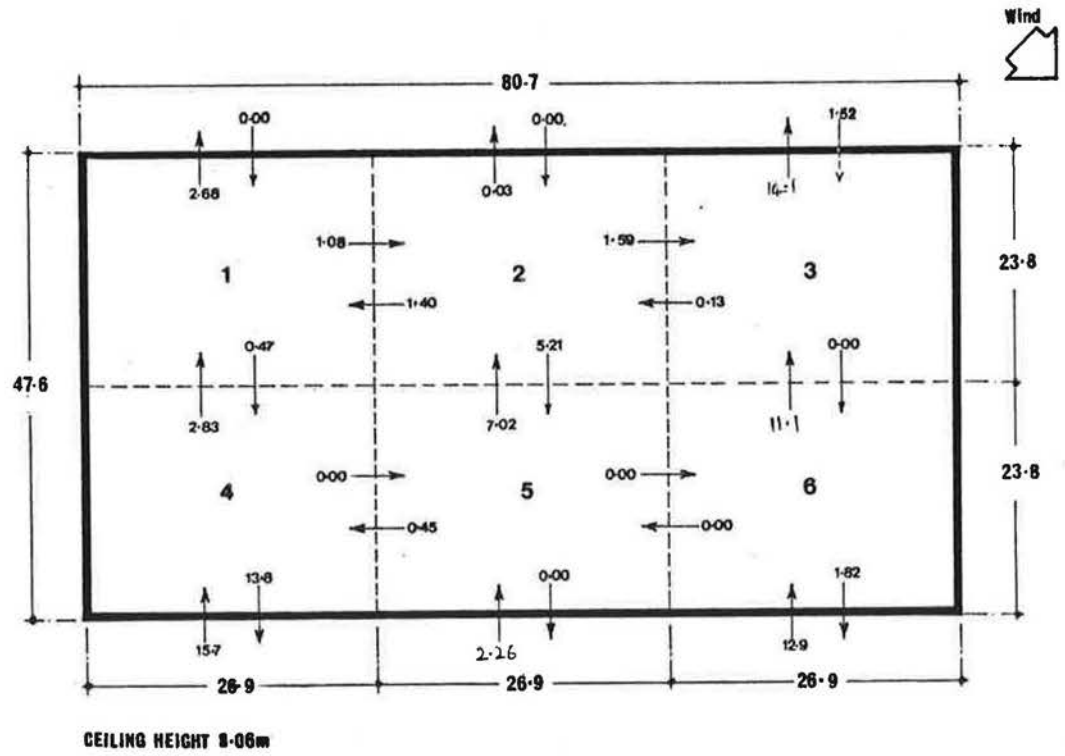

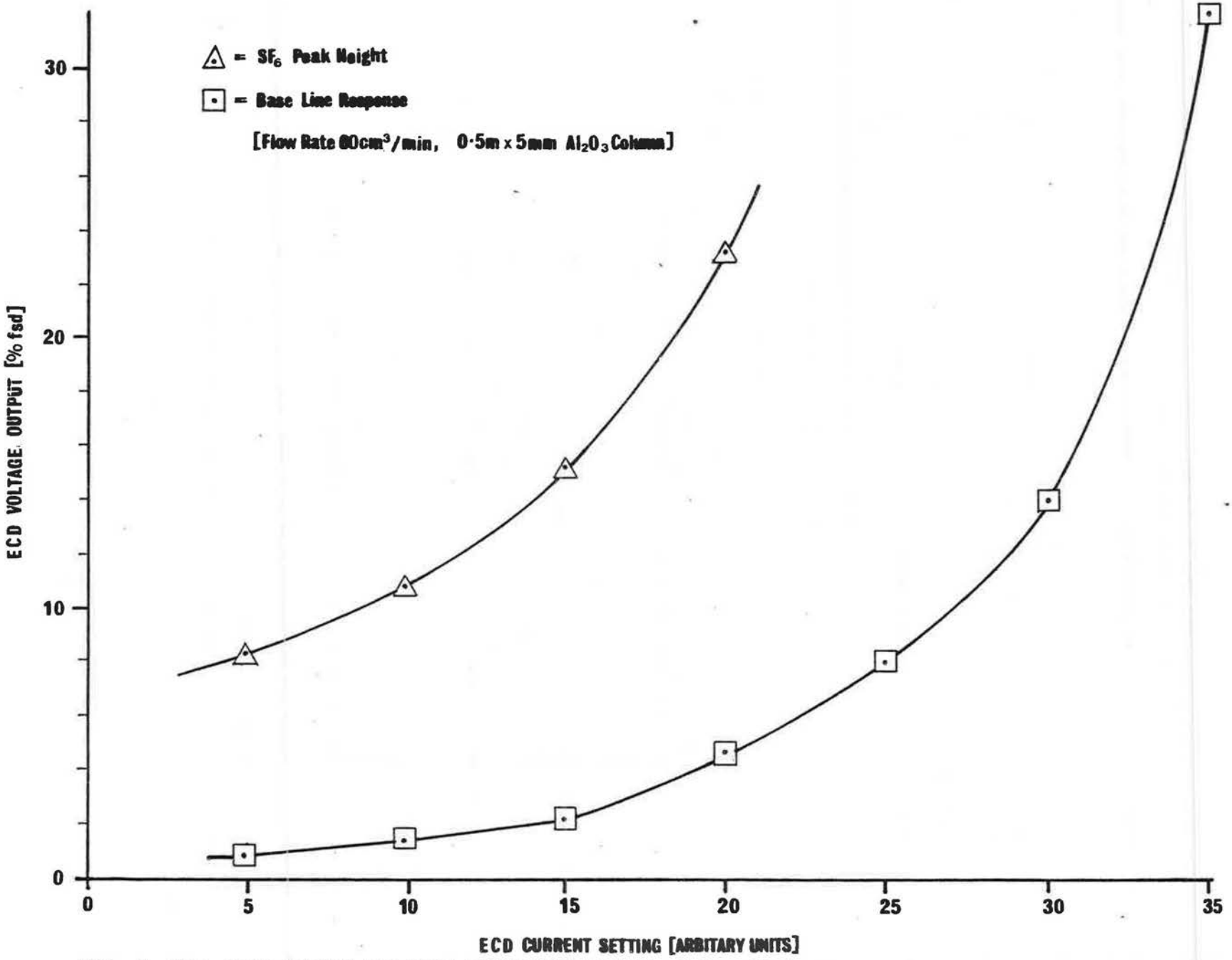

FIG 1 SF6 PEAK HEIGHT AND BASE LINE RESPONSE VERSUS E CURR

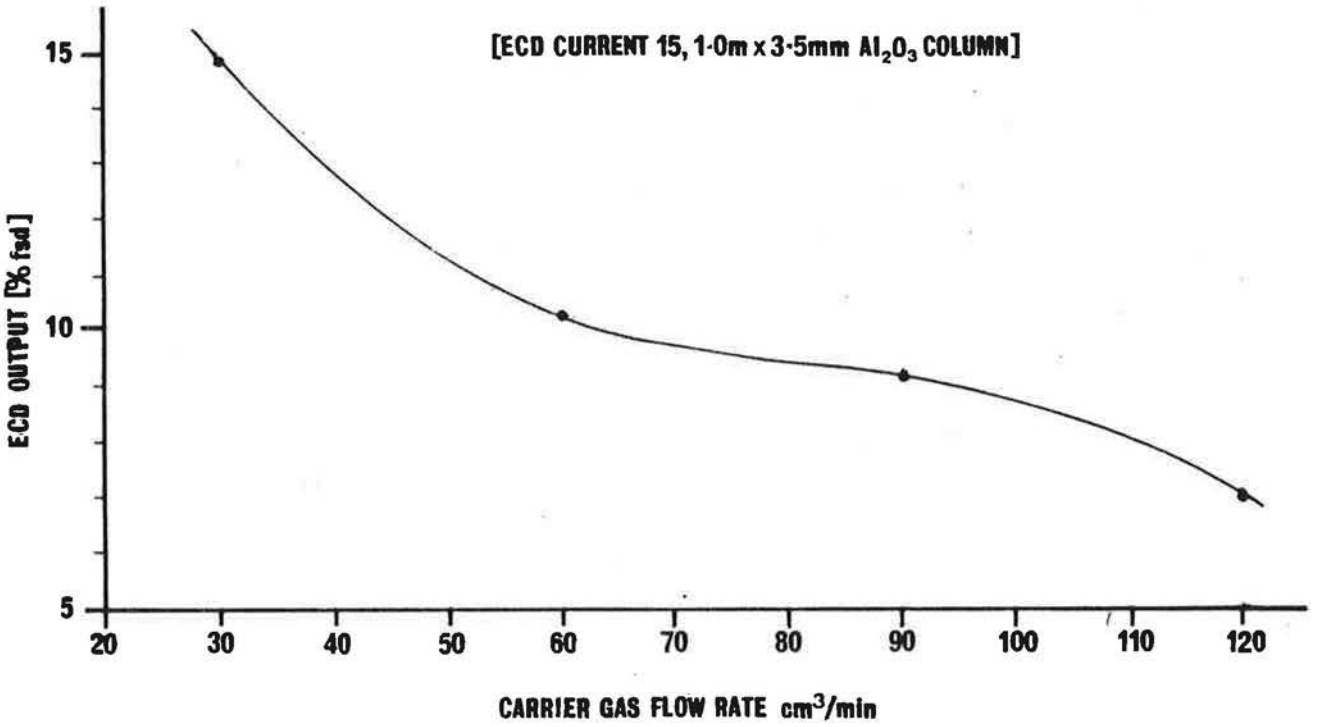

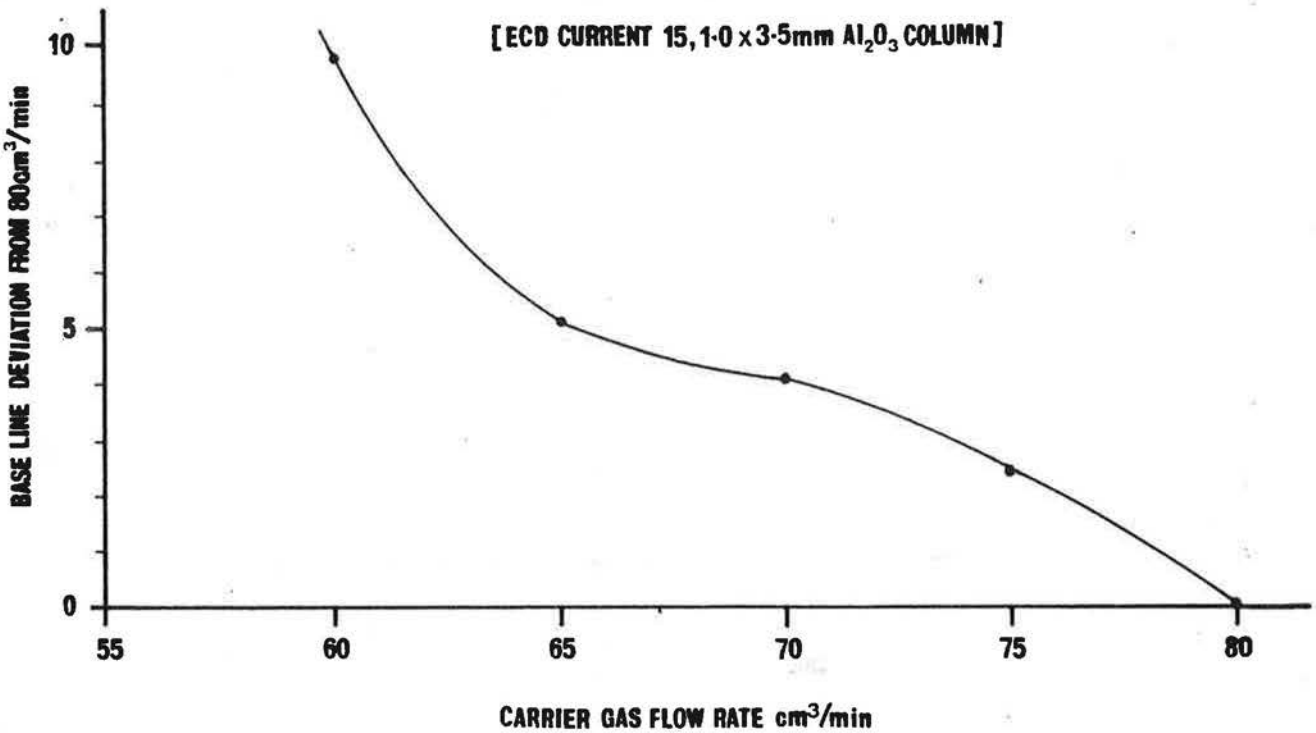

FIG.2 SF_6 PEAK HEIGHT AND BASE LINE RESPONSE VERSUS CARRIER GAS FLOW RATE

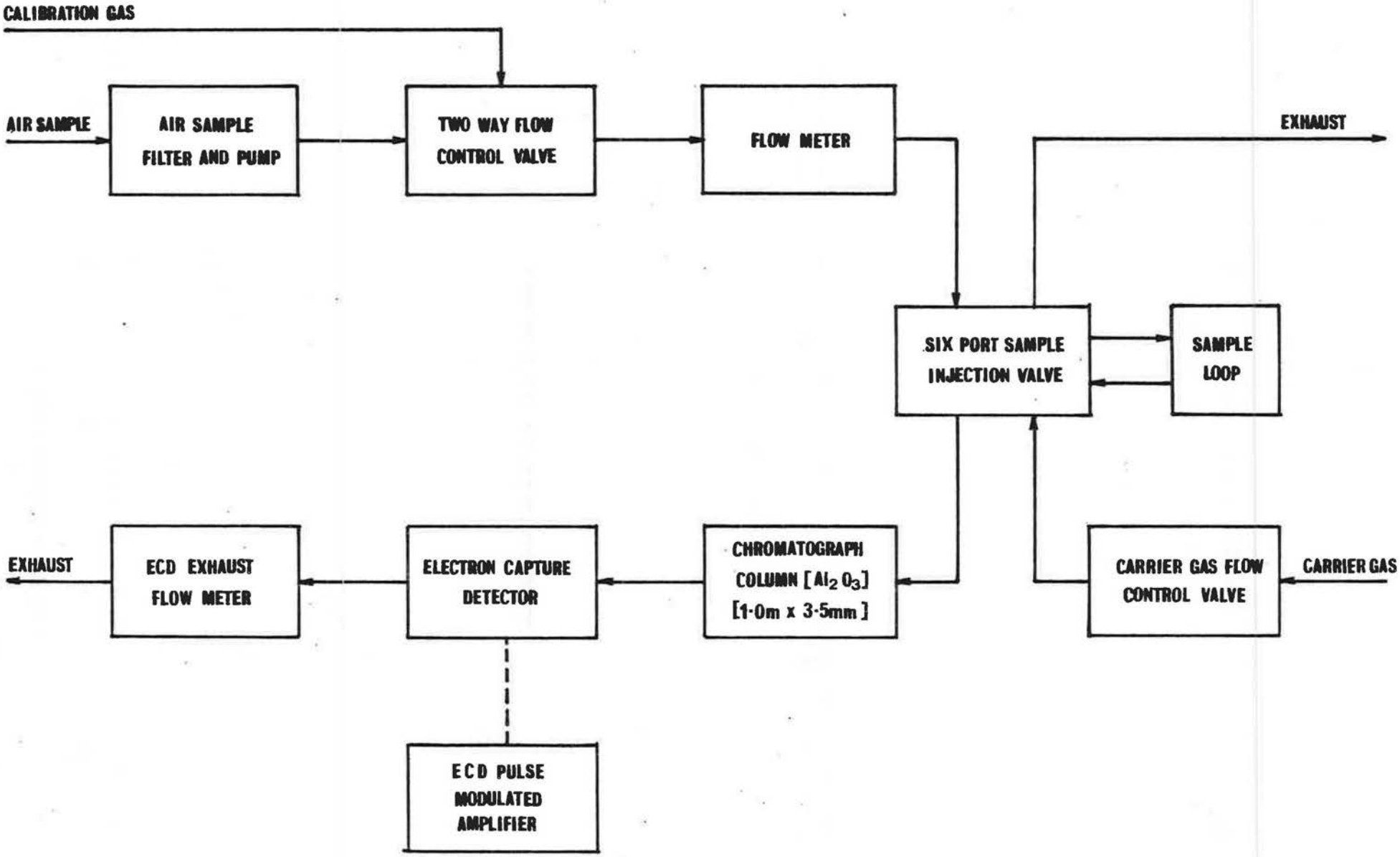

GAS ANALYSER UNIT : LAYOUT

FIG. 3 GAS ANALYSER UNIT BLOCK DIAGRAM

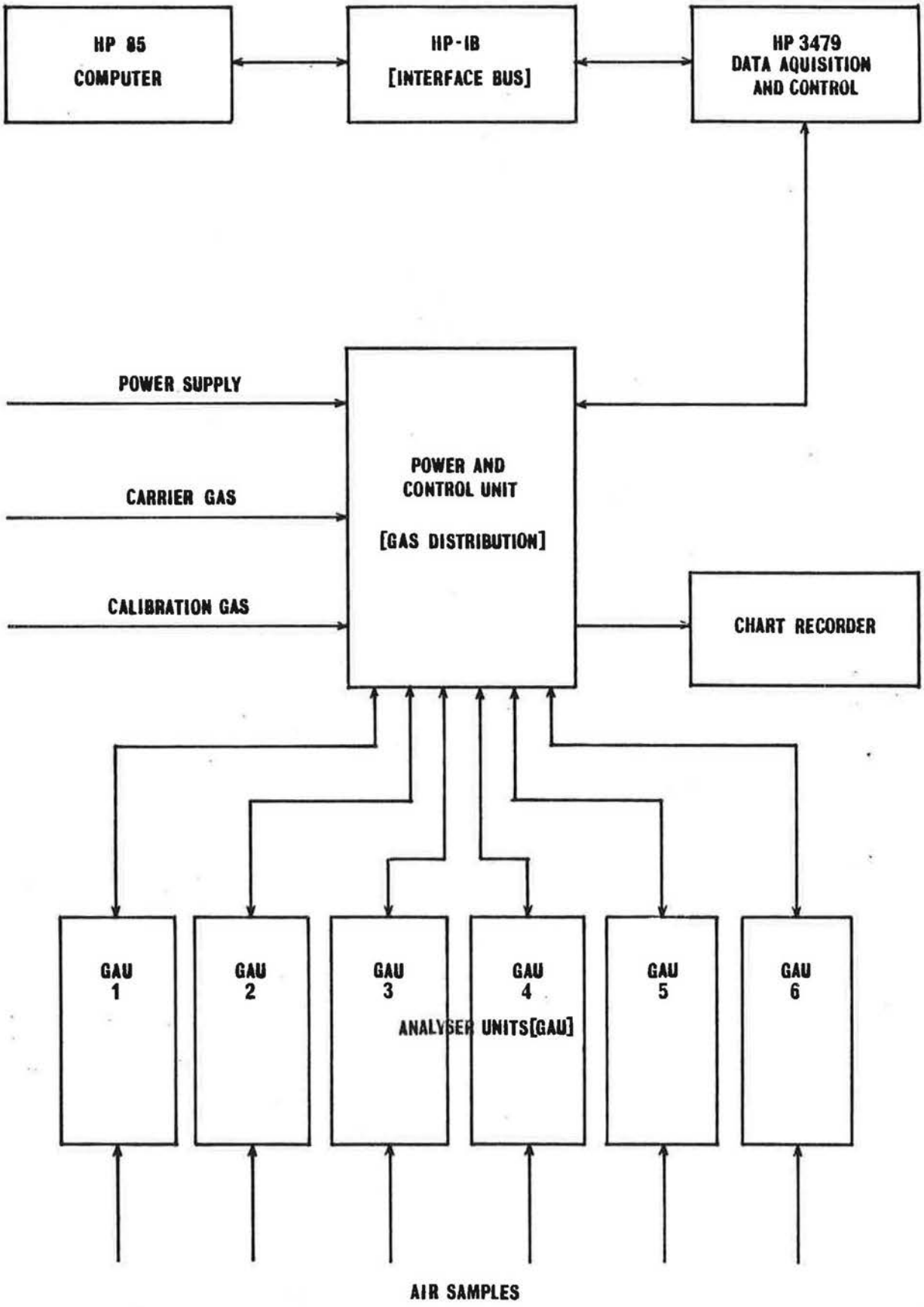

FIG 4 TRACER GAS MONITORING SYSTEM BLOCK DIAGRAM

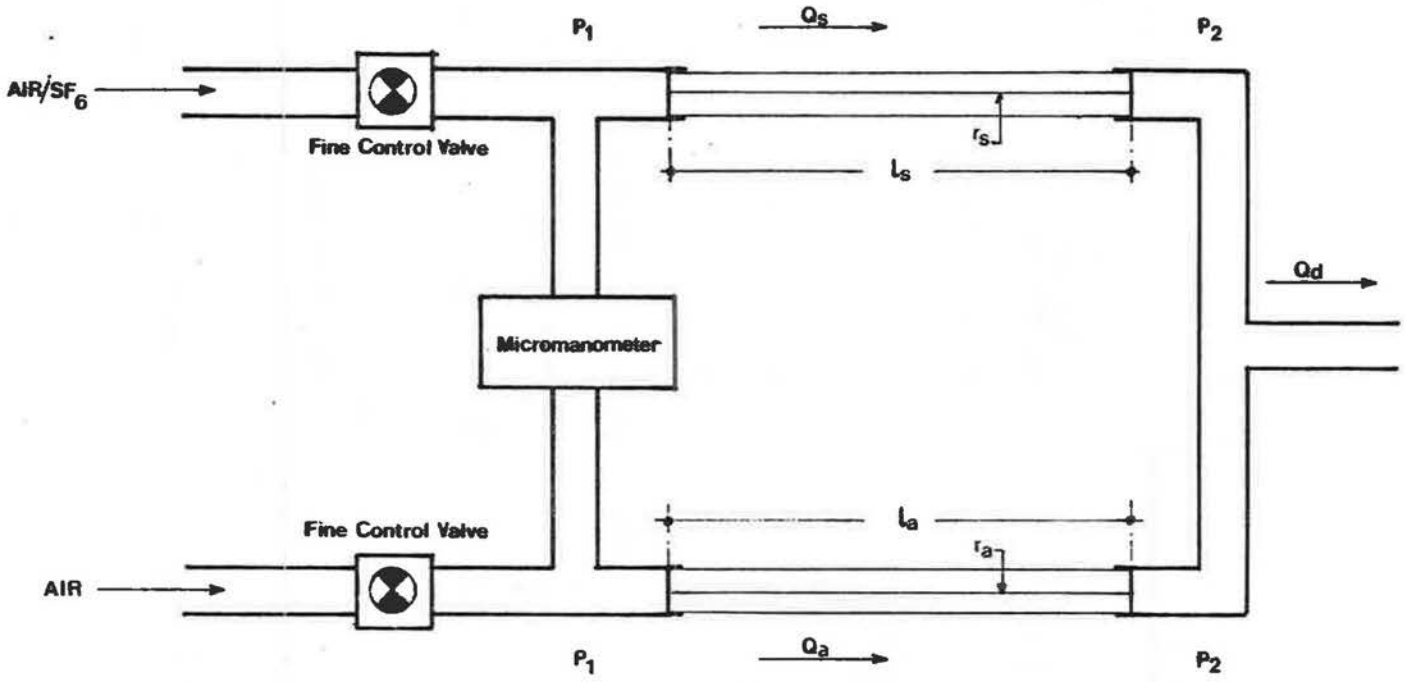

FIG 5 TRACER DILUTION AND CALIBRATION ARRANGEMENT

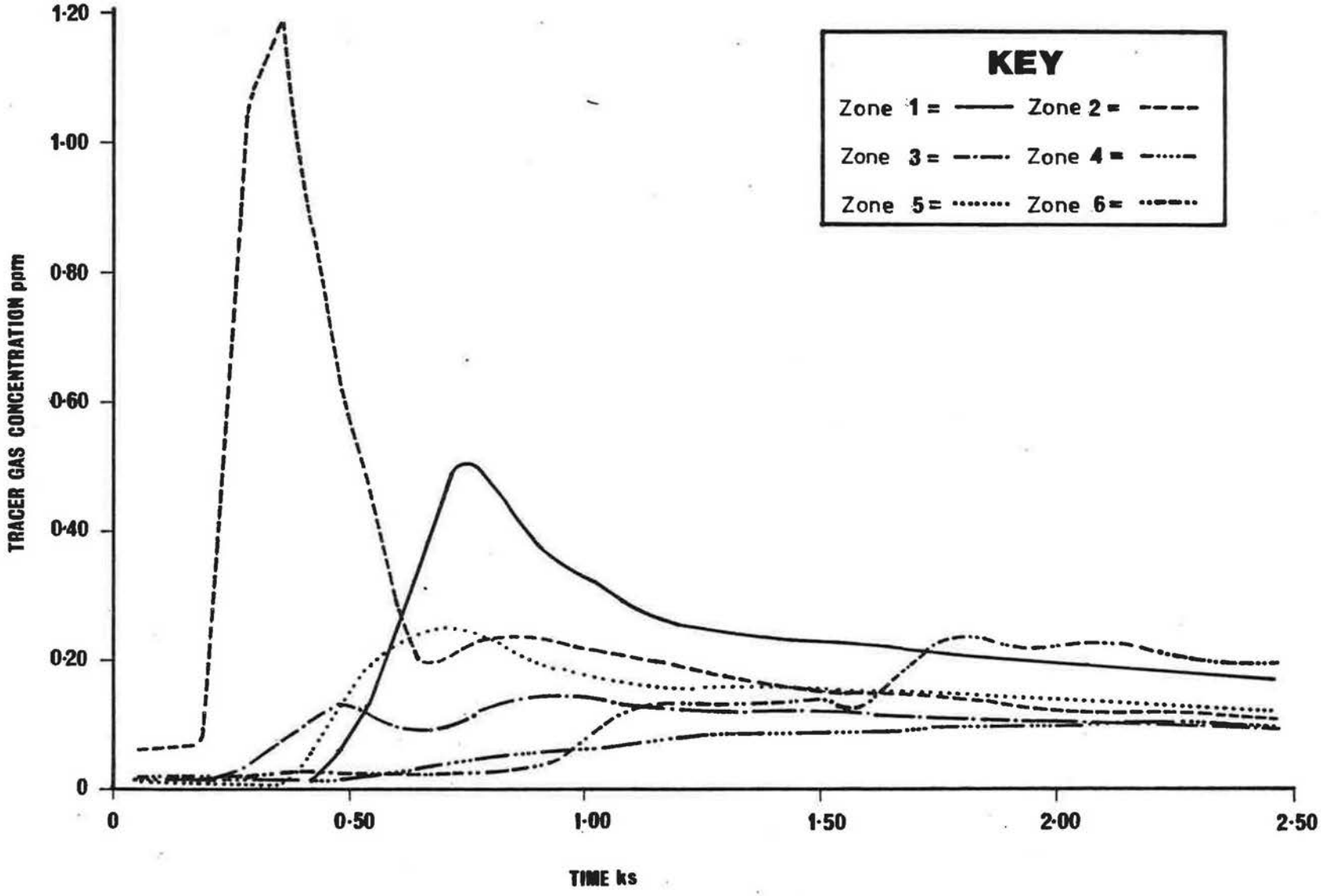

FIG 6 MEASURED TRACER DECAY CURVES SHOWING OSCILLATION DUE TO TIME LAGS.

THE EVALUATION OF CONTAMINANT CONCENTRATIONS AND AIR FLOWS IN A MULTIZONE MODEL OF A BUILDING

J.R. WATERS and M.W. SIMONS

Building and Environment

Building and Environment, Vol. 22, No. 4, pp. 305–315, 1987.
Printed in Great Britain.

0360–1323/87 $3.00 + 0.00

The Evaluation of Contaminant Concentrations and Air Flows in a Multizone Model of a Building

J. R. WATERS*
M. W. SIMONS*

Improvements to tracer decay techniques for measuring flow rates in multi-cell buildings are proposed on the basis of a study of the governing equations. A detailed examination of the forward solution, in which tracer gas concentrations are predicted from known flow rates, has been carried out. This has revealed properties of the decay curves, which, if recognised, can assist in the extraction of flow rates from measured tracer concentrations. Proposals are made for tracer gas seeding strategy, and for computational procedures.

NOMENCLATURE

a_i concentration coefficient to ith eigenvector
f_{ij} $F_{ij}V_j^{-1}$
F_{ij} volumetric flow rate from zone i to zone j ($m^3\ s^{-1}$)
n number of zones
r_i $S_iV_i^{-1}$
S_i sum of flows into zone i ($m^3\ s^{-1}$)
V_i volume of zone i (m^3)
$c(t)$ concentration in zone i

$$\underline{c}(t) = \begin{bmatrix} c_1(t) \\ c_2(t) \\ \vdots \\ c_n(t) \end{bmatrix}$$

$$\underline{x}_i = \begin{bmatrix} x_{i1} \\ x_{i2} \\ \vdots \\ x_{in} \end{bmatrix}$$ ith eigenvector

Greek symbol
λ_i ith eigenvalue

1. INTRODUCTION

IN AIR movement studies it is convenient to represent a building as an assembly of interconnected zones, each zone being capable of exchanging air with any other zone. Usually, one zone is taken to represent external air, so that air movement between inside and outside may be represented as well as air movement within the building. If the interzonal flow rates are known, the multizone model may be used to compute the time evolution of the spread of an airborne contaminant. This may be particularly useful in certain types of buildings such as factories and hospitals. On the other hand, if flow rates are not known, the model can be used to obtain them from appropriate measurements of contaminant concentrations.

The differential equations governing contaminant distribution in a multizone model are well known, and have been given by Sinden [1] and Sandberg [2], both of whom make general remarks concerning their solution. However, in the particular case of the evaluation of flow rates from contaminant concentrations, as in the tracer decay method, it is of great advantage to understand the properties of the solution in considerable detail. Such an understanding is of value in, (i) determining the best initial distribution for the tracer gas, i.e. the most advantageous seeding strategy; (ii) avoiding poorly defined results due to ill-conditioning or linear dependency in the solution; (iii) maximising the information that can be obtained from a set of experimental data.

Perera and Walker [3] have considered some of these points, but their discussion is mostly confined to a particular building, and cannot, therefore, be easily generalized. Indeed, as will be shown later, the more general approach adopted here leads to conclusions which differ in some respects. The purpose of this paper is to examine the theory of the multizone air movement model in order to improve strategies for the derivation of interzonal air flows from tracer decay measurements. This has been done by examining in some detail the forward solution from known interzonal flow rates in order to identify pertinent features of the decay curves. These features are then used to sugest how both seeding strategy and the analysis of decay curves may be carried out to best advantage. The theory and discussion are restricted to the case of a single tracer gas.

* Department of Civil Engineering and Building, Coventry (Lanchester) Polytechnic, Priory Street, Coventry CV1 5FB, U.K.

2. FUNDAMENTAL THEORY AND THE GENERATION OF DECAY CURVES FROM KNOWN FLOW RATES

The fundamental equations of a multi-zone air movement model have been stated by several authors, but are repeated here for completeness and consistency. Figure 1, due originally to ref. [1], and also given by ref. [2], illustrates the essentials of the model, in which a number of zones, $0, 1, \ldots, n$, are connected by one way passages through which air is flowing. The air in each zone is assumed to be fully mixed. Initially each zone contains a known concentration of tracer gas, and because we are restricting the problem to the tracer decay method, it is assumed that there is no generation of tracer gas in the system after time zero. Taking a volumetric balance on tracer gas in zone j, and balancing the total flow into and out of zone j gives

$$V_j \dot{c}_j(t) = \sum_{\substack{i=0 \\ i \neq j}}^{n} F_{ij} c_i(t) - c_j(t) S_j, \tag{1}$$

where S_j is the summation of the flows into or out of zone j, and is given by the conservation equation

$$S_j = \sum_{\substack{i=0 \\ i \neq j}}^{n} F_{ij} = \sum_{\substack{i=0 \\ i \neq j}}^{n} F_{ji}. \tag{2}$$

In matrix form, equation 1 becomes

$$V\underline{\dot{c}}(t) = F\underline{c}(t) \tag{3}$$

where

$$V = \begin{bmatrix} V_0 & 0 & \cdots & 0 \\ 0 & V_1 & \cdots & 0 \\ \vdots & \vdots & & \\ 0 & 0 & & V_n \end{bmatrix}$$

$$F = \begin{bmatrix} -S_0 & F_{10} & F_{20} & \cdots & F_{n0} \\ F_{01} & -S_1 & F_{21} & \cdots & F_{n1} \\ \vdots & & \ddots & & \\ F_{0n} & & & \ddots & -S_n \end{bmatrix}.$$

This is a system of of first order differential equations with the general solution

$$\underline{c}(t) = \sum_{k=0}^{n} a_k \underline{x}_k \, e^{\lambda_k t},$$

where $n+1$ values of λ_k and $\underline{x}_k$ are, respectively, the eigenvalues and eigenvectors of the equation

$$\lambda V\underline{x} = F\underline{x} \tag{4}$$

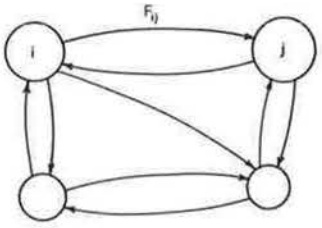

Fig. 1. The multizone air movement model of a building.

and the coefficients a_k are determined by the initial conditions. Sinden pointed out that (i) one eigenvalue, λ_0, is always zero, and that the corresponding eigenvector $\underline{x}_0$ is real and has equal components, (ii) all other eigenvalues and eigenvectors may be real or complex, (iii) complex values always occur in conjugate pairs, and (iv) all eigenvalues apart from λ_0 have negative real parts. Assigning infinite volume to zone 0 causes this zone to represent external air. The model then represents a building with n internal zones.

If tracer gas is not present in external air, the concentration in zone 0 is always zero. Hence $x_0(t)$ and the first row and first column of the vectors V and F may be deleted from Equation (2). The solution simplifies to

$$\underline{c}(t) = \sum_{k=1}^{n} a_k \underline{x}_k \, e^{\lambda_k t}. \tag{5}$$

The zero eigenvalue and its eigenvector no longer appear and the remaining λ_k and $\underline{x}_k$ are obtained from

$$\lambda V'\underline{x} = F'\underline{x}, \tag{6}$$

where

$$V' = \begin{bmatrix} V_1 & O & \cdots & 0 \\ 0 & V_2 & & \\ \vdots & & \ddots & V_n \end{bmatrix}$$

$$F' = \begin{bmatrix} -S_1 & F_{21} & \cdots & F_{n1} \\ F_{12} & -S_2 & & \\ \vdots & & \ddots & \\ F_{1n} & & & -S_n \end{bmatrix}.$$

Sinden's conditions (ii), (iii) and (iv) still apply. However, in the case of a two zone building ($n = 2$) only, Sinden showed that the two eigenvalues and their eigenvectors are always real. This indicates that for the two zone case, oscillatory solutions are impossible, whereas for all other cases ($n \geq 3$), oscillatory solutions exist for appropriate combinations of flow rates.

Solution of Equation (6) requires computation of the eigenvalues and eigenvectors of $E' = V'^{-1} F'$, which for $n > 3$ generally requires the use of numerical computation procedures. Such methods are certain to fail if E' has repeated eigenvalues and linearly dependent eigenvectors. That repeated eigenvalues can occur in quite normal situations can be demonstrated by some simple examples.

Example 1. *Repeated eigenvalues, 2 zone building*

For the general 2 zone building shown in Fig. 2, the eigenvalues can easily be shown to satisfy

$$\lambda = -\frac{1}{2}\left(\frac{S_1}{V_1} + \frac{S_2}{V_2}\right) \pm \frac{1}{2}\left[\left(\frac{S_1}{V_1} + \frac{S_2}{V_2}\right)^2 - 4\left(\frac{S_1 S_2}{V_1 V_2} - \frac{F_{12} F_{21}}{V_1 V_2}\right)\right]^{1/2} \tag{7}$$

from which it can be seen that repeated eigenvalues occur when

$$\left(\frac{S_1}{V_1} + \frac{S_2}{V_2}\right)^2 - 4\left(\frac{S_1 S_2}{V_1 V_2} - \frac{F_{12} F_{21}}{V_1 V_2}\right) = 0.$$

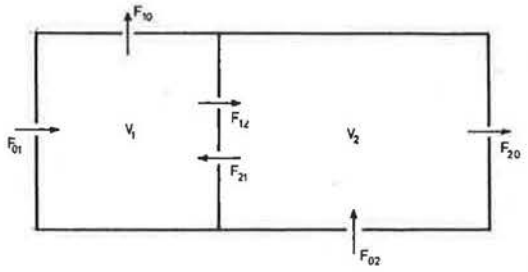

Fig. 2. The general 2 zone building.

Writing

$$r_1 = \frac{S_1}{V_1}, \quad r_2 = \frac{S_2}{V_2}, \quad f_{12} = \frac{F_{12}}{V_2}, \quad f_{21} = \frac{F_{21}}{V_1},$$

this becomes

$$(r_1 - r_2)^2 + 4 f_{12} f_{21} = 0.$$

Since all quantities are real non-negative numbers, this requires

$$(r_1 = r_2) \quad \text{and} \quad (f_{12} = 0 \quad \text{or} \quad f_{21} = 0).$$

The most obvious case which satisfies these conditions occurs when $V_1 = V_2$ and $F_{10} = F_{02} = F_{21} = 0$, which corresponds to a simple uni-directional flow of air through the building. The solution for $c_1(t)$ and $c_2(t)$ can be found directly as:

$$\left.\begin{aligned} c_1(t) &= a_1 e^{\lambda t} \\ c_2(t) &= (a_1 t + a_2) e^{\lambda t} \end{aligned}\right\} \tag{8}$$

where

$$\lambda = -\frac{S_1}{V_1} = -\frac{S_2}{V_2}.$$

More generally, if $V_1 \neq V_2$ and only $F_{21} = 0$, then the condition $r_1 = r_2$ will be met if

$$F_{12} = \frac{V_1}{V_2} F_{20} - F_{10}$$

and the solution for $c_1(t)$ and $c_2(t)$ becomes

$$\left.\begin{aligned} c_1(t) &= a_1 e^{\lambda t} \\ c_2(t) &= (a_1 f_{12} t + a_2) e^{\lambda t} \end{aligned}\right\} \tag{9}$$

Example 2. *Repeated eigenvalues, 3 zone building*

The eigenvalues will be the roots of a cubic equation

$$\lambda^3 + a\lambda^2 + b\lambda + c = 0.$$

Again writing

$$r_i = \frac{S_i}{V_i} \quad \text{and} \quad f_{ij} = \frac{F_{ij}}{V_j},$$

it is a simple matter to show that

$$a = r_1 + r_2 + r_3$$

$$b = r_1 r_2 + r_2 r_3 + r_3 r_1 - f_{12} f_{21} - f_{23} f_{32} - f_{13} f_{31}$$

$$c = r_1 r_2 r_3 - r_1 f_{23} f_{32} - r_2 f_{13} f_{31} - r_3 f_{12} f_{21} - f_{12} f_{23} f_{31} - f_{13} f_{32} f_{21}$$

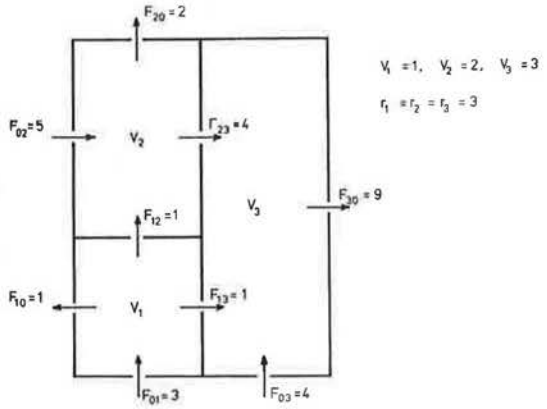

Fig. 3. A 3 zone building with repeated eigenvalues.

From elementary algebra, the cubic may be re-written as

$$x^3 + px + q = 0,$$

where

$$p = b - \frac{a^2}{3}, \quad q = c - \frac{ab}{3} + \frac{2a^3}{27} \quad \text{and} \quad \lambda = x - \frac{a}{3}.$$

The condition for repeated roots is that the discriminant is zero, i.e.

$$4p^3 + 27q^2 = 0.$$

Now, by substitution for a and b, p may be shown to be

$$p = -[f_{12} f_{21} + f_{23} f_{32} + f_{13} f_{31} + \tfrac{1}{6}\{(r_1 - r_2)^2 + (r_2 - r_3)^2 + (r_3 - r_1)^2\}].$$

Since all r_i and f_{ij} must be real and non negative, then $p \leqslant 0$, and real solutions to the discriminant exist. Thus combinations of r_i and f_{ij} exist which give repeated roots. In the particular case when all three roots are equal (and therefore real), then if this root is m, it may be shown that

$$b = \frac{a^2}{3}, \quad c = \frac{a^3}{27}, \quad p = q = 0, \quad \text{and} \quad m = -\frac{a}{3}.$$

Clearly $p = 0$ when $r_1 = r_2 = r_3$ and $f_{21} = f_{32} = f_{31} = 0$, and a typical building configuration where this might occur, with suggested values, is shown in Fig. 3. In this particular example the solution is

$$c_1(t) = \alpha e^{-3t}$$

$$c_2(t) = \beta e^{-3t} + \frac{\alpha}{2} t e^{-3t}$$

$$c_3(t) = \gamma e^{-3t} + \left(\frac{\alpha}{4} + \frac{4\beta}{3}\right) t e^{-3t} + \frac{\alpha}{3} t^2 e^{-3t}$$

where α, β, γ are determined by the initial conditions.

In general, the existence of repeated eigenvalues may be found by examining the Jordan canonical form of the matrix E'. Clearly the condition

$$r_1 = r_2 = \ldots = r_n \quad \text{with some} \quad f_{ij} = 0$$

is of particular significance, but whether or not this is a necessary condition has not been explored here. The

possibility exists, therefore, that in general repeated eigenvalues will occur for a variety of conditions on r_i and f_{ij}. The physical significance of a repeated eigenvalue in the 2 and 3 zone examples given above is that one zone in the system does not receive a flow from any other zone (except zone 0 which is the outside), indicating that contaminant concentrations in this zone are unaffected by contaminant concentrations elsewhere in the building. It is possible that a repeated eigenvalue has the same physical significance in buildings of 4 or more zones.

3. PRINCIPAL PROPERTIES OF THE DECAY CURVES

The solution to the tracer decay problem, Equation (5), is in practice obtained in two stages. First, from the known interzone flow rates F_{ij} the eigenvalues and their associated eigenvectors are found. It is convenient to label the largest eigenvalue and its associated eigenvector λ_1 and $\underline{x}_1$ respectively. It should be noted that the eigenvalues and eigenvectors are completely determined by the set of F_{ij}. If one F_{ij} is altered, all λ_k and $\underline{x}_k$ are also altered. Secondly from the known initial contaminant concentrations, the coefficients a_k are calculated, each one being associated with one eigenvalue. Again, the a_k are determined by the set of initial conditions. Changing the initial conditions in any one zone will change all the a_k, but not the λ_k or $\underline{x}_k$.

The solution has a number of properties which, if recognised, can aid the interpretation of measured decay curves. The following points are of particular value.

(i) Whatever the initial conditions, a time will be approached when the largest eigenvalue dominates, after which all zones will decay at essentially the same rate, and the concentrations in the zones will be in the same ratio as the components of $\underline{x}_1$. Since by definition the contaminant concentrations in all zones are real positive numbers, it follows that λ_1 is a real negative number, and that a_1 and all components of $\underline{x}_1$ are real positive. The remaining eigenvalues, eigenvectors and coefficients may be real or complex. However, complex values always occur in conjugate pairs [Sinden's rule (iii)], and so if there are an even number of zones, there must always be at least one more real λ_k, $\underline{x}_k$ and a_k.

(ii) The time taken to reach the point at which the largest eigenvalue dominates, and a uniform decay is established in all zones depends on the initial distribution and the magnitude of the flow rates. If the initial distribution is such that the concentrations in the zones are in the same ratio as the corresponding components of $\underline{x}_1$, then uniform decay is established instantaneously, which implies that $a_1 = 1$ and $a_2 = a_3 = \ldots\ a_n = 0$. If the initial distribution is such that only the zone assoicated with the smallest component of the dominant eigenvector is contaminated, the time to reach uniform decay rate is maximised.

(iii) Starting from a non-uniform initial distribution, especially where only one zone is contaminated, it is likely that the other zones will show an increase in contaminant concentration in the early part of the process. However, conservation considerations require that the zone with the highest concentration at any given time must be decaying. Thus the concentration in any zone where it is rising must reach a peak not later than the time at which it equals the concentration in the zone which until then had shown the highest value. In particular, if the concentration versus time curves for any two zones in a system is such that the decaying concentration in one of them (say zone 1) intersects the rising concentration in the other (say zone 2) when the concentration in 2 is at its peak, then immediately it may be possible to infer that the only non-zero flow into 2 is from 1. This occurs frequently in practical situations, and it may be proved by writing the flow equation for zone 2 (from equation 1) in the form

$$c_2(t) = \frac{\Sigma F_{i2} c_i(t) - V_2 \dot{c}_2(t)}{S_2},$$

or more simply, since at the point in question, $\dot{c}_2(t) = 0$,

$$c_2(t) = f_{02}c_0(t) + f_{12}c_1(t) + f_{22}c_2(t) + \ldots f_{n2}c_n(t)$$

The coefficients f_{ij} must be such that

$$f_{i2} = \frac{F_{i2}}{S_2}, \quad \sum_{i=0}^{n} f_{i2} = 1, \quad 0 \leqslant f_{i2} \leqslant 1 \quad \text{and } f_{22} \equiv 0.$$

Now if at the point of intersection $c_1(t) > c_i(t)$ for all other i (except $i = 2$), the equality $c_2(t) = c_1(t)$ can only be satisfied if all f_{i2} are zero except f_{12}, which proves that F_{12} is the only non-zero flow *into* zone 2. The condition that $c_1(t)$ is greater than all other $c_i(t)$ may be relaxed for those $c_i(t)$ where it is already known from other considerations (e.g. building geometry) that the corresponding f_{i2} is zero. Thus, if $c_1(t) = c_2(t)$ when $\dot{c}_2(t) = 0$, it follows that F_{12} is the only flow into zone 2 if $c_1(t)$ is the maximum in the subset of zones which have a possible connection to zone 2.

(iv) It is not possible to associate any eigenvalue with an individual zone, neither is it possible to associate any flow rate with an eigenvalue. This is an obvious consequence of the fact than an alteration in only one of the F_{ij} will alter all the λ_k. In particular, the dominant eigenvalue which governs the later stages of decay does not relate to the overall fresh air infiltration rate of the whole building. However when internal interzonal flow rates become very large relative to the infiltration flow rates, the building will approximate to a fully mixed single zone, and in these circumstances λ_1 may become a good measure of the overall infiltration rate.

4. AN ILLUSTRATIVE EXAMPLE

The properties discussed in Section 3 can be illustrated by a hypothetical but nevertheless realistic example. Consider a four zone building, as shown in Fig. 4, in which the significant infiltration openings are

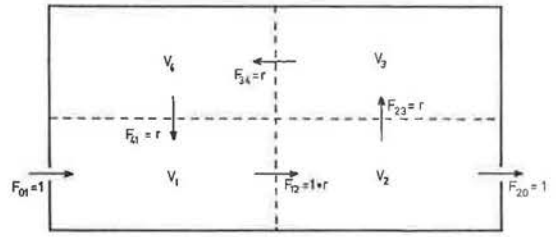

Fig. 4. A 4 zone building example.

concentrated in zones 1 and 2. Wind pressure will create a flow into zone 1, a flow from zone 1 to zone 2, and an outflow from zone 2. Superimposed on this there may be a circulation through zones 3 and 4, generated perhaps by entrainment or by internal stirring mechanisms. This example is a simplified model of a common natural ventilation situation; Fig. 4 may be visualized as a plan view, in which zones 3 and 4 are rooms with no direct link to the outside, or, as in an industrial building, the figure could represent a vertical section, in which zones 3 and 4 are the roof space.

Taking the total volume of the building as 3600 m^3, then with $F_{01} = F_{20} = 1\ m^3\ s^{-1}$, the fresh air infiltration rate is 3600 $m^3\ h^{-1}$ or 1 air change per hour. For values of the circulation flow rate, r greater than zero, zonal concentrations may be calculated from Equation (5), using values of λ_k and $\underline{x}_k$ found from Equation (6). This has been done for $r = 0.25$, $r = 1$ and $r = 4\ m^3\ s^{-1}$, giving a range of values from well below to well above the infiltration flow rate. The resulting eigenvalues and their eigenvectors are shown in Table 1. When $r = 0$, zones 3 and 4 are isolated from zones 1 and 2, and become stagnant areas, leaving a uni-directional flow through zones 1 and 2, exactly as in example 1 in Section 2. In this case $c_3(t) = c_4(t) = 0$, and the solutions for $c_1(t)$ and $c_2(t)$ are given by Equations 8, with

$$\lambda = -\frac{S_1}{V_1} = -\frac{S_2}{V_2} = -\frac{1}{900}.$$

The coefficients a_k have also been computed for a range of cases, illustrating the effect of different initial conditions. The values of a_k are shown in Table 2, in which the notation 1, 0, 0, 0 indicates that initially zone 1 was seeded with contaminant, whereas zones 2, 3 and 4 were contaminant free. The time evolution of the contaminant concentrations have also been calculated for these cases, and the results are plotted in Figs 5–11. Inspection of Tables 1 and 2 show, as explained in paragraph 3 (i), that λ_1 is always real negative, and that a_1 and all components of $\underline{x}_1$ are real positive. Where complex values arise, they are in conjugate pairs, and because there are an even number of zones, there are always in total at least two real sets of λ_k, $\underline{x}_k$ and a_k.

The effect of initial distribution on the time taken to reach a uniform decay is shown in Figs 5–9. The components of the dominant eigenvector are, from Table 1, in the order $x_{11} < x_{12} < x_{13} < x_{14}$. Therefore, from 3 (ii), the time to reach uniform decay from the seeding of a single zone should be greatest if zone 1 is seeded, becoming less in order as zone 2 or 3 or 4 is the zone seeded. When all zones are equally seeded the time to uniformity should be least. Inspection of the graphs tends to confirm this; the time at which all four zone concentrations settle into their final relative order [i.e. $c_4(t) > c_3(t) > c_2(t) > c_1(t)$] is a useful indication. However, a better criterion is to compare the ratios of the concentrations at a suitable point in time (say 2 time constants) with the components of $\underline{x}_1$. The closer these ratios are to $\underline{x}_1$, the closer is the decay process to uniformity. The comparison is shown in Table 3, which confirms the expectation. In practice, it can be seen that if, initially, all zones are uniformly contaminated, the time taken to reach uniform decay will always be short, whereas if, initially, any one zone only is contaminated, the time to uniform decay will be long. The effect of flow rate on the speed with which uniformity is established is shown in Figs 10 and 11, which show the effect of increasing r to 1 and then 4 for the 1, 0, 0, 0 case.

The effect described in 3 (iii) is most clearly shown in Figs 5, 10 and 11, in which seeding is in zone 1. In each

Table 1. Eigenvalues and eigenvectors for 4 zone building

	$i=1$		$i=2$		$i=3$		$i=4$	
				Case 1, $r=4$				
λ_i	-2.68×10^{-4}	0	-5.00×10^{-3}	4.67×10^{-3}	-5.00×10^{-3}	-4.67×10^{-3}	-9.73×10^{-3}	0
x_{i1}	0.840	0	0.1	0.839	0.1	−0.839	−0.752	0
x_{i2}	0.882	0	1	0	1	0	1	0
x_{i3}	0.939	0	−0.111	−0.939	−0.111	0.939	−0.840	0
x_{i4}	1	0	−0.869	0.210	−0.869	−0.210	0.705	0
				Case 2, $r=1$				
λ_i	-2.33×10^{-4}	0	-1.67×10^{-3}	1.20×10^{-3}	-1.67×10^{-3}	-1.20×10^{-3}	-3.10×10^{-3}	0
x_{i1}	0.558	0	0.250	0.539	0.250	−0.539	−0.395	0
x_{i2}	0.623	0	1	0	1	0	1	0
x_{i3}	0.790	0	−0.354	−0.763	−0.354	0.763	−0.558	0
x_{i4}	1	0	−0.458	0.539	−0.458	−0.539	0.311	0
				Case 3, $r=0.25$				
λ_i	-1.40×10^{-4}	0	-4.64×10^{-4}	0	-1.20×10^{-3}	0	-1.53×10^{-3}	0
x_{i1}	0.223	0	0.300	0	0.134	0	−0.0995	0
x_{i2}	0.247	0	0.452	0	1	0	1	0
x_{i3}	0.498	0	−0.672	0	−0.300	0	−0.223	0
x_{i4}	1	0	1	0	0.0903	0	0.0495	0

Table 2. Coefficients for 4 zone building

	Initial distribution zone				Real and imaginary components of coefficients							
r	1	2	3	4	a_1		a_2		a_3		a_4	
0.25	1	0	0	0	2.24	0	−4.21	0	4.66	0	−4.53	0
0.25	0	1	0	0	0.202	0	−0.280	0	0.662	0	0.450	0
0.25	0	0	1	0	0.909	0	−0.931	0	0.421	0	−0.224	0
0.25	0	0	0	1	0.450	0	0.627	0	−1.40	0	1.01	0
0.25	1	1	1	1	1.785	0	−1.01	0	4.30	0	−3.39	0
1	1	0	0	0	0.274	0	0.354	−0.299	0.354	0.299	−0.879	0
4	1	0	0	0	0.263	0	0.070	−0.289	0.070	0.289	−0.372	0

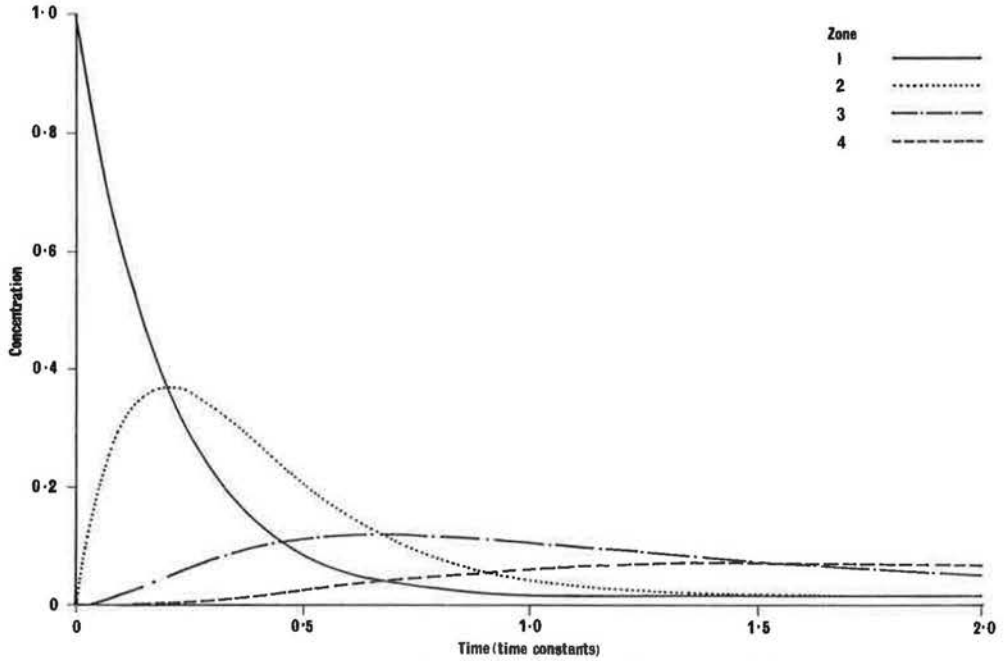

Fig. 5. Tracer decay, 4 zone building, $r = 0.25$, zone 1 seeded.

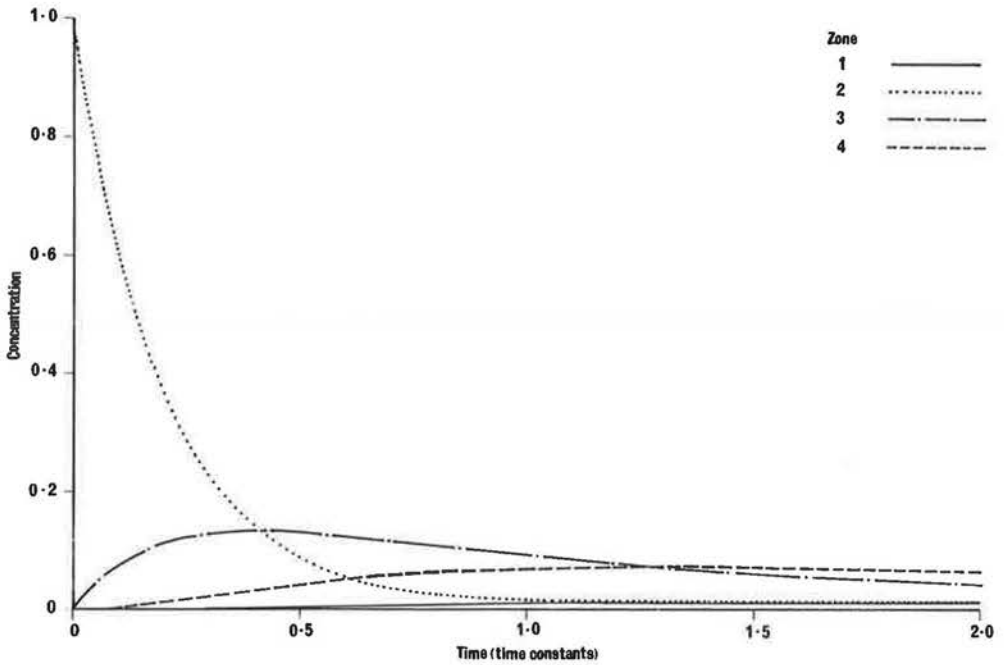

Fig. 6. Tracer decay, 4 zone building, $r = 0.25$, zone 2 seeded.

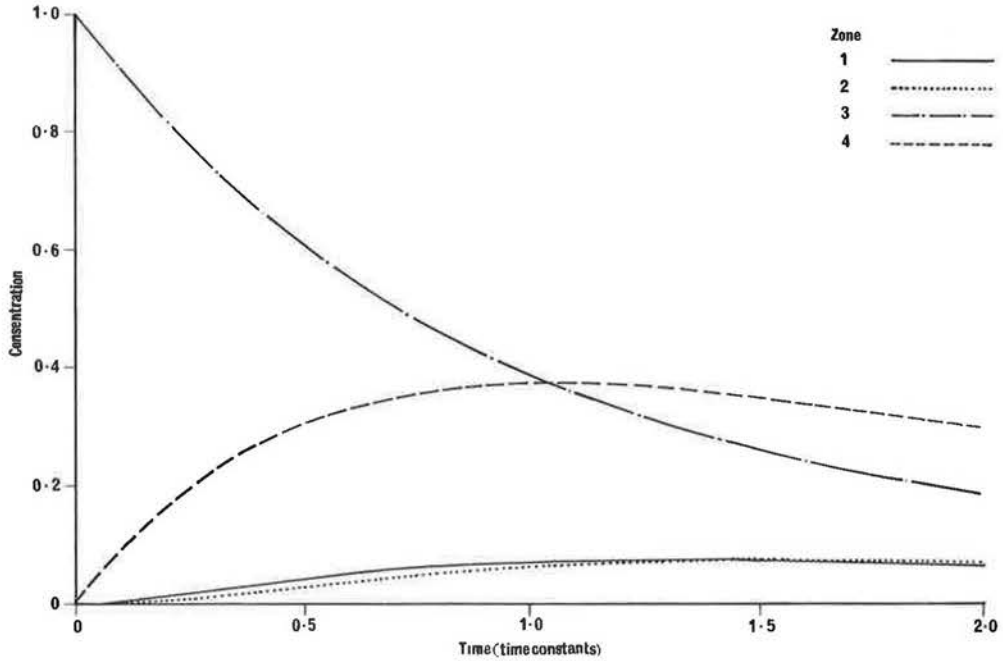

Fig. 7. Tracer decay, 4 zone building, $r = 0.25$, zone 3 seeded.

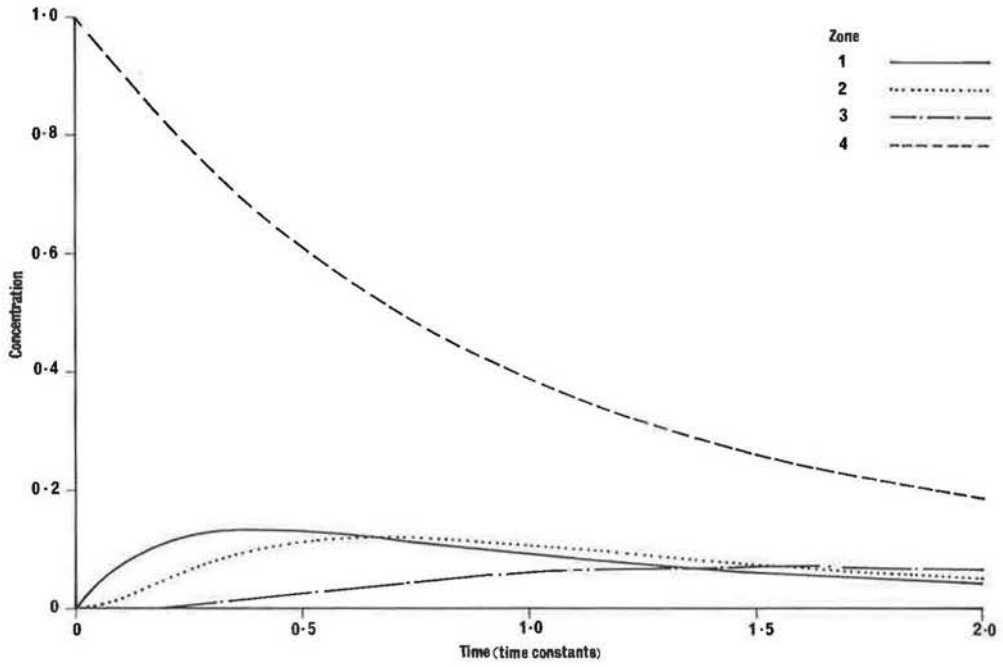

Fig. 8. Tracer decay, 4 zone building, $r = 0.25$, zone 4 seeded.

Table 3. Difference between concentration ratios and components of the dominant eigenvector at 2 time constants

		Seeded zone							
		1		2		3		4	
Zone i	x_{1i}	c_i	$\lvert c_i - x_{1i}\rvert$	c_i	$\lvert c_i - x_{1i}\rvert$	c_i	$\lvert c_i - x_{1i}\rvert$	c_i	$\lvert c_i - x_{1i}\rvert$
1	0.223	0.207	0.016	0.210	0.013	0.214	0.009	0.231	0.008
2	0.247	0.213	0.034	0.218	0.029	0.225	0.022	0.270	0.023
3	0.498	0.753	0.255	0.677	0.179	0.626	0.128	0.359	0.139
4	1	1	0	1	0	1	0	1	0
$\Sigma\lvert c_i - x_{1i}\rvert$			0.305		0.221		0.159		0.170

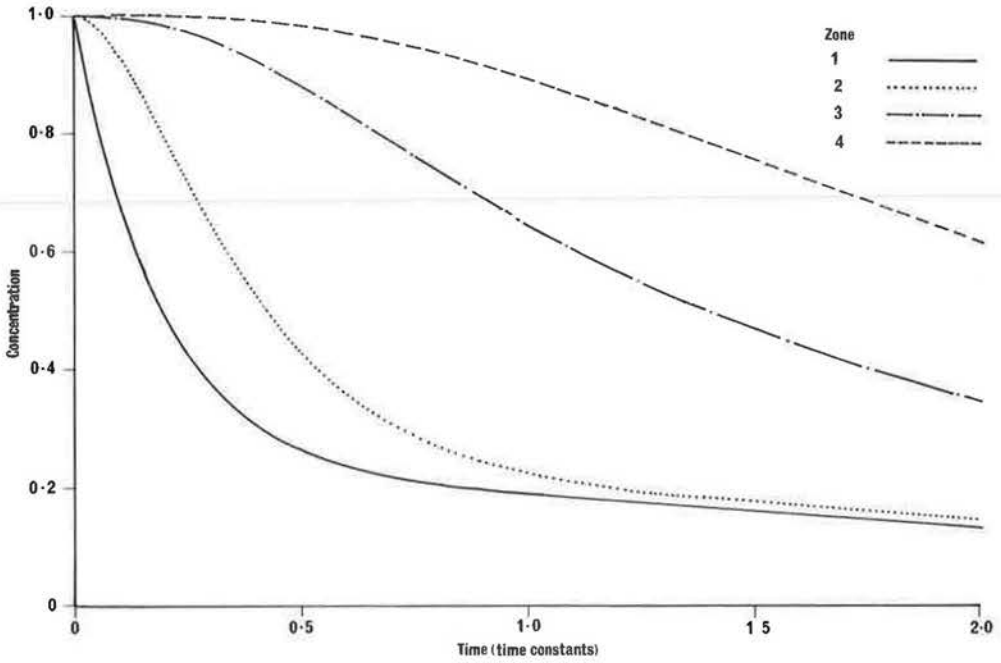

Fig. 9. Tracer decay, 4 zone building, $r = 0.25$, all zones uniformly seeded.

of these, the decaying concentration in zone 1 intersects the concentration in zone 2 when the latter is at its peak, indicating that all F_{i2} are zero except for F_{12}. Similarly, zone 2 intersects zone 3, and then zone 3 intersects zone 4, indicating that all F_{i3} and F_{i4} are zero except for F_{23} and F_{34}. Note also that seeding other zones gives less information. In Fig. 8, the intersection of $c_1(t)$ with $c_2(t)$ occurs when $\dot{c}_2(t)$ is zero, but it is necessary to assume that the diagonal flow F_{42} is zero in order to infer that F_{12} is the only flow into zone 2. Also in Fig. 8, because geometry does not preclude that $F_{43} = 0$, the fact that $c_2(t)$ intersects $c_3(t)$ when $\dot{c}_3(t)$ is zero does not necessarily require F_{23} to be the only flow into zone 3.

The relationship between the dominant eigenvalue, λ_1, and fresh air infiltration rate, as discussed in paragraph 3 (iv), can be found by multiplying λ_1 by 3600 to obtain air changes per hour. Table 4 shows how λ_1, expressed in units of h^{-1}, varies with r. Even with $r = 4$, the infiltration measured from the long term slope of the decay curves would be 4% below the true value of 1 air change

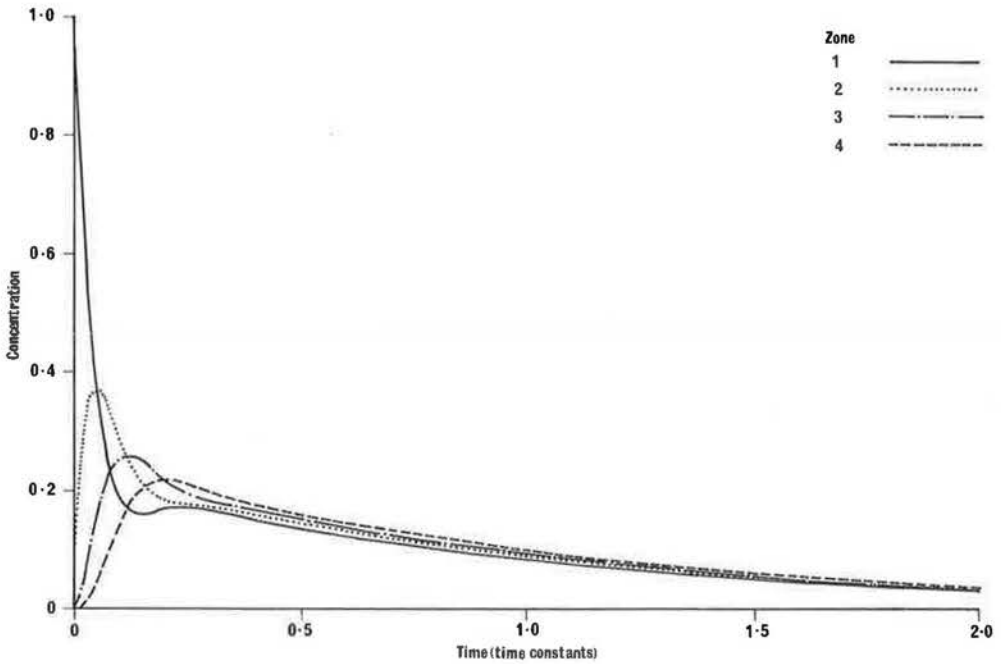

Fig. 10. Tracer decay, 4 zone building, $r = 1$, zone 1 seeded.

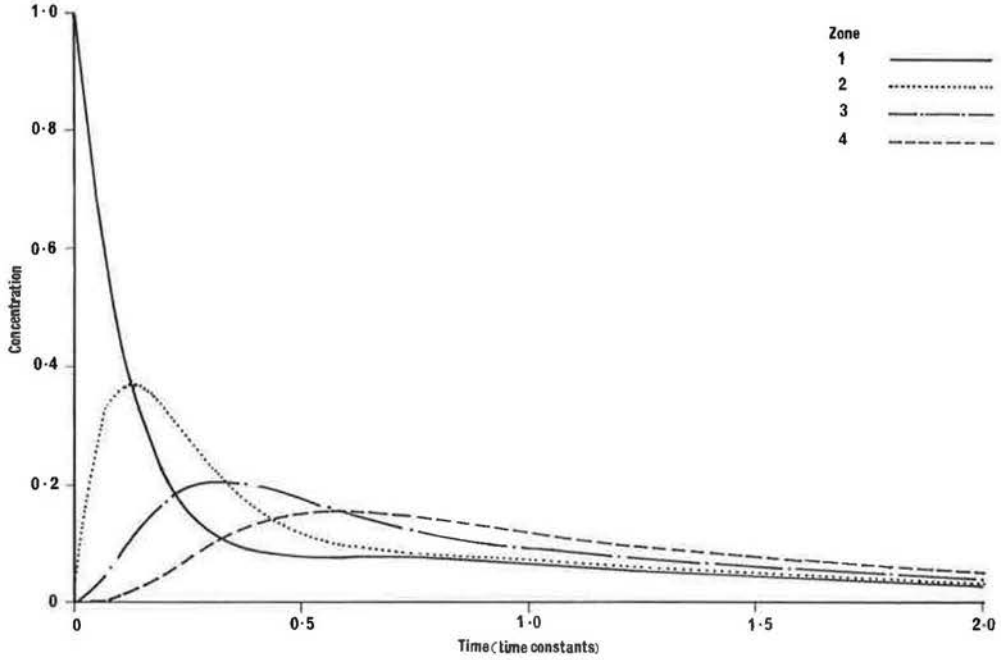

Fig. 11. Tracer decay, 4 zone building, $r = 4$, zone 1 seeded.

per hour, whereas at $r = 0$, it would be only 25% of the true value. Whilst it is obvious from this example that, for $r = 0$, the value of λ would give the correct fresh air infiltration rate if it were associated with the volume of zone 1 only, this cannot be done from the decay curves alone, without first establishing that F_{21}, F_{31} and F_{41} are all zero.

Paragraph 3(iv) above, and the results of this example throw some light on remarks made by Perera and Walker [3] concerning the association of eigenvalues with particular flow rates. Using computations from their own five-zone building, they concluded that "eigenvalues do not necessarily equate either to the fresh air infiltration or to the total air change rate of a zone". This is in agreement with the work presented here. However, they also state that the dominant eigenvalue must represent air movement between the building and the outside, and that the dominant eigenvalue is relatively unaffected by changes in interzone flows. This must be incorrect as it is clearly contrary to both the theory and example considered here.

5. THE EXTRACTION OF FLOW RATES FROM TRACER DECAY MEASUREMENTS

The problem encountered in practice is the opposite of that considered so far i.e. knowledge is required about air movement patterns within buildings and across their external fabric from tracer gas decay observations. In a system of n zones each connecting with the outside there are n^2+n flows, F_{ij}. The necessary n^2+n equations may be formed from the n flow conservation equations (2) and measurement of the concentrations $c_1(t), \ldots, c_n(t)$ and their derivatives $\dot{c}_1(t), \ldots, \dot{c}_n(t)$ on n occasions since each set of measurements yields n tracer gas conservation equations (1).

Table 4. Apparent fresh air infiltration rate, 4 zone building

r	λ_1	Air change rate (h^{-1})
4	-2.68×10^{-4}	0.96
1	-2.33×10^{-4}	0.84
0.25	-1.40×10^{-4}	0.50
0	-1.11×10^{-3}	0.25

If the c_i data set is error free and gives perfect tracer decay curves, there is no difficulty in solving for the F_{ij} providing the $c_i(t)$ and $\dot{c}_i(t)$ can be obtained at n sufficiently different points in time to yield the necessary n^2 equations. There are however certain precautions that must be taken in order to avoid an inaccurate solution.

(i) As explained in Section 4, irrespective of initial conditions, zonal concentrations tend to relative magnitudes equivalent to the components of $\underline{x}_1$. If more than one set of $c_i(t)$ and $\dot{c}_i(t)$ are taken as this condition is approached, an ill conditioned set of equations and hence an inaccurate solution will result. It follows that it is necessary to ensure that adequate time is available for collecting well conditioned data, i.e. before the equilibrium concentrations are approached. This is most easily achieved by strategic seeding of the zones, especially, as explained in Section 4, by seeding the zone with lowest equilibrium concentration. Although this zone may often be identified intuitively, it is most easily obtained from the results of a preliminary set of measurements based on an arbitrary seeding pattern which is allowed to run until equilibrium concentration ratios are apparent.

(ii) Care must be taken when seeding buildings of symmetrical layout. In the case of the building shown in Fig. 12, if zone 2 alone was initially seeded the

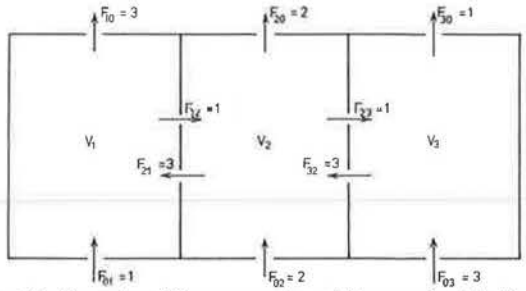

Fig. 12. Example of flow symmetry which may lead to linear dependence.

concentration in zone 1 would, for all time, be greater than that of zone 3 in the ratio of 3 to 1. As a consequence there would be linear dependence between the conservation equations and hence no unique solution. In the case of a real building, experimental scatter would mask the problem causing the linear dependence to give way to ill conditioning and an inaccurate solution.

This problem may be quite easily overcome by ensuring that the symmetry does not exist. In the above example, seeding zone 1, zone 3 or any combination of more than one zone instead of zone 2 alone, would be satisfactory.

(iii) Situations where there may be repeated eigenvalues, as in examples 1 and 2 in Section 2, may create difficulties if the wrong zone is seeded. In those particular examples, it is obvious that it is necessary to seed zone 1, otherwise not all the decay curves will be present. In the case of a real building where there is no pre-knowledge of the flow pattern, incorrect seeding may fail to reveal an important flow. In example 2, if zone 2 was seeded, there would be no measured tracer in zone 1. Nevertheless, a valid set of measurements would be obtained, the solution of which would lump the F_{12} flow in with F_{02}.

The solutions to examples 1 and 2 show that the solutions for the concentrations are not wholly independent, as $c_2(t)$ and $c_3(t)$ can be expressed in terms of $c_1(t)$. However, this dependency varies with time, and so it is still possible to obtain the necessary n^2 equations from the tracer conservation equation. In the 2 zone case, if t_1 and t_2 are the two times at which $c_1(t)$, $\dot{c}_1(t)$, $c_2(t)$ and $\dot{c}_2(t)$ are measured, then it may be shown by substituting equations 8 into equation 1, that the determinant of the coefficient matrix for the F_{ij} is exactly $(t_1-t_2)^2$. As this is only zero when $t_1 = t_2$ a unique solution should always be possible.

In practice, an experimental data set is subject to scatter from a variety of sources, and in many cases experimental technique provides measured values at discrete points in time only. As the direct solution technique relies on measurement of gradient as well as magnitude, the resulting errors in the F_{ij} may be substantial. Walker [4] has attempted an analysis of errors by considering suitable norms of the appropriate matrices. This is useful for examining the theoretical upper bounds of the errors, but does not help to quantify the probable error arising from a particular data set. Nevertheless, from the analysis presented in this paper, it is possible to deduce in a qualitative sense a series of measures which should reduce the effect of errors in the data set and improve the quality of the computed F_{ij}. Seeding strategy has already been discussed, and there are some other possibilities.

5.1. *Noise on the data*

If the data set is large enough, it is possible to use Sinden's suggestion, and integrate Equation (11) over different time intervals. Penman and Rashid (5) have used this method. The disadvantage is that decisions must be made concerning the length of the time intervals and their positions in the data set. There is no simple criterion which will resolve the conflicting requirements of long time intervals (to maximise noise suppression) and sufficiently different time intervals to avoid ill conditioning. This difficulty is avoided if a straightforward smoothing technique is adopted. For example if the data points are equally spaced in time, the method of fourth differences [6] may be applied. This gives smoothed values of both $c_i(t)$ and $\dot{c}_i(t)$ according to simple algebraic formulae. Where the smoothing is carried out over, say, five adjacent data points, we have:

$$C_i(t) = c_i(t) - 3/35[c_i(t-2s) - 4c_i(t-s) + 6c_i(t) - 4c_i(t+s) + c_i(t+2s)]$$

$$\dot{C}_i(t) = \frac{-2c_i(t-2s) - c_i(t-s) + c_i(t+s) + 2c_i(t+2s)}{10s}$$

where $C_i(t)$ and $\dot{C}_i(t)$ are the smoothed values of $c_i(t)$ and $\dot{c}_i(t)$, and s is the time interval between successive points. This method has been used in ref. [7].

5.2. *Reducing the number of unknowns*

It is rare in practical situations for all possible flows, F_{ij}, to exist, and therefore some of the F_{ij} can be set to zero from geometrical considerations alone. Of the remaining F_{ij}, some may also be set to zero if it is observed that any of the decay curves intersect as in paragraph 3 (iii). Furthermore, when a single zone is seeded, additional information can be obtained from an examination of the decay curves in the neighbourhood of the origin. If only one zone is seeded, say zone i, then at $t = 0$, this will be the only zone to contain tracer gas, and Equation (1) reduces to

$$V_i\dot{c}_i(0) = -c_i(0)S_i.$$

Thus

$$S_i = -V_i\frac{\dot{c}_i(0)}{c_i(0)} \tag{10}$$

and the limiting value as $t \to 0$ can conveniently be found by plotting the ratio $\dot{c}_i(t)/c_i(t)$ against time. Also, for any zone, j, which has a flow connection to zone i, equation 1 at time $t = 0$ can be reduced to

$$V_j\dot{c}_i(\theta) = F_{ij}c_i(0)$$

and so

$$F_{ij} = V_j\frac{\dot{c}_j(0)}{c_i(0)}.$$

However, this likely to over-estimate F_{ij} because time lags in the flow paths make it difficult to synchronise the

measurements of $\dot{c}_j(0)$ and $c_i(0)$. If $c_i(0)$ is taken as the value of $c_i(t)$ at the time (usually slightly after $t = 0$) that the measured gradient in zone j is a maximum, then $c_i(0)$ is probably too low, and it is safer to write

$$F_{ij} \leqslant \frac{V_j \dot{c}_j 0}{c_i(0)}. \tag{11}$$

Again, it is convenient to plot the ratio of $\dot{c}_j(t)/c_i(t)$ against time.

5.3. *Application of least squares methods to measured data sets*

Once the data has been smoothed, and the number of unknown F_{ij}'s has been reduced to a minimum, a solution of Equations 1 and 2 may be attempted. A least squares technique is appropriate, but in multi-zone buildings it is often found that the optimum solution contains negative values for some of the F_{ij} [5, 7]. Clearly negative values of F_{ij} are physically impossible, and so it is necessary to apply the constraint $F_{ij} \geqslant 0$. Penman and Rashid achieved this by using the constrained least squares method described in ref. [8], and found that they were then able to obtain satisfactory results. Lawrance has done likewise, but has taken the idea further by including the extra information obtained from Equations 10 and 11 as additional constraints. The least squares solution could possibly be further refined if the equations obtained from the data set were weighted according to their position in the time series, in order to compensate for the fact that, as time progresses, the equations approach linear dependence. This, however, would require a criterion for evaluating appropriate weighting factors.

5.4. *Time delays*

In large buildings, zones may be sufficiently far apart for there to be a significant time lag between zones. This not only has the effect of displacing the decay curves for the zones by different amounts with respect to time, but can also affect the pattern of the decay process. This effect has been examined for a simple two zone building [9]. For the two zone case, it was found that the introduction of time lags creates an oscillation on the decay curves. Similar effects could occur in multizone cases, and may therefore need to be included in the analysis.

6. CONCLUSION

Solutions to the equations for the distribution of a contaminant in a multizone air movement model have been examined in detail, with a view to improving the evaluation of interzone flow rates from measured decay curves. The principal conclusions are;

(i) the most advantageous seeding strategy is to seed a single zone. Preferably this should be the zone in which the tracer concentration will as time progresses fall below the concentration in any other zone.

(ii) The number of unknown F_{ij}'s can be reduced not only from considerations of building geometry, but also if the decay curves exhibit certain features.

(iii) The values of all non-zero F_{ij}'s can be constrained to be greater than zero, and some can be constrained to other values or to an upper limit from close examination of the decay curves.

(iv) It is not possible to determine the overall fresh air infilitration of a building by measuring the dominant eigenvalue from the final uniform decay rate. The fresh air infiltration rate can only be found by first solving for the F_{ij}, and then summing to find

$$S_0 = \sum_{i=1}^{n} F_{i0} = \sum_{i=1}^{n} F_{0i}.$$

REFERENCES

1. F. W. Sinden, Multi-chamber theory of air infiltration. *Bldg. Envir.* **13**, 21–28 (1978).
2. M. Sandberg, The multi-chamber theory reconsidered from the viewpoint of air quality studies. *Bldg. Envir.* **19**, 221–233 (1984).
3. M. D. A. E. S. Perera and R. R. Walker, Strategy for measuring infiltration rates in large, multicelled and naturally ventilated buildings using a single tacer gas. *BSER & T* **6**, 82–88 (1985).
4. R. R. Walker, Interpretation and error analysis of multi-tracer gas measurements to determine air movement in a house. Paper 53, 6th AIC Conference, Ventilation strategies and measurement techniques, Netherlands (September 1985).
5. J. M. Penman and A. A. M. Rashid, Experimental determination of air-flow in a naturally ventilated room using metabolic carbon dioxide. *Bldg. Envir.* **17**, 253–256 (1982).
6. C. Lanczos, *Applied Analysis*. Pitman, London (1957).
7. J. R. Waters and G. V. Lawrance, Ventilation and air movement measurements at Duddestone Mill Maintenance Depot. Report No. CB/85/0002, Coventry (Lanchester) Polytechnic (January 1987).
8. C. L. Lawson and R. J. Hanson, *Solving Least Squares Problems*. Prentice–Hall, Englewood Cliffs, N.J. (1974).
9. J. R. Waters, The effect of time lags in a two zone air movement model. *BSER & T* (in press).

MEASUREMENTS OF INFILTRATION AND AIR MOVEMENT IN FIVE LARGE SINGLE CELL BUILDINGS

G.V. LAWRANCE and J.R. WATERS

8th AIVC Conference
Uberlingen
September 1987

SYNOPSIS

A six channel, computer controlled, tracer gas detection system for the measurement of infiltration rates and air movement in large single-cell industrial buildings has been designed, constructed and calibrated. This has been used for over 50 sets of tracer decay measurements in five single-cell buildings ranging in size from 4000 to 31000 m³. The buildings included a sports hall, a vehicle maintenance depot, two factory workshops and an aircraft hanger. Infiltration rates and interzonal flows were derived from the tracer decay curves using methods based on multizone theory. The analysis method includes a specially developed, constrained least squares technique which gives both infiltration rate and internal flow rates.

The equipment and method of analysis are briefly described, and results for each data set presented. A comparison of infiltration rates, derived from interzonal flows and from averaged tracer decay data is also given. In addition examples are given of comparisons between measured decay curves and theoretical decay curves reconstructed from the measured flow rates. Finally inconsistencies in the data and the model are discussed, together with suggestions for improvements to the experimental technique and the method of analysis.

1. INTRODUCTION AND OBJECTIVES

Although modern industrial buildings are often equipped with sophisticated mechanical ventilation systems, many new ones and most existing ones still rely on a combination of natural ventilation, infiltration and localised extract fans for control of indoor temperature and air quality. As with any other type of building, the potential for energy saving by reducing infiltration must be balanced against the need to maintain air quality, and this balance should be evaluated if any building improvement actions are to be judged. Knowledge of infiltration rates and internal contaminant concentrations is of considerable value in determining the need for such action and its subsequent effectiveness. The significant characteristic of industrial buildings is that they consist of a small number of large spaces, or cells, within each of which there are likely to be strong spatial variations in the effective infiltration rate and in the distribution of contaminated air. Therefore it is necessary that a measurement system should be capable of yielding information not only on whole building infiltration rates but also on the internal air movement patterns which give rise to the spatial variations. Furthermore, the distribution of contaminant concentrations within industrial buildings is due as much to the industrial activity as to the design of the building. Any realistic assessment must therefore be based on measurements of the building in use.

The objective of the study was to develop equipment and a methodology which would enable measurements to be made on industrial buildings which would give values of whole building infiltration rates, and in addition information on air movement patterns within the building. As it was the intention to conduct measurements on buildings in use, acceptability to the building's occupants was an important consideration. A subsidiary objective, therefore, was that the technique should cause minimum disturbance to activities within the building, and that it should be possible to conduct measurements and produce the results within a short time span, say, less than a day. Clearly the complete determination of internal air movement patterns requires very detailed measurements, and this is incompatible with the aim of minimising disturbance to the occupant. The approach therefore has been to adopt procedures which are acceptable to building occupiers, and to determine the extent to which air infiltration rates and air movement patterns can be obtained from a practical number of measurements.

2. THE MEASUREMENT SYSTEM

A detailed description of the tracer gas measurement system has been given by Waters et.al.[1] The need to measure internal air movements imposes a limitation on the choice of tracer gas method. Methods which require some additional imposed stirring throughout the monitoring period will upset the internal air movements which are to be measured. Therefore the tracer decay method is to be preferred to the constant concentration or constant injection methods. Also it is necessary to use tracer gases which are unlikely to be present in industrial atmospheres, and which, because of the large volumes of such buildings, are detectable at low concentrations. Although there are advantages in using multiple tracer systems, especially where internal flows are to be measured, it was considered simpler to choose a single tracer, and to optimise the detection system for that tracer. Sulphur hexafluoride was chosen and has been found to be entirely satisfactory. The measurement system is therefore a tracer gas monitoring device, in which detection is achieved by six independent custom built gas chromatograph units. The use of six independent units permits rapid sampling from at least six sample points, and the use of pulse modulated electron capture detectors within the chromatographs provides both high sensitivity and good linearity over a wide range of tracer concentrations.
A comprehensive evaluation of the detector behaviour was carried out, from which it was possible to optimise the chromatograph parameters with respect to sulphur hexafluoride. Because the system uses six separate detector units, calibration is of particular importance. Therefore a special calibration rig was built, based on the accurate dilution of a sulphur hexafluoride/ air mixture. A standard mixture is used at intervals during actual measurements to give a check on the relative performance of the six units.

The whole system, complete with calibration gases, data acquisition unit, and control computer, is mounted in a small covered trailer, which in most cases may be parked within the building under investigation.

3. MEASUREMENT METHODOLOGY

The theoretical basis of the methodology that has been adopted is that the large volume of air enclosed by a single-cell building can be notionally subdivided, or discretised, by imaginary boundaries into a large number of small volumes, or zones. Although the boundaries between the zones are hypothetical, in practice many single-cell buildings contain partitions screens or furniture which give physical reality to some of the boundaries. If each zone is small enough the distribution of contaminants, including the tracer gas, within the zone will be sufficiently uniform for the air in the zone to be considered well mixed. The system is then identical to the usual multizone model[2] of air flow within a building, and the interzone flow rates will be a measure of the magnitude and direction of the air movement within the complete volume. A detailed theoretical analysis of single gas tracer decay in a multizone model has been carried out by Waters and Simons[3]. This showed that the best seeding strategy is to seed a single zone, and that this should be the zone associated with the smallest component of the dominant eigenvector in the solution of the multizone equations. This is also the zone which, as the transients die out and the process approaches a steady decay, exhibits the lowest value of the tracer concentration. It can therefore be identified by a preliminary measurement. If this is not convenient, it can also be identified as the zone receiving the largest inflow of fresh air, and is therefore likely to be the most exposed zone on the windward side of the building. Fortunately, it is almost as satisfactory to seed any single zone, provided that in the subsequent measurements it is possible to detect tracer gas in all zones in the system. Nevertheless the analysis also revealed two possible difficulties. One occurs with particular flow patterns, which give rise to repeated eigenvalues in the multizone solution. The other occurs when there are certain kinds of symmetry in the interzonal flows, which, when a particular zone is seeded, leads to decay curves in which the concentration in one zone is a constant ratio of the concentration in another zone. The latter leads to linear dependency in the solution for the inter-zone flows, which because of experimental scatter in the data, manifests itself as ill-conditioning. Seeding strategy had to take account of these possible difficulties. The actual measurement procedure is conventional. The trailer is parked either within the building, or immediately outside, so that it is only necessary to run tubing from the trailer to the sample points. The position of the sample points is chosen according to building geometry and the extent of internal obstructions. In open buildings with few obstructions, the building is divided into imaginary zones of approximately equal volume, with a sample point at the centre of

each zone. Where internal obstruction are significant, sample points are placed to represent the spaces that obstructions delineate. However, in occupied buildings, it is often necessary to displace the sample point from the desired position to avoid interference with building activities. The sampling heads themselves consist of a small cylindrical manifold from which radiate nine 1 cm lengths of copper tubing, in the manner of the spokes of a wheel. At each sample point, therefore, air is collected from nine equally spaced points around the circumference of a 2 m circle. This provides some spatial integration of the sample collection within each zone. Pure sulphur hexafluoride is injected into a single zone on the windward side of the building, with stirring during the injection process, and the tracer decay is followed for between one and two hours.

4. MEASUREMENT PROGRAMME

A total of 58 sets of measurements have been obtained, distributed approximately equally between the following five buildings:

1. Abbey School Sports Hall, Kenilworth, Volume 4220 m^3
2. Courtaulds Engineering Workshop, Coventry, Volume 14370 m^3
3. Courtaulds Pattern Making Shop, Coventry, Volume 6420 m^3
4. Hangar 5, Coventry Airport, Volume 31300 m^3
5. British Gas Maintenance Depot, Birmingham, Volume 31020 m^3

Except for the Sports Hall, all the buildings were in use during the measurements; in Hangar 5 all measurements were taken with the aircraft doors closed. In all cases, six sampling points were used, which were positioned to represent equal volumes, except where internal obstructions were significant, in which case they were positioned to represent the spaces that the obstructions created.

All the buildings were naturally ventilated, but Courtaulds Pattern Making Shop and British Gas Maintenance Depot had fume extract systems at strategic positions. Also, the British Gas building had an experimental mechanical ventilation and heat recovery system which was switched off for all but three of the measurements.

5. ANALYSIS OF RESULTS

Results for each measurement set were processed in two ways:

1. Readings for all six sample points were averaged to give a single overall average tracer concentration for the whole building. The decay of the average concentration was used to obtain the fresh air infiltration rate of the whole building.

2. Using multizone theory, a constrained least squares technique was used to determine the complete set of interzone flow rates. The fresh air infiltration rate of the whole building was found by summing the flows between individual zones and the outside.

For both methods of analysis, the data set for each run was split into sections, and each section analysed separately. These sections were:

1. the first third of the data in the time series

2. the second third

3. the last third

4. the first two thirds

5. the last two thirds

6. the whole data set.

Thus for each method of analysis there were six sets of results for each run.

The justification for the first method of analysis follows from the standard solution to the multizone problem. If $\underline{c}(t)$ is the vector representing the tracer concentration in the n zones of a building, then

$$\underline{c}(t) = \sum_{k=1}^{n} a_k \, \underline{x}_k \, e^{\lambda_k t}$$

where λ_k and $\underline{x}_k$ are the eigenvalues and their associated eigenvectors of the solution, and the a_k are the constants associated with the initial condition (i.e. the seeding strategy). The average concentration $\bar{c}(t)$ of the n zones is, if the zones are of equal size, given by

$$\bar{c}(t) = \frac{1}{n}\left[a_1(x_{11} + x_{12} + ..)e^{\lambda_1 t} + a_2(x_{21} + x_{22} + ..)e^{\lambda_2 t} + ..\right]$$

$$= \frac{1}{n} \sum_{k=1}^{n} A_k \, e^{\lambda_k t}$$

where $A_k = a_k(x_{k1} + x_{k2} + ..)$.

The decay of the average concentration is therefore governed by the same set of eigenvalues. Now Waters and Simons[3] have demonstrated that as the internal flow rates increase, the dominant eigenvalue decreases, and approaches the value that would apply if the whole building were a single fully mixed zone. At the same time the other eigenvalues also get smaller, approaching in the limit $-\infty$. The implications of this for the decay of the average concentration, $\bar{c}(t)$, are shown in figure 1, in which the natural logarithm of $\bar{c}(t)$ is plotted against time. Now the gradient of the decay curve for the fully mixed case gives the whole building infiltration rate.

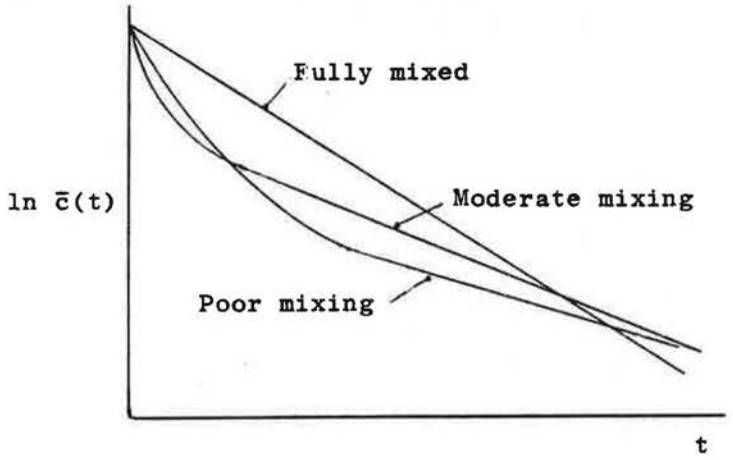

Figure 1. The effect of mixing on the decay of $\bar{c}(t)$

It can be seen therefore that in all other cases the gradient from the early part of the decay will over-estimate the whole building ventilation rate, whereas the gradient from the later stages where the dominant eigenvalue is in control will under-estimate it. These two values must give the limits within which the whole building infiltration lies, and the average gradient of the whole data set will lie close to the true value.

The solution for the individual flows is found by direct substitution of measured tracer concentrations and concentration gradients in the fundamental equations. However, the problem is first reduced by determining, from building geometry and from examination of the decay curves, which of the interzonal flows, F_{ij} are zero. Secondly, constraints are applied. Obviously we must have all $F_{ij} \geq 0$, but in addition examination of the decay curves in the seeded zone and zones adjacent to it, at times close to the start of the process, provides the possibility of including further constraints. If i is the seeded zone, and j a zone with a flow connection to i, then it may be shown (ref.3) that at time $t = 0$,

$$\sum_{j=0}^{n} F_{ji} = \sum_{j=0}^{n} F_{ij} = -V_i \frac{\dot{c}_i(0)}{c_i(0)}$$

and $$F_{ij} \leqslant V_j \frac{\dot{c}_j(0)}{c_i(0)}$$

where V_i is the volume of zone i. Using the method described by Lawson and Hanson[4], these constraints are applied to the least squares solution.

6. PRESENTATION AND DISCUSSION OF RESULTS

Tables 1 to 5 inclusive give the results for the whole building infiltration rate, calculated by both methods of analysis. For each run, the first row, marked AC, gives values computed from the average concentration, and the second row, marked IF, gives values computed from the interzonal flows. The last column gives the best value of the infiltration rate, which is assumed to be that given by the whole data set, and the range, which is the difference between the best value and the extreme values expressed as a percentage. Each table also includes a plan diagram of the building, with the interzonal flows computed from one of the runs superimposed.

For each run, the infiltration rates obtained from the average concentration vary according to the data subset from which they have been calculated in the expected manner. With very few exceptions, the highest value comes from the first third of data and lowest from the final third. The range is often much greater on the positive side than the negative side. This again is to be expected, because the early decay rate is primarily a function of the flow rates out of the seeded zone, which may be very large. It is likely, therefore, that a large value on the positive side over-estimates the probable error in the best value.

If the data set were free from experimental error, and if the assumptions of multizone theory were valid in these buildings, the infiltration rates computed from interzone flows would be the same whichever data subset was used in the analysis. Neither condition is true, and the results often show marked variability. Comparing the infiltration rates from the interzone flows with the 'best value' from the average concentration suggests that where agreement is good, variability is low, and vice versa. For example, taking as a measure of the variability of the six IF values in any run the ratio of the standard deviation to the mean, the following three runs illustrate the trend:

Building 1	Best Value	IF Value	SD/mean
Run 13	4.15 ach	1.09 ach	0.61

Building 3	Best Value	IF Value	SD/mean
Run 36	2.69 ach	3.05 ach	0.43

Building 3	Best Value	IF Value	SD/mean
Run 39	2.57 ach	2.48 ach	0.30

One possible explanation for the variability is that the length of the data sets was determined arbitarily by the time available for each run. Waters and Simons[3] demonstrated that for single zone seeding the decay process is close to uniformity at a time of two time constants from the start, where the time constant is defined as the reciprocal of the dominant eigenvalue. The inclusion of data beyond this time may be weighting the least squares solution towards linear dependency. Some of the results were recalculated with the data set restricted to two time constants, where the time constant was assumed to be given with sufficient accuracy by the reciprocal of the 'best value' infiltration rate. In table 6 run 13

TABLE 6

EFFECT OF RESTRICTING DATA SET TO TWO TIME CONSTANTS

	Infiltration rate, ach, from interzonal flows Data Subset						SD/means
	1	2	3	4	5	6	
Run 13							
Full data	0.72	0.83	0.48	0.63	2.13	1.09	0.61
2t	1.48	0.19	0.69	3.98	0.03	0.84	1.21
Run 36							
Full data	5.71	4.10	1.88	3.35	1.97	3.05	0.43
2t	3.09	3.24	4.05	3.72	1.39	1.58	0.39

the variability and agreement with the 'best value' are worse, and for run 36 there is no improvement. The individual interzonal flows also show considerable variation between the solutions from different data subsets, and again there is a tendency for the variability to be less where agreement for the infiltration rates is good. The extreme sensitivity of the interzonal flows to the manner in which the data is selected and processed has also been noted by Afonso et.al[5] who also used a single tracer gas. Nevertheless, they were able to get reasonable agreement with independently measured values of the interzonal flows, but it is of interest to note that they were using only 2 zones in an experimental set-up which was designed to match the assumptions of the multizone model.

As a further indicator of the quality of the interzonal flow results, theoretical decay curves were computed from the flows, and compared with the original measured curves. This is a severe test, and where the flow results are in doubt because the whole building infiltration rates are inconsistent, the reconstituted curves bear little resemblance to the measured originals. However, where there is some measure of consistency in the infiltration

rates, the two sets of curves can show at least a reasonable similarity. Figs 2-4 show as an example run 36. This run also illustrates one of the major reasons for the difficulties in obtaining good matching. It can be seen from the measured curve that there is a time lag effect, shown by tracer concentration peaks in standing above the general trend of the decay. This is not possible on the basis of the normal multizone model.

7. CONCLUSIONS

The results for infiltration rate computed from the average concentration appear to be sufficiently consistent to be considered reliable, and show that it is comparatively easy to obtain reasonable values for buildings in the size range considered without recourse to elaborate technique or analysis. The values for the infiltration rates were in most cases surprisingly high, but all these buildings were very leaky, with large badly fitting doors, which in some cases were left open during normal working.

The results for interzone flows were always plausible, but this was due to the imposition of constraints on the solution technique. In most cases, lack of consistency and poor agreement with the infiltration rates obtained from the averaged data, suggest that at the present stage of development the interzone results are too unreliable to be useful. The most probable explanations for the poor results are:

1. The size of the hypothetical zones was too large to give adequate discretisation of the internal volume of these buildings. The choice of six channels for the measurement system was dictated partly by experience from a preceding pilot study and partly by available resources. Thus, in these buildings, each zone was large enough for there to be spatial variations within it.

2. The 2 metre diameter sampling head used in each zone was small in relation to the size of each zone, and therefore may not have given a reasonable measure of the average tracer concentration in that zone.

3. Because artificial mixing of the air in these buildings has been deliberately avoided, the normal multizone model is not strictly applicable, even with discretisation into small zones.

Each of these problems can be overcome to some degree. The first two could be ameliorated by increasing the number of zones, either by adding extra channels to the equipment, or by multiplexing the existing channels. At the same time, the sampling arrangement could be altered to give a more representative value of the concentration in each zone. Unfortunately, both of these possible courses of action would increase the disturbance caused to the building occupier.

The third problem has been approached by reconsidering the air flow model of the building. Instead of considering the air volume as an assembly of perfectly mixed zones, it is more realistic to consider it as a combination of pockets of good mixing (or zones) linked by air streams in which the air flow is predominantly in one direction. These latter approximate to ducts. An alternative model is therefore, an assembly of perfectly mixed zones linked by ducts in which the flow is unidirectional. The solution of this alternative model is much more difficult. Nevertheless a solution has been obtained for the case of two zones linked by two ducts (reference 6). The most significant feature of the solution is that the decay curves can exhibit the time delays and oscillatory behaviour which has often been observed in our measured decay curves. It would be very interesting to solve a model of six zones connected by unidirectional flow ducts, but this has not yet been achieved.

8. REFERENCES

1. J.R. Waters, G.V. Lawrance and N. Jones, A tracer gas decay systems for monitoring air infiltration and air movement in large single-cell buildings. Symposium on Design and Protocol for Monitoring Indoor Air Quality, ASTM, Cincinnati, April 1987 .

2. F.W. Sinden, Multi-chamber theory of air infiltration. Building and Environment, 13, 21-28, 1978 .

3. J.R. Waters and M.W. Simons, The evaluation of Contaminant Concentrations and air flows in a multizone model of a building. Building and Environment.

4. C.L. Lawson and R.J. Hanson, Solving least squares problems. Prentice-Hall, Englewood Cliffs, N.J., 1974 .

5. C.F.A. Afonso, E.A.B. Maldonado and E. Skaret, A Single tracer-gas method to characterize multi-room air exchanges. Energy and Buildings, 9, 273-280, 1986.

6. J.R. Waters, The effect of time lags in a two zone air movement model. BSER & T

Table 1

BUILDING 1 : ABBEY SCHOOL SPORTS HALL

Run No	Wind Vel m/s	Analysis Method	Whole Building Infiltration Rate (ach) Data Subset 1	2	3	4	5	6	Best Value & Range %
12	5.1	AC	4.95	4.04	3.59	4.24	3.73	3.83	3.83 +29 -6
		IF	5.70	6.71	80.8	?.08	28.4	14.1	
13	5.7	AC	5.56	4.25	3.83	4.60	3.97	4.15	4.15 +34 -8
		IF	0.72	0.83	0.48	0.63	2.13	1.09	
14	6.9	AC	5.39	4.78	4.35	4.91	4.49	4.56	4.56 +18 -5
		IF	1.89	10.3	0.86	2.45	3.42	1.68	
16	5.1	AC	3.64	3.69	3.53	3.68	3.58	3.58	3.58 +3 -1
		IF	1.60	4.99	293	0.33	4.27	4.57	
17	3.1	AC	4.23	4.41	3.99	4.37	4.12	4.13	4.13 +7 -3
		IF	3.69	0.77	1.17	1.14	2.46	1.93	
18	5.1	AC	3.60	3.13	3.28	3.24	3.23	3.26	3.26 +10 -14
		IF	0.98	1.27	2.85	1.86	0.45	2.31	
19	6.2	AC	4.66	3.32	2.95	3.61	3.07	3.20	3.20 +46 -8
		IF	4.06	3.50	14.8	2.77	9.07	2.25	

Interzone Flows ms^{-1} , Run 13 Data Subset 6

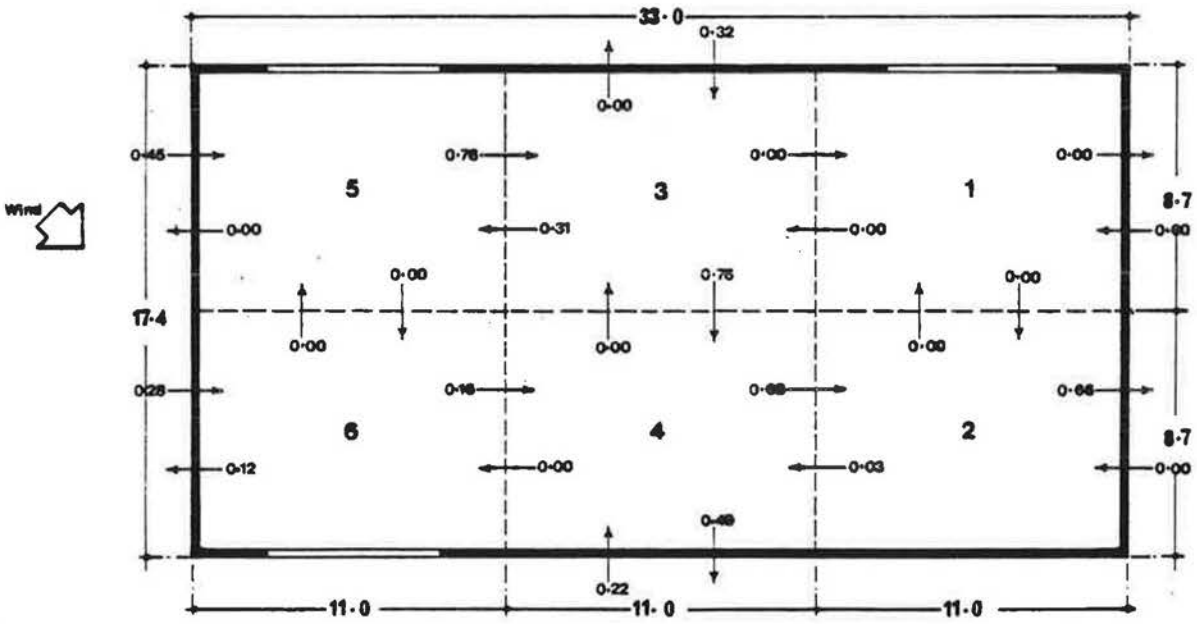

Table 2

RUILDING 2 : COVENTRY AIRPORT HANGER 5

Run No	Wind Vel m/s	Analysis Method	Whole Building Infiltration Rate (ach) Data Subset 1	2	3	4	5	6	Best Value & Range %
21	6.2	AC	9.27	6.33	4.97	6.81	5.36	5.57	5.57 +66 -11
		IF	9.86	3.11	6.02	7.91	2.94	7.10	
22	7.2	AC	5.69	5.84	5.70	5.81	5.74	5.74	5.74 +2 -1
		IF	5.35	2.17	395	3.16	4.04	6.53	
23	6.7	AC	5.64	5.02	4.69	5.13	4.79	4.84	4.84 +17 -3
		IF	3.72	1.26	106	4.66	7.34	3.62	
24	6.7	AC	5.24	4.20	3.34	4.42	3.61	3.73	3.73 +40 -10
		IF	7.14	3.24	54.1	3.11	10.8	11.7	
26	5.1	AC	4.17	3.34	2.58	3.52	2.81	2.92	2.92 +43 -12
		IF	4.23	4.85	30.2	2.48	57.2	3.91	
27	3.6	AC	5.84	4.66	3.94	4.89	4.16	4.27	4.27 +37 -8
		IF	9.48	10.1	16.8	6.08	5.21	10.6	
28	5.1	AC	5.24	4.16	3.58	4.33	3.74	3.84	3.84 +36 -7
		IF	1.95	1.58	2.60	2.47	5.62	3.14	
30	3.6	AC	6.98	3.72	3.00	4.41	3.22	3.51	3.51 +99 -15
		IF	3.82	2.11	0.47	1.48	2.37	1.19	

Interzone Flows ms^{-1} , Run 28 Data Subset 6

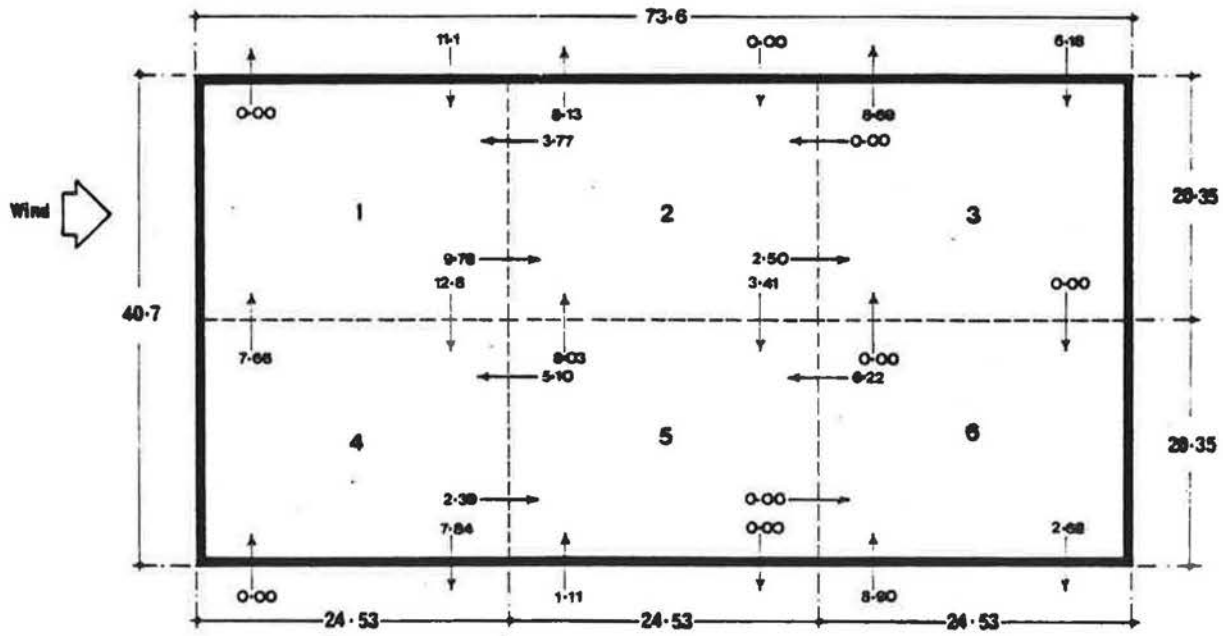

Table 3

BUILDING 3 : COURTAULDS FITTING SHOP

Run No	Wind Vel m/s	Analysis Method	Whole Building Infiltration Rate (ach) Data Subset 1	2	3	4	5	6	Best Value & Range %
31	6.7	AC	5.05	3.10	2.31	3.47	2.55	2.71	2.71 +86 -15
		IF	4.83	8.66	18.9	13.2	11.4	6.49	
32	4.1	AC	4.24	2.72	2.15	3.00	2.32	2.44	2.44 +74 -5
		IF	3.89	2.58	1.01	2.97	3.33	1.67	
34	2.6	AC	4.36	2.85	2.19	3.21	2.40	2.58	2.58 +69 -15
		IF	1.43	0.88	1.78	2.65	0.75	2.60	
35	1.5	AC	4.27	2.64	2.04	2.95	2.22	2.36	2.36 +81 -14
		IF	2.10	2.11	2.01	4.94	3.95	2.52	
36	1.5	AC	4.75	3.02	2.34	3.34	2.54	2.69	2.69 +77 -13
		IF	5.71	4.10	1.88	3.35	1.97	3.05	
38	4.1	AC	3.72	2.48	1.91	2.70	2.08	2.18	2.18 +71 -5
		IF	3.61	0.20	1.40	3.68	1.31	3.83	
39	3.1	AC	4.53	2.88	2.22	3.21	2.42	2.57	2.57 +76 -14
		IF	2.16	2.47	1.88	1.51	0.99	2.48	

Interzone Flows ms^{-1} , Run 34 Data Subset 6

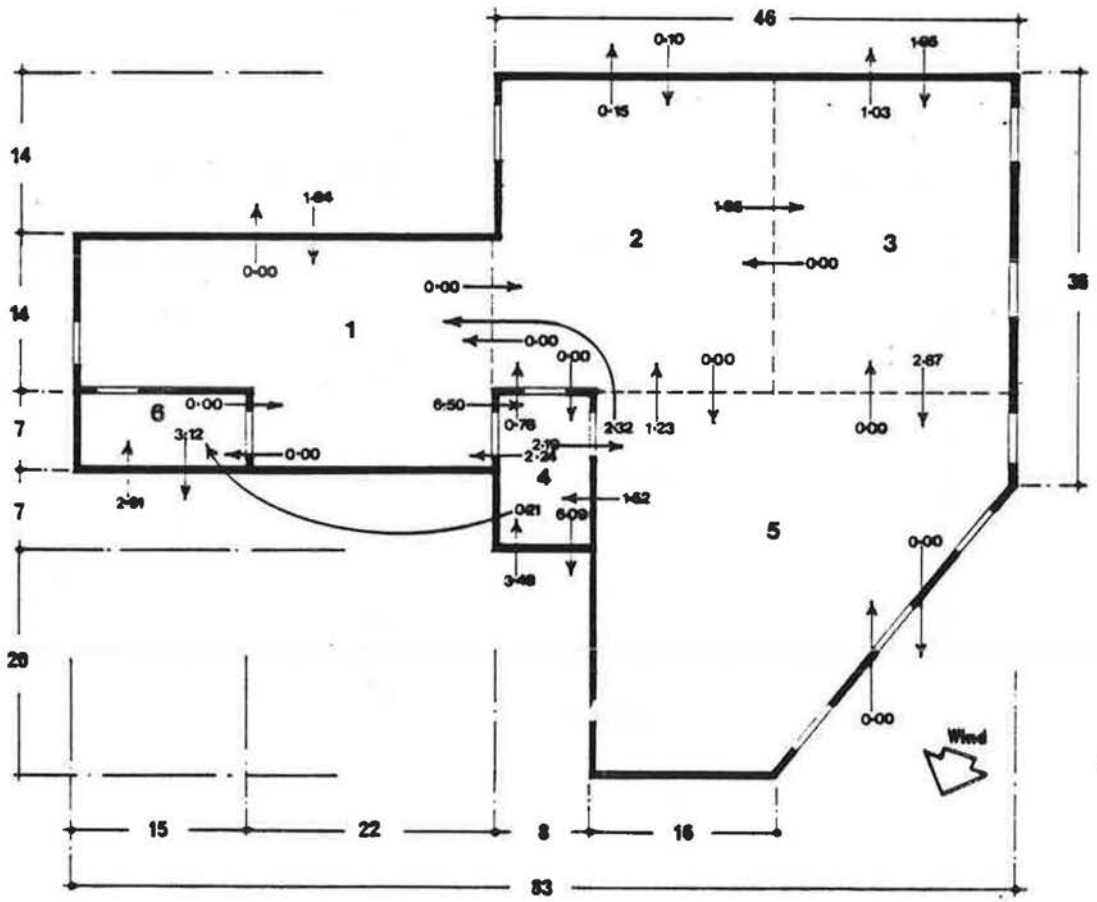

Table 4

BUILDING 4 : COURTAULDS PATTERN SHOP

Run No	Wind Vel m/s	Analysis Method	Whole Building Infiltration Rate (ach) Data Subset 1	2	3	4	5	6	Best Value & Range %
41	6.2	AC	2.54	1.91	1.63	2.01	1.71	1.75	1.75 +45 -7
		IF	5.70	1.05	1.33	2.93	0.96	1.64	
42	7.2	AC	2.38	1.75	2.10	1.84	2.00	2.01	2.01 +18 -13
		IF	2.50	1.74	4.75	1.06	1.34	3.44	
43	1.5	AC	2.09	1.69	1.35	1.76	1.45	1.48	1.48 +41 -9
		IF	1.04	2.90	2.99	2.71	3.05	0.80	
45	5.7	AC	1.93	1.47	1.61	1.55	1.57	1.59	1.59 +21 -8
		IF	2.04	3.81	1.52	2.05	2.27	3.18	
46	5.7	AC	2.37	1.90	1.70	1.99	1.76	1.80	1.80 +32 -6
		IF	0.91	1.16	3.22	0.93	1.45	1.36	
47	10	AC	2.84	2.23	2.08	2.35	2.13	2.17	2.17 +31 -4
		IF	0.72	1.53	2.29	2.94	2.01	1.30	
48	6.2	AC	3.61	2.70	3.11	2.91	2.98	3.03	3.03 +19 -11
		IF	7.83	1.41	6.36	1.89	4.44	3.38	
49	8.2	AC	2.65	2.09	1.95	2.19	1.99	2.03	2.03 +31 -4
		IF	3.10	1.26	1.43	1.29	3.47	0.88	
50	9.3	AC	2.94	2.72	2.69	2.76	2.70	2.72	2.72 +8 -1
		IF	0.49	1.42	3.34	1.01	0.68	0.29	

Interzone Flows ms^{-1} , Run 49 Data Subset 6

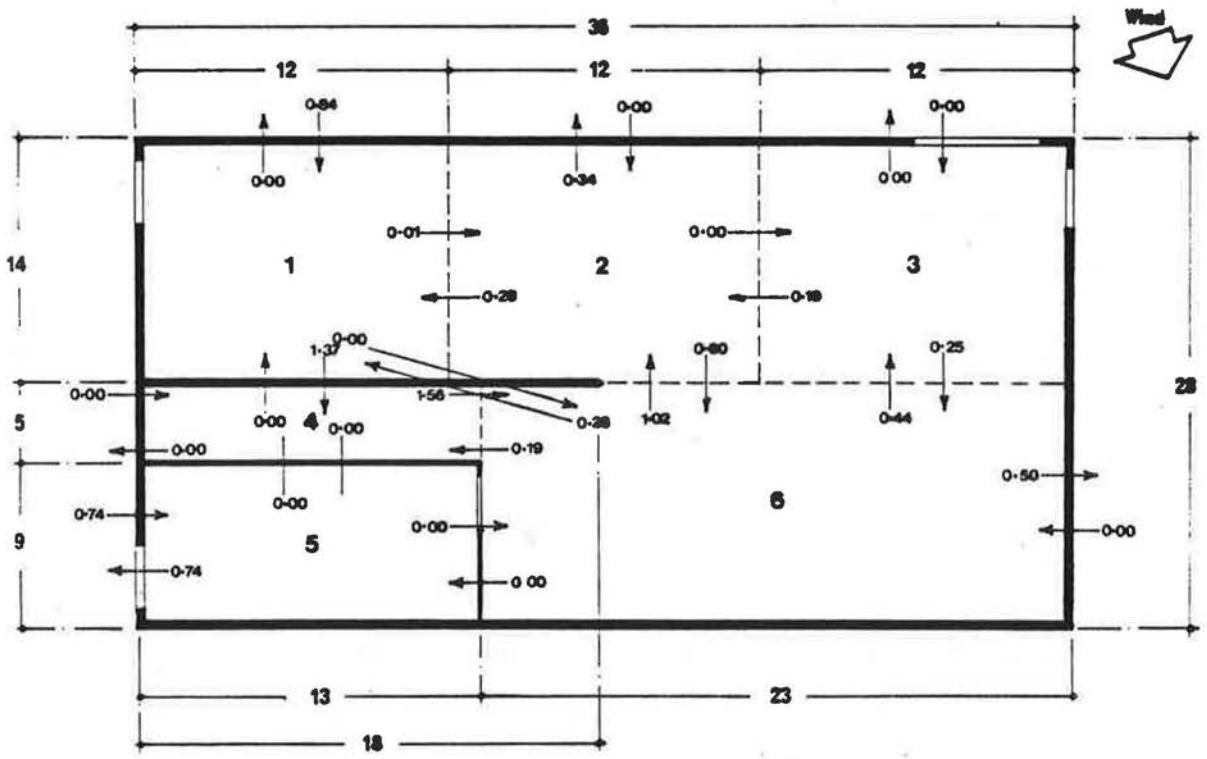

Table 5

BUILDING 5 : BRITISH GAS MAINTAINANCE DEPOT

Run No	Wind Vel m/s	Analysis Method	Whole Building Infiltration Rate (ach) Data Subset 1	2	3	4	5	6	Best Value & Range %
63	5.1	AC	3.54	2.54	2.83	2.77	2.74	2.81	2.81 +26 -10
		IF	3.65	4.05	6.08	2.01	4.65	2.20	
65	3.6	AC	3.14	2.47	2.46	2.60	2.46	2.51	2.51 +25 -2
		IF	0.53	1.00	2.12	2.26	1.66	0.91	
66	2.6	AC	6.42	4.29	3.65	4.79	3.86	4.09	4.09 +57 -11
		IF	1.75	1.38	0.81	0.46	1.78	0.80	
67	2.6	AC	4.29	3.26	2.96	3.50	3.06	3.17	3.17 +35 -7
		IF	1.40	4.04	4.33	2.98	4.94	3.76	
68	3.6	AC	9.29	6.07	4.91	6.82	5.28	5.63	5.63 +65 -13
		IF	6.55	2.89	5.14	2.33	4.94	4.36	
69	4.6	AC	2.97	2.59	2.83	2.46	2.76	2.69	2.69 +10 -9
		IF	0.88	1.97	1.28	0.61	2.31	1.17	
71	2.6	AC	4.47	3.85	3.36	4.00	3.52	3.61	3.61 +24 -7
		IF	0.54	2.16	3.71	0.99	2.15	0.75	
73	2.6	AC	2.92	2.52	2.56	2.61	2.55	2.58	2.58 +13 -2
		IF	0.96	2.85	1.14	0.54	1.05	1.21	
74	2.1	AC	3.44	2.73	2.81	2.94	2.78	2.87	2.87 +20 -5
		IF	6.05	3.06	4.33	3.42	5.75	4.19	

Interzone Flows ms^{-1} , Run 67 Data Subset 6

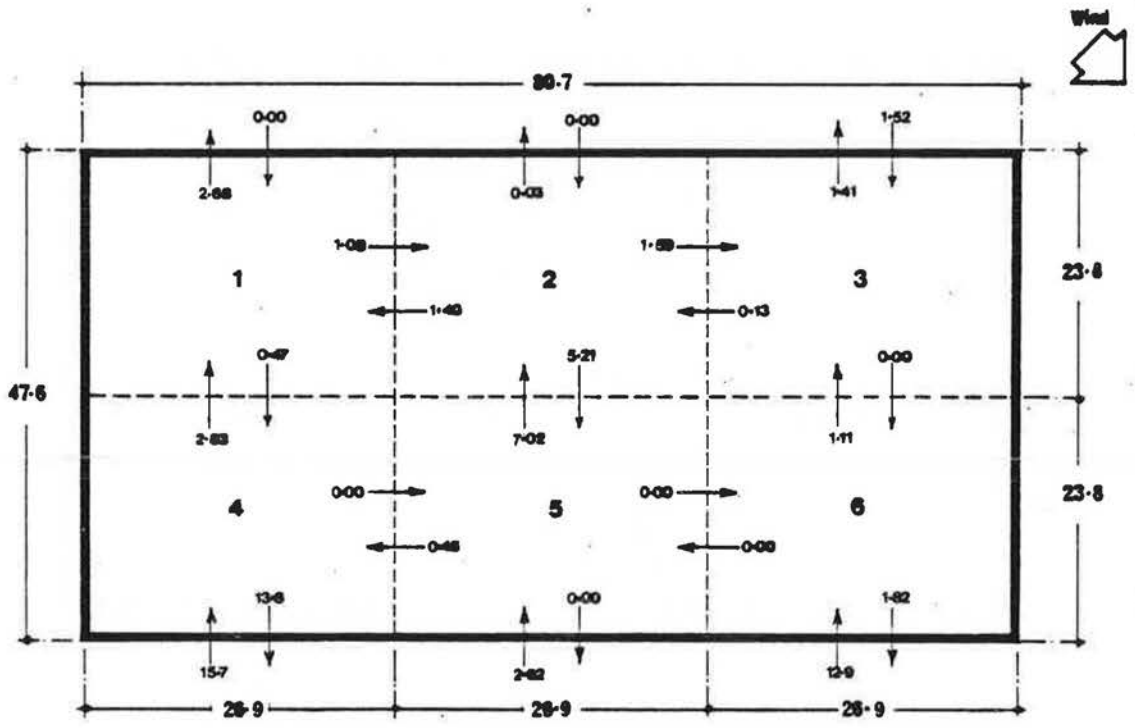

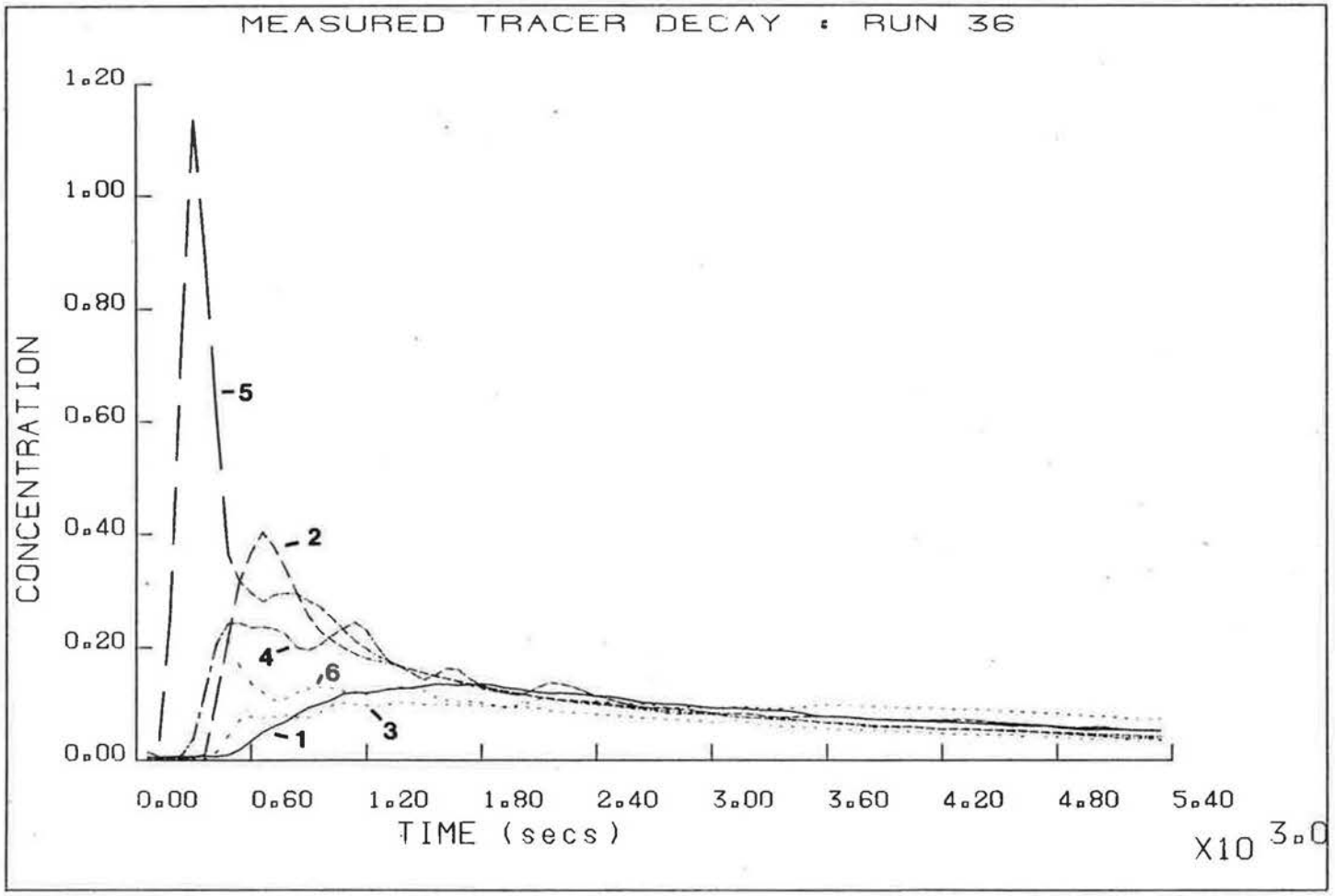

Figure 2. Measured tracer decay in Building 3, run 36

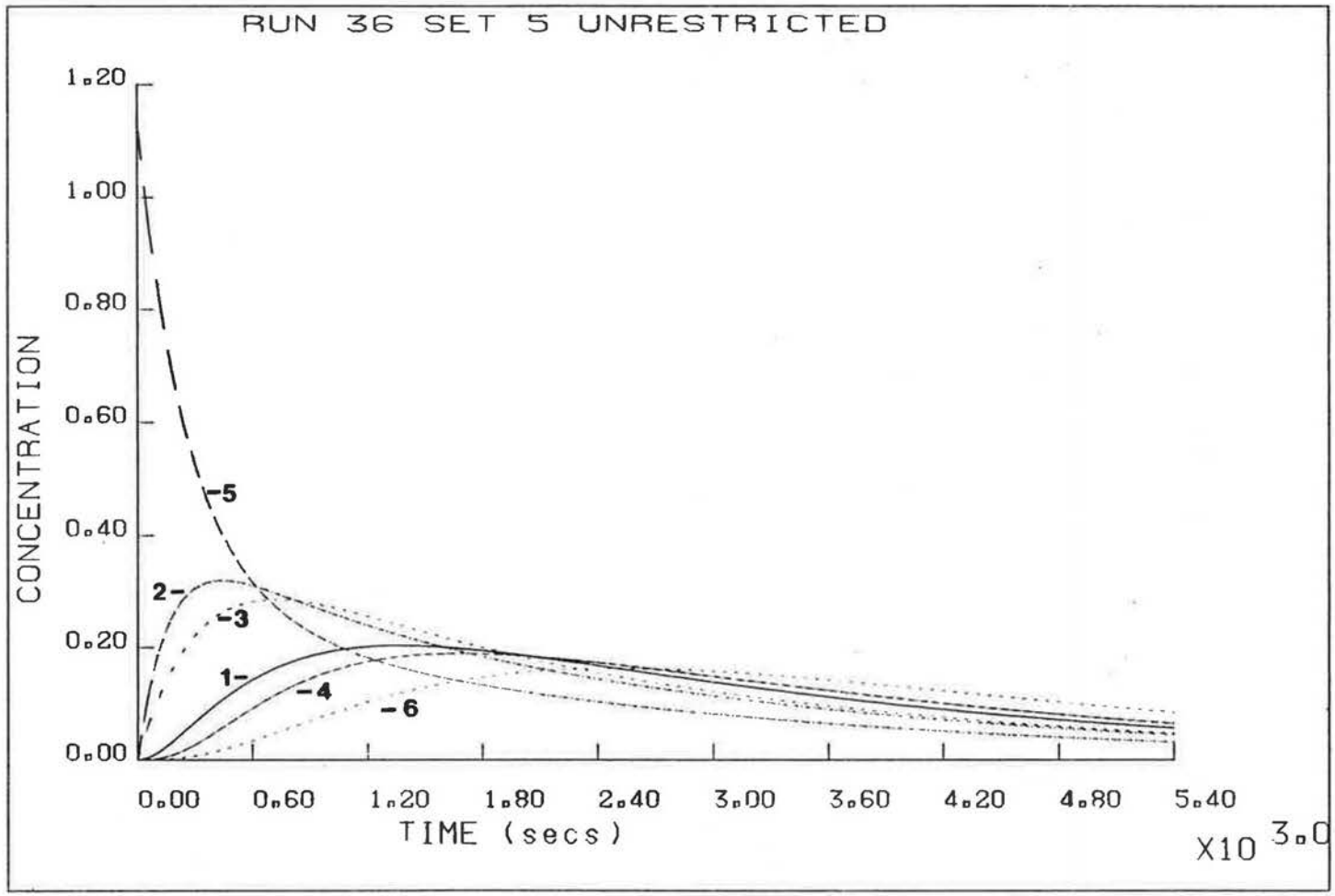

Figure 3. Computed tracer decay in Building 3, run 36
Interzonal flows obtained from data subset 5 of full data

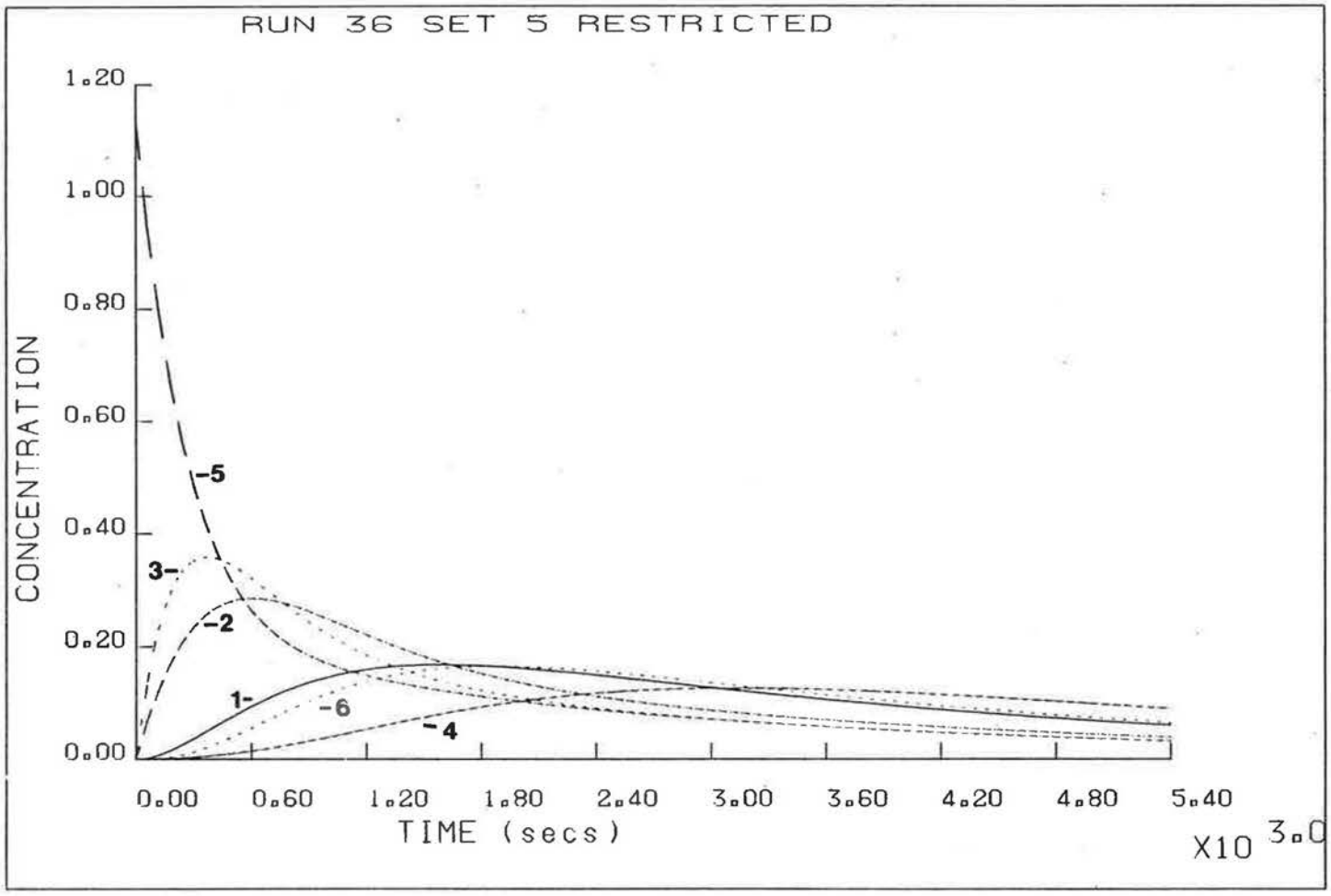

Figure 4. Computed tracer decay in Building 3, run 36
Interzonal flows obtained from data subset 5 of
data restricted to 2 time constants

Ventilation and Air Movement Measurements at Duddestone Mill Maintenance Depot, Birmingham

J R Waters, BSc, MPhil, PhD, MCIBSE
and G V Lawrance, BSc

Report No: CB/85/0002

January 1987

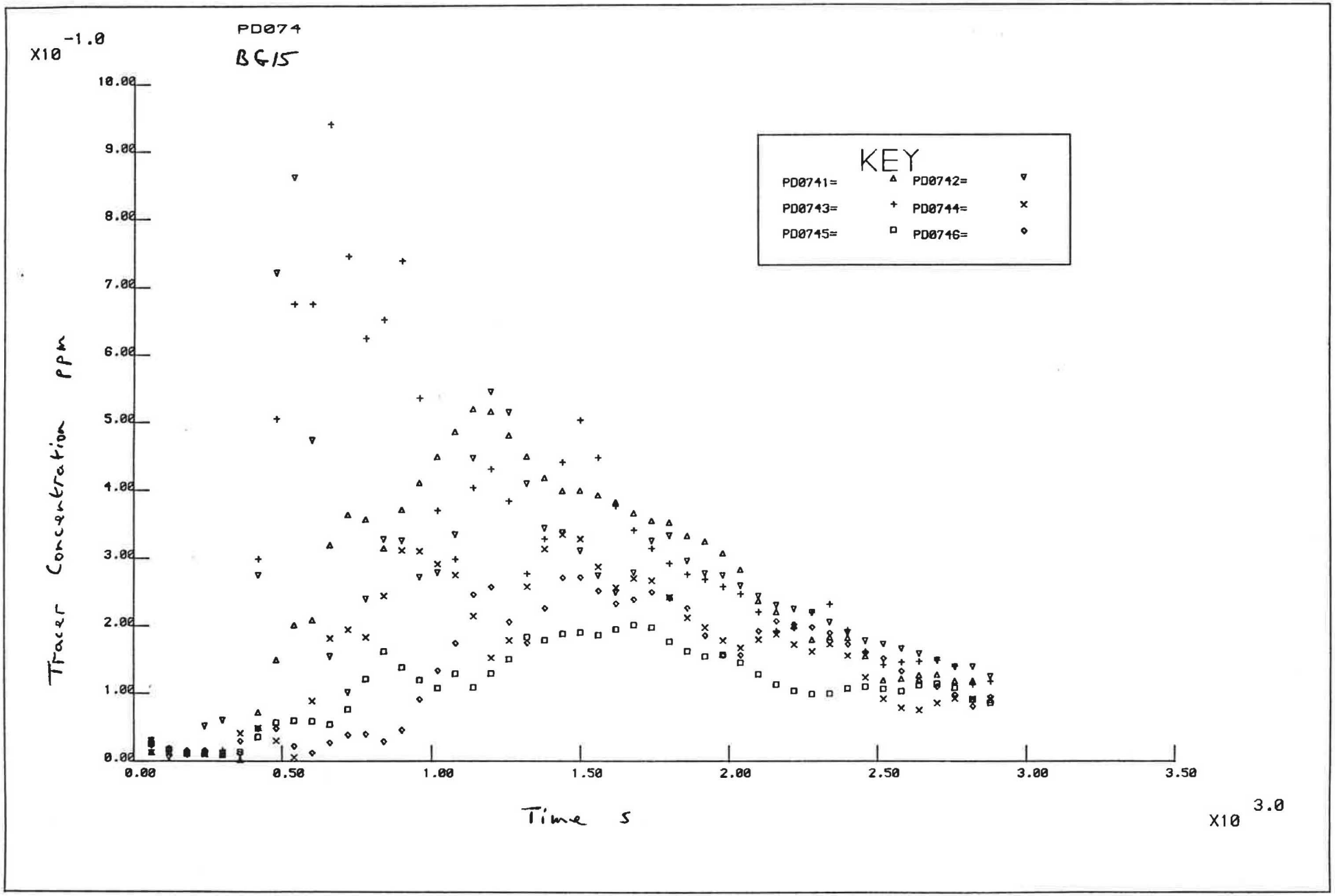
PD074
BG15
X10 -1.0
10.00
9.00
8.00
7.00
6.00
5.00
4.00
3.00
2.00
1.00
0.00
Tracer Concentration ppm
0.00
0.50
1.00
1.50
2.00
2.50
3.00
3.50
Time s
X10 3.0
KEY
PD0741=
PD0742=
PD0743=
PD0744=
PD0745=
PD0746=

Ventilation and Air Movement Measurement System

Coventry (Lanchester) Polytechnic
Dept Civil Engineering and Building
G.V.Lawrance B.Sc.

Date: 23.9.86 Time: 12.00 Run: BG 15

Location: British Gas Duddestone Mill Matainance Depot

Program: VAMMS6 Data Number PD 074

Comments:

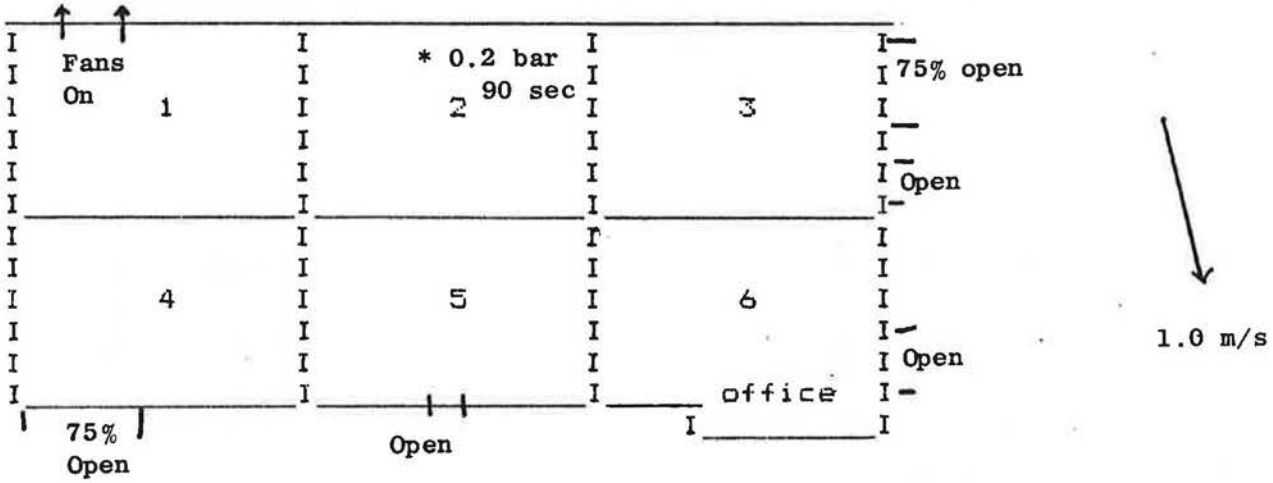

Air Handling System On (10% Fresh Air)
BA Wind Data 330°, 4 knots (7)
Constraints i) $F_{21} \leq 10.3$, $41.7 \leq F_{02} + F_{12} + F_{32} + F_{52} \leq 92.3$, $F_{23} \leq 22.6$ $F_{25} \leq$

ii) All $F \geq \emptyset$

Air Change Rates for Whole Building

Data Used	Flow ACH	Graph ACH	Constraints Applied
1st 1/3	6.046	3.44	i & ii
2nd 1/3	3.064	2.73	"
3rd 1/3	4.332	2.81	"
1st 2/3	3.417	2.94	"
Last 2/3	5.753	2.78	"
All	4.185	2.87	"
All	0.482		ii only
All	3.603		none

Ventilation and Air Movement Measurements at Duddestone Mill Maintenance Depot, Birmingham

J R Waters, BSc, MPhil, PhD, MCIBSE and G V Lawrance, BSc

Introduction

The ventilation research team at Coventry Lanchester Polytechnic has been investigating methods of determining ventilation rates and air movement patterns in large single cell buildings of the industrial type. A specially designed automated tracer gas monitoring system has been built, calibrated and commissioned for this purpose. A program of measurements in different types of industrial environment is being carried out in order to gain experience of operating the equipment, and to provide a data bank of results. The data bank is being used to refine data analysis techniques and to provide a practical basis for improving the background theory.

British Gas has a long-standing interest in the ventilation of all types of building. Furthermore, the West Midlands Region of British Gas has been investigating the heating of industrial premises, and to this end has installed an engine driven heat pump set at its Transport Maintenance Depot at Duddestone Mill, Birmingham. An important component in the monitoring of the performance of the heat pump set is the fresh air infiltration rate of this building.

As a result of their common interest, British Gas and Coventry Polytechnic arranged a joint program of measurements at the Duddestone Mill Maintenance Depot. In September 1986, measurements were made with the objective of determining the fresh air infiltration rate with the building in normal use. The results of these measurements are reported here. Additional measurements were made in October and November 1986 in order to study variations in the measurement technique; these are not reported here.

Theory

The standard methods of measuring ventilation rate by a tracer gas method require that the air in the building (or part of a building) be uniformly mixed. In small buildings this is easily achieved by small mixing fans. When mixing if uniform, the decay of a tracer gas measured at a single point follows a simple exponential law, with a single decay constant, and the decay constant may be equated to the fresh air infiltration rate of the building.

However in large buildings, especially when they are in use, it is rarely practicable to stir the air sufficiently to achieve uniform mixing. Even if it were practical, it is often not appropriate because in normal use, internal air movements and the positions of openings tend to create a variation in the effective infiltration rate throughout the building. Instead of attempting to stir the air, it may therefore be preferable to increase the number of sampling points in the building. It may be expected that by averaging the tracer concentrations from all the sample points, a simple exponential decay would again be obtained, and that the decay constant would again equate to the fresh air infiltration rate. Unfortunately, Waters and Simons (1) have shown that this is not strictly true, and that it is theoretically better to treat each sample point as representing the region or zone which surrounds it. This allows multizone theory to be used, from which may be derived the flow rates between zones, and between each zone and the outside. Summing the individual flows into each zone from the outside gives the overall infiltration rate of the whole building.

Unfortunately, the current state of knowledge is insufficient to give reliable guidance on several key features of the use of multizone methodology in large single cell buildings. These are:-

(i) The number of zones/sampling points in relation to the size of the building.

(ii) The seeding strategy for the tracer gas.

(iii) The most appropriate method of analysing the experimental data, and

(iv) The extent of the validity of multizone theory and hence the likely reliability of the derived flow rates.

Thus, multizone treatment is theoretically superior as it yields more detailed and more realistic information. Nevertheless, the difficulties in applying it are such that the magnitude of the errors in the results are not known.

Method

Duddestone Mill Maintenance Depot is a simple rectangular building approximately 80.7 m x 47.6 m x 8.0 m. Figure 1 is a sketch plan of the building, showing those doors which were in use during the test measurements.

Apart from the office, the store and the spray booth, the interior is a single volume, obstructed only by the vehicles and their associated repair equipment. For the purposes of measurement the building was considered as an assembly of six contiguous zones of approximately equal volume. The tracer gas sampling points were placed at the centre of each zone on plan, but because of the need to maintain adequate clearance for passing vehicles, they were suspended at a height of approximately three-quarters of the overall height of the building. Following the theoretical considerations of Waters and Simons, for each experimental run, sulphur hexafluoride tracer gas was injected into one of the zones. During the injection process, a small fan was used to give some initial mixing in that zone only. After injection, the fan was switched off, and the tracer gas concentrations in all six zones measured for a period between one and two hours. Results for each run were then processed in two ways:-

(i) Readings for all six sample points were averaged to give a single overall average tracer concentration for the whole building. The decay of this average concentration was fitted using a standard least squares technique to a simple exponential decay law, the decay constant being taken as the fresh air infiltration rate (or graph air change rate) of the whole building.

(ii) Using multizone theory, a specially developed constrained least squares technique was used to determine the complete set of inter-zone flow rates. The fresh air infiltration rate of the whole building was found by summing the flows from the outside into each zone (giving the flow air change rate).

For both methods of analysis, the data set for each run was split into sections, and each section analysed separately. These sections were:-

(i) the first third of the data in the time series

(ii) the second third

(iii) the last third

(iv) the first two thirds

(v) the last two thirds

(vi) the whole data set.

Thus for each method of analysis there are six sets of results for each run. In addition, as an indication of the effect of the constraints, the multizone solution has been obtained from the full data set with reduced constraints and also with all constraints removed.

A total of nine runs were found suitable for complete processing. Table 1 shows the conditions existing during each run, and gives a summary of the results of the infiltration rate, in air changes per hour, obtained by both methods of analysis. The remaining tables, graphs and plans give detailed results for each run. In each case the plan shows predicted interzone flows, expressed in $m^3 s^{-1}$, as calculated by multizone theory. Each plan also shows the flow air change rate (Fach) and the graph air change rate (Gach) for each zone, expressed in air changes per hour. The Fach number is the total air exchange of each zone including both internal and external exchange, calculated from the flow rates. The Gach number is the overall average decay constant for the decay curve for a single zone; the strict theoretical interpretation of this number is in some doubt, as it is unlikely to be an indicator of the fresh air infiltration rate of the zone.

Reliability of the results

It can easily be proved that when the air in a building is not uniformly mixed, the tracer decay curve, whether from a single point or from an average of several points, does not follow a simple exponential decay. Compared with uniformly mixed single zone theory, the tracer concentration usually falls more rapidly during the early stages of decay, and less rapidly during the later stages of decay. Thus the Gach figure from the first third of the data set tends to over estimate the infiltration rate, whereas the Gach figure from later portions of the data set may underestimate it. The Gach figure from the whole data set may, fortuitously, be close to the true value. Table 2 shows the most probable values of the whole building infiltration rate, obtained from the Gach figure for the whole data set, together with the probable range.

Table 2 - Whole Building Infiltration Rates

Run	Infiltration Rate, ach		
	Min	Best estimate	Max
BG4	2.54	2.81	3.54
BG6	2.46	2.51	3.14
BG7	3.65	4.09	6.42
BG8	2.96	3.17	4.29
BG9	4.91	5.63	9.29
BG10	1.97	2.69	2.83
BG12	3.36	3.61	4,47
BG14	2.52	2.58	2.92
BG15	2.73	2.87	3.44

The reliability of the interzone flow rates is not known. Walker (2) has published a theoretical analysis of errors in multizone measurements, but it is insufficient to allow an estimate of the error in each individual flow rate to be made. If the data sets were free from experimental error, and if the fundamental assumptions of multizone theory were actually realised in this particular building, the flow air change rates would be the same whichever section of the data set was used for analysis. Neither condition is true, and so the errors in the computed flow rates are probably large. However, interzone flow rates give an indication of internal flows, and show how fresh air is distributed throughout the building. The experience gained from the measurements will contribute to improvements in the technique for obtaining interzone flow rates.

References

1) J R Waters and M W Simons, "The evaluation of contaminant concentrations and air flows in a multizone model of a building." To be published.

2) R R Walker, "Interpretation and error analysis of multi-tracer gas measurements to determine air movement in a house", Paper 53, 6th AIC Conference, Netherlands, September 1985.

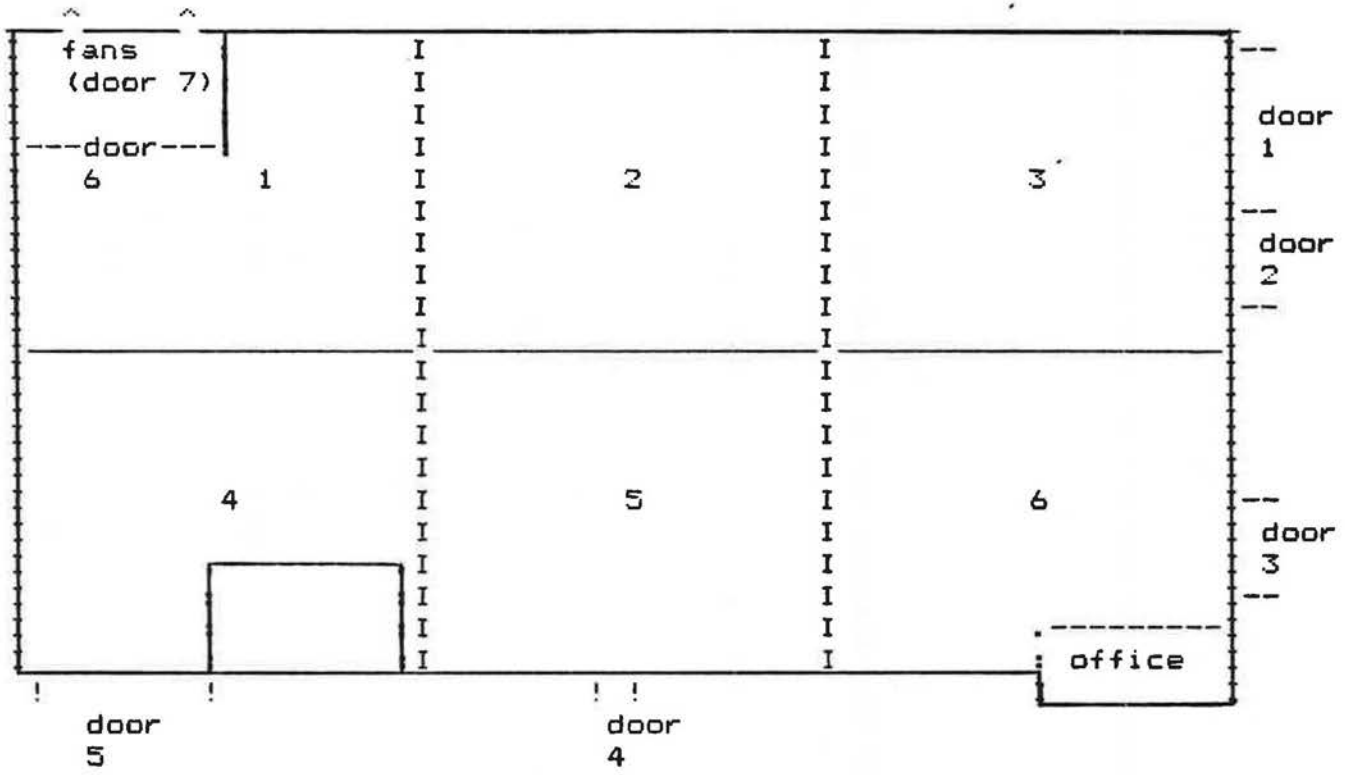

Figure 1 - Plan, Duddeston Mill Transport Depot

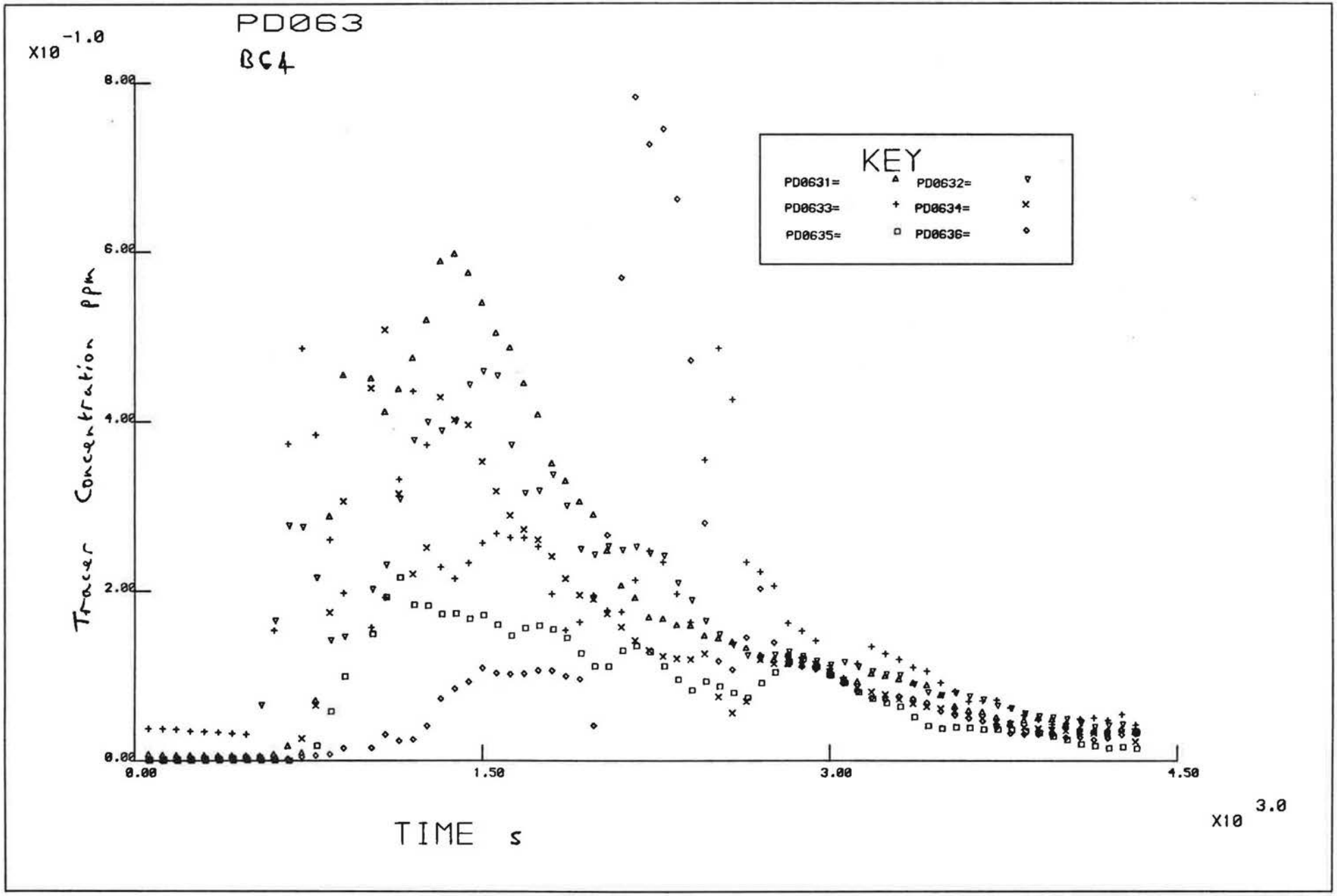
PD063
BC4
X10 -1.0
8.00
6.00
4.00
2.00
0.00
Tracer Concentration ppm
KEY
PD0631=
PD0632=
PD0633=
PD0634=
PD0635=
PD0636=
0.00
1.50
3.00
4.50
X10 3.0
TIME s

Ventilation and Air Movement Measurement System

Coventry (Lanchester) Polytechnic
Dept Civil Engineering and Building
G.V.Lawrance B.Sc.

Date: 12.09.86 Time: 13.45 Run: BG4

Location: British Gas Duddestone Mill Matainance Depot

Program: VAMMS6 Data Number PD063

Comments:

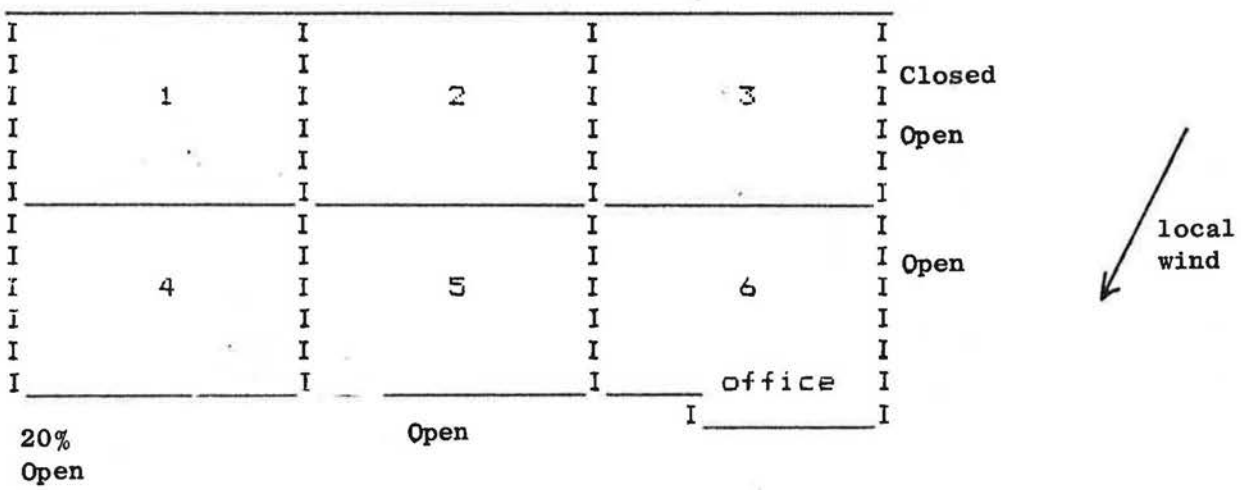

Air Handling System Off. BA Wind Data : 60^{o}, 10 knots

Constraints i) $F_{32} \leqslant 47.2$, $19.8 \leqslant F_{03} + F_{23} + F_{63} \leqslant 23.4$, $F_{36} \leqslant 0.51$

ii) All $F \geqslant 0.00$

Data Used	Flow ACH	Graph ACH	Constraints Used
1st $\frac{1}{3}$	3.65	3.54	i & ii
2nd $\frac{1}{3}$	4.05	2.54	"
3rd $\frac{1}{3}$	6.08	2.83	"
1st $\frac{2}{3}$	2.01	2.77	"
last $\frac{2}{3}$	4.65	2.74	"
All	2.20	2.81	"
All	0.27		ii only
All	0.84		none

Coventry Polytechnic
Department of Civil Engineering and Building
G.V.Lawrance B.Sc.

British Gas , Duddestone Mill Depot

BG4/PD063 12/09/86 1345hrs

Flow Map from All of Data Set , Fully Constrained

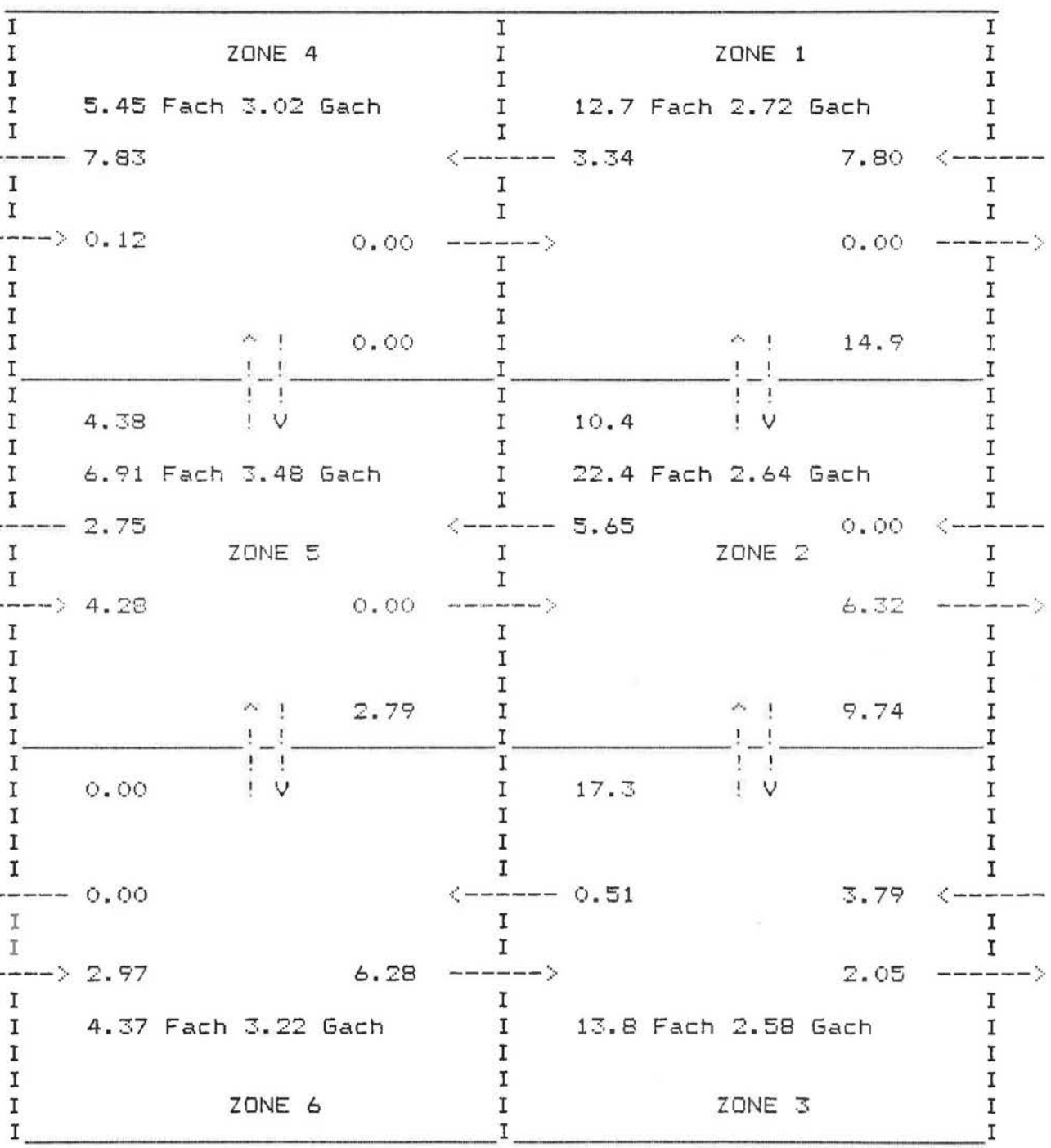

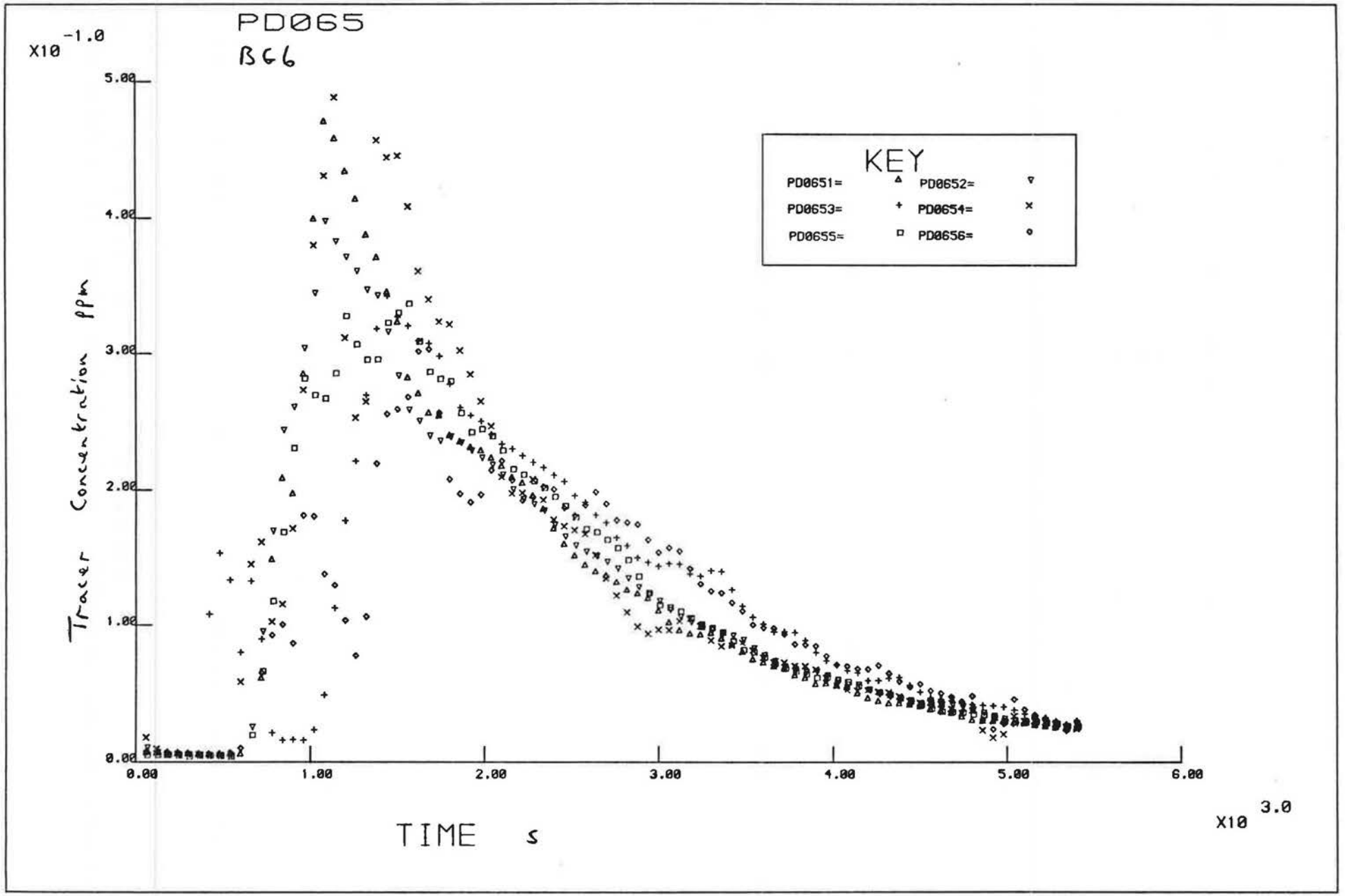
PD065
BG6
X10 -1.0
5.00
4.00
3.00
2.00
1.00
0.00
Tracer Concentration ppm
KEY
PD0651=
PD0652=
PD0653=
PD0654=
PD0655=
PD0656=
0.00
1.00
2.00
3.00
4.00
5.00
6.00
X10 3.0
TIME s

Ventilation and Air Movement Measurement System

Coventry (Lanchester) Polytechnic
Dept Civil Engineering and Building
G.V.Lawrance B.Sc.

Date: 15.9.86 Time: 1300 Run: BG6

Location: British Gas Duddestone Mill Matainance Depot

Program: VAMMS6 Data Number PD065

Comments:

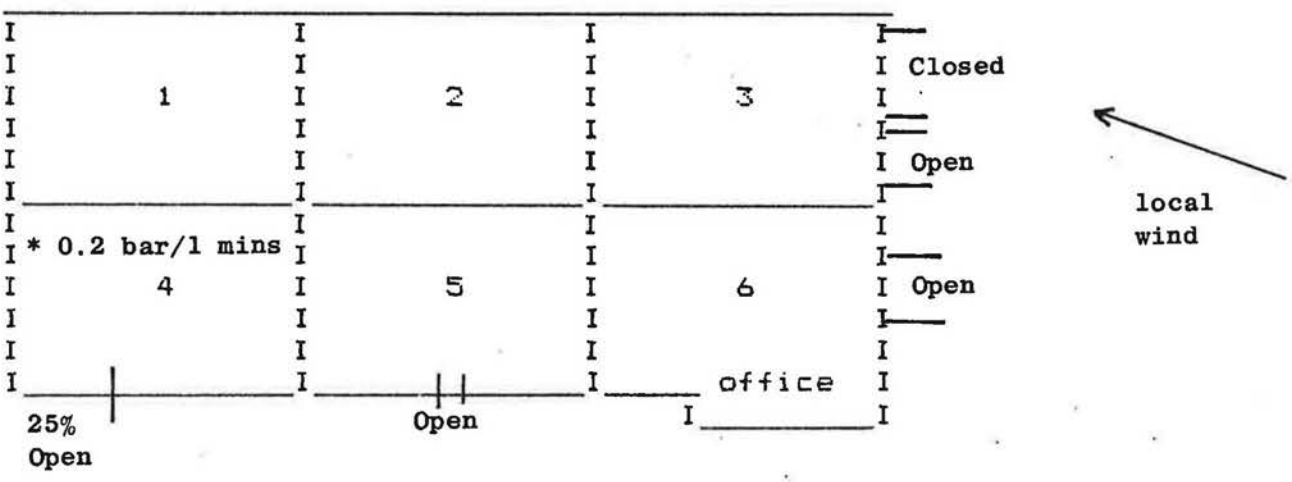

Air Handling System Off: BA Wind Data 30°, 7 knots

Constraints i) $F_{41} \leq 25.2$, $3.8 \leq F_{04} + F_{14} + F_{54} \leq 13.3$, $F_{45} \leq 38.9$

ii) All $F \geq 0.00$

Data Used	Flow ACH	Graph ACH	Constraints
1st $\frac{1}{3}$	0.53	3.14	i & ii
2nd $\frac{1}{3}$	1.00	2.47	"
3rd $\frac{1}{3}$	2.12	2.46	"
1st $\frac{2}{3}$	2.26	2.60	"
last $\frac{2}{3}$	1.66	2.46	"
All	0.91	2.51	"
All	0.78		ii only
All	0.31		none

Coventry Polytechnic
Department of Civil Engineering and Building
G.V.Lawrance B.Sc.

British Gas , Duddestone Mill Depot

BG6/PD065 15/09/86 1300hrs

Flow Map from All of Data Set , Fully Constrained

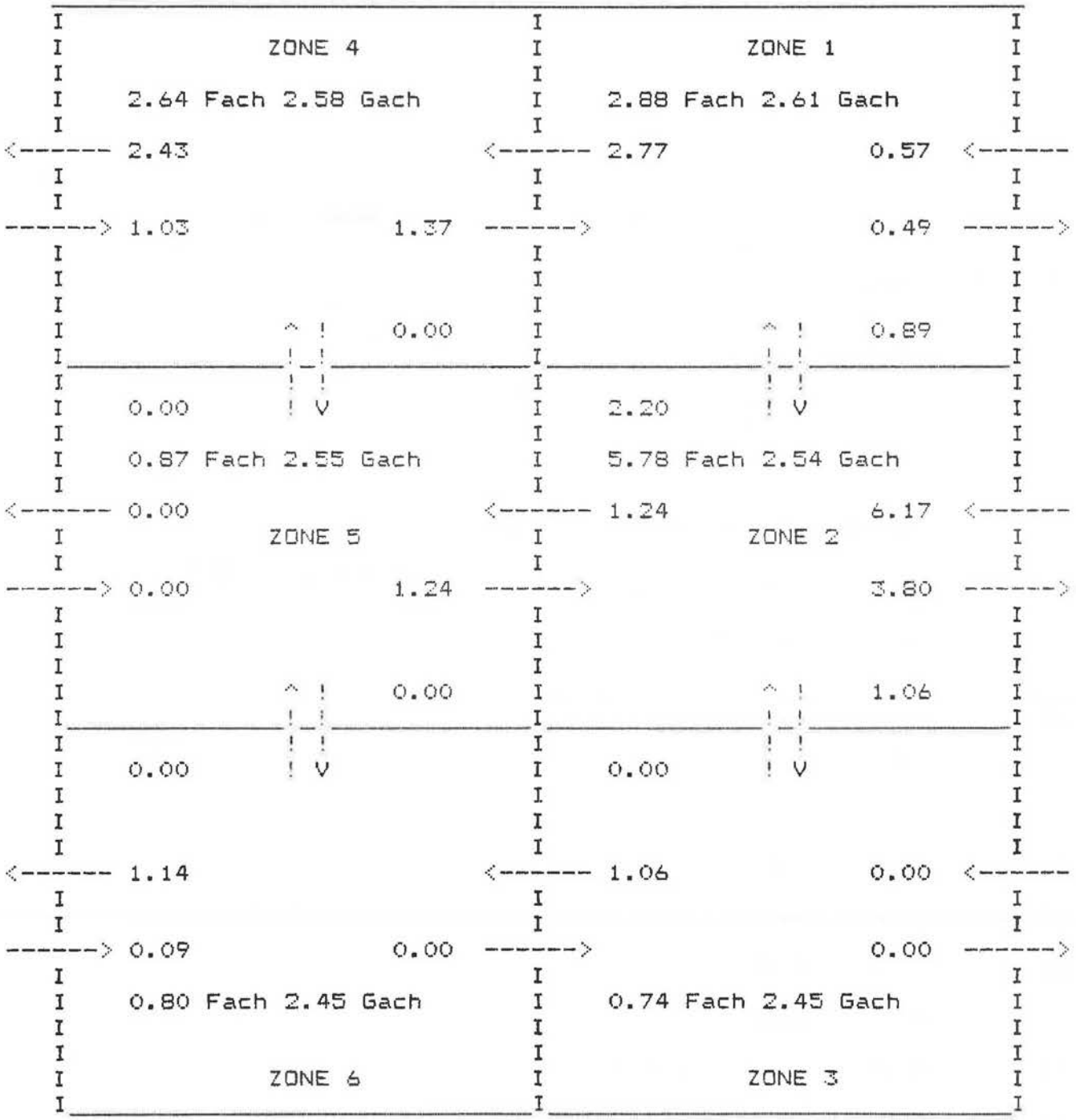

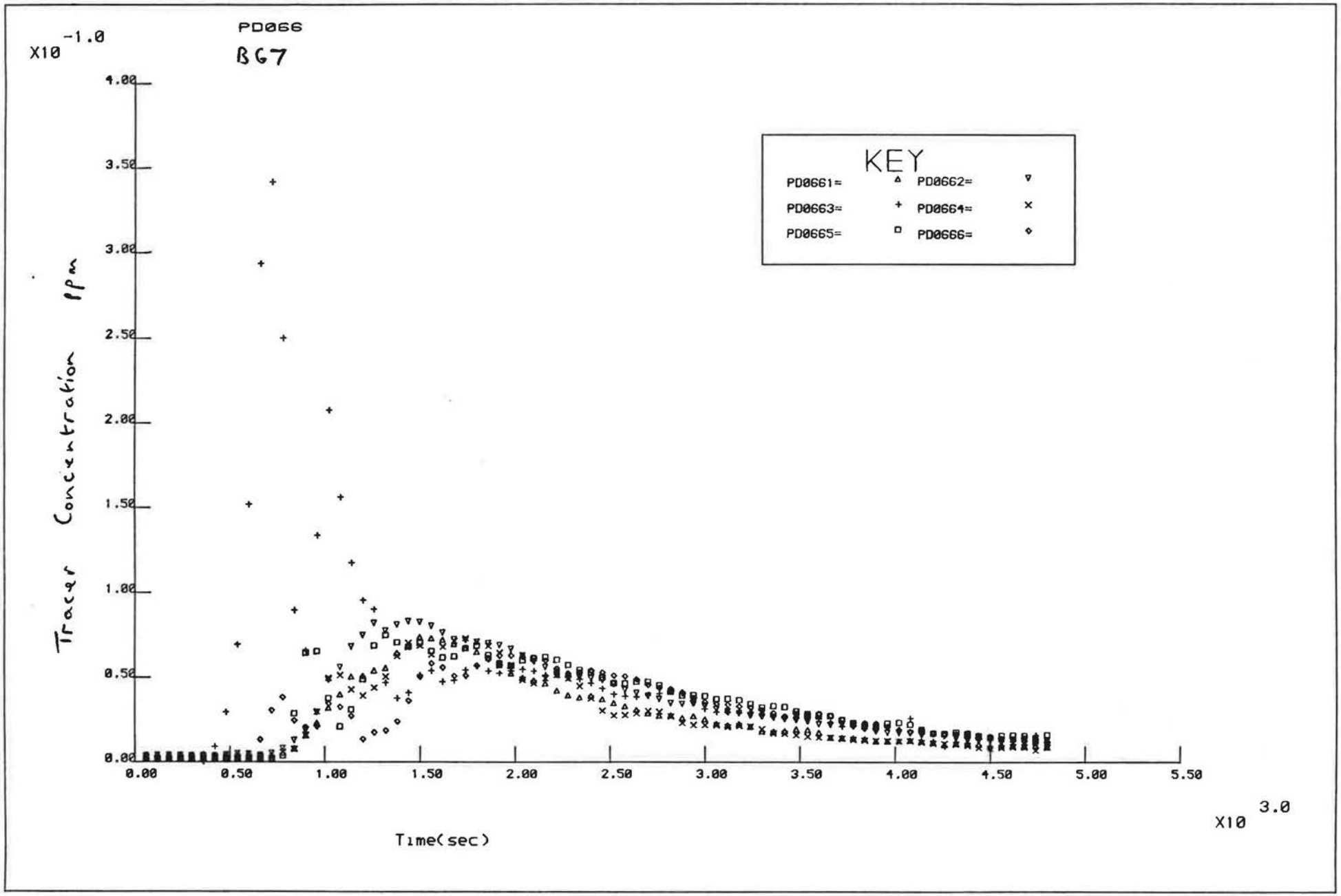
PD066
BG7
X10 -1.0
4.00
3.50
3.00
2.50
2.00
1.50
1.00
0.50
0.00
Tracer Concentration ppm
KEY
PD0661=
PD0662=
PD0663=
PD0664=
PD0665=
PD0666=
0.00
0.50
1.00
1.50
2.00
2.50
3.00
3.50
4.00
4.50
5.00
5.50
X10 3.0
Time(sec)

Ventilation and Air Movement Measurement System

Coventry (Lanchester) Polytechnic
Dept Civil Engineering and Building
G.V.Lawrance B.Sc.

Date: 17.9.86 Time: 11.15 Run: BG7

Location: British Gas Duddestone Mill Matainance Depot

Program: VAMMS6 Data Number PD 066

Comments:

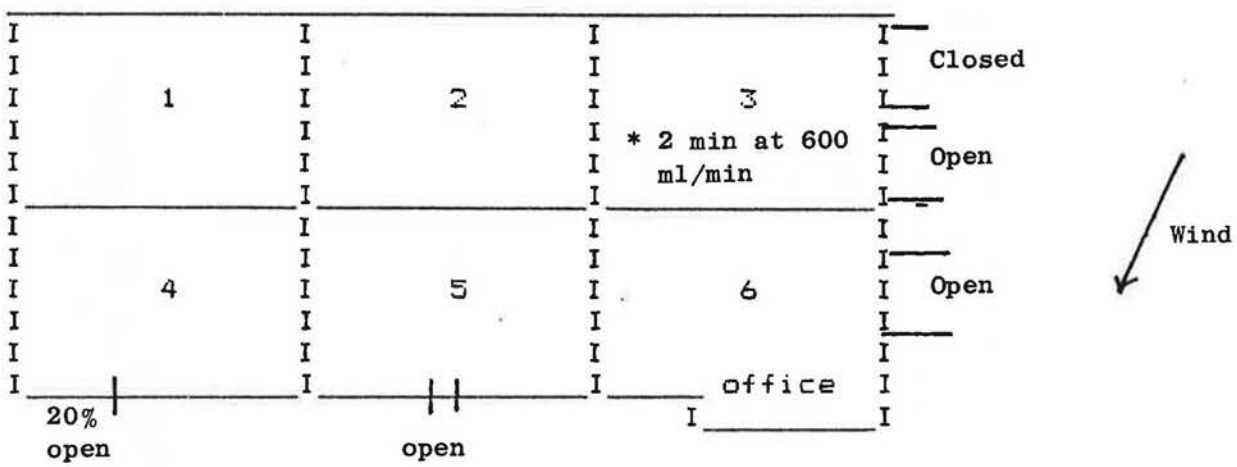

Air Handling System Off: BA Wind Data, 360° 5 (9) knots
Constraints i) $F_{32} \leq 8.7\ m^3/5$, $3.6 \leq F_{03} + F_{23} + F_{63} \leq 63.3$, $F_{36} \leq 3.13$

ii) All $F \geq \emptyset$ (zero)

Data Used	Flow ACH	Graph ACH	Constraints
1st 1/3	1.75	6.42	i and ii
2nd 1/3	1.38	4.29	"
3rd 1/3	0.81	3.65	"
1st 2/3	0.46	4.79	"
last 2/3	1.78	3.86	"
All	0.80	4.09	"
All	0.09		ii only
All	1.48		none

Coventry Polytechnic
Department of Civil Engineering and Building
G.V.Lawrance B.Sc.

British Gas , Duddestone Mill Depot

BG7/PD066 17/09/86 1115hrs

Flow Map from First Third of Data Set , Fully Constrained

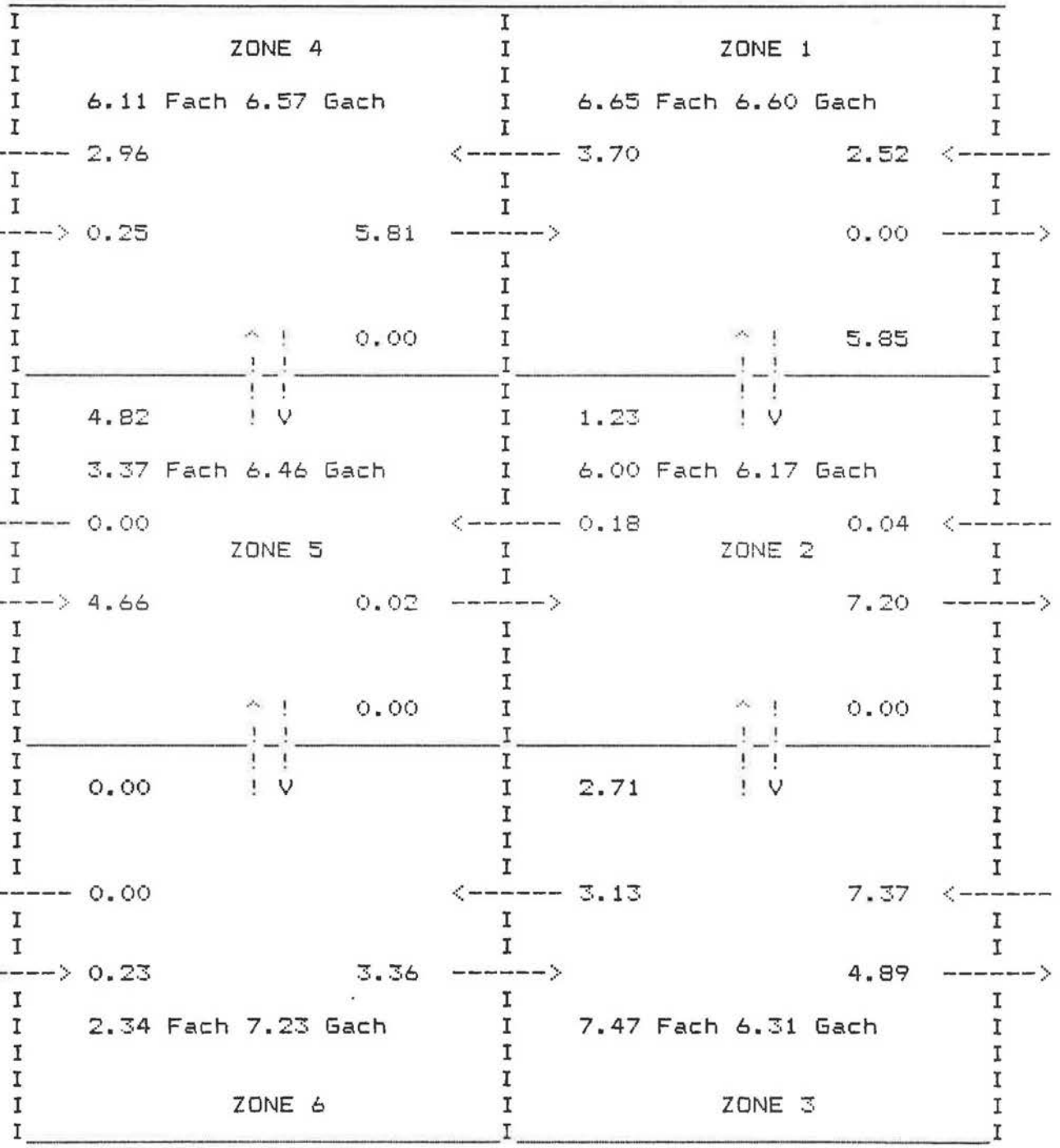

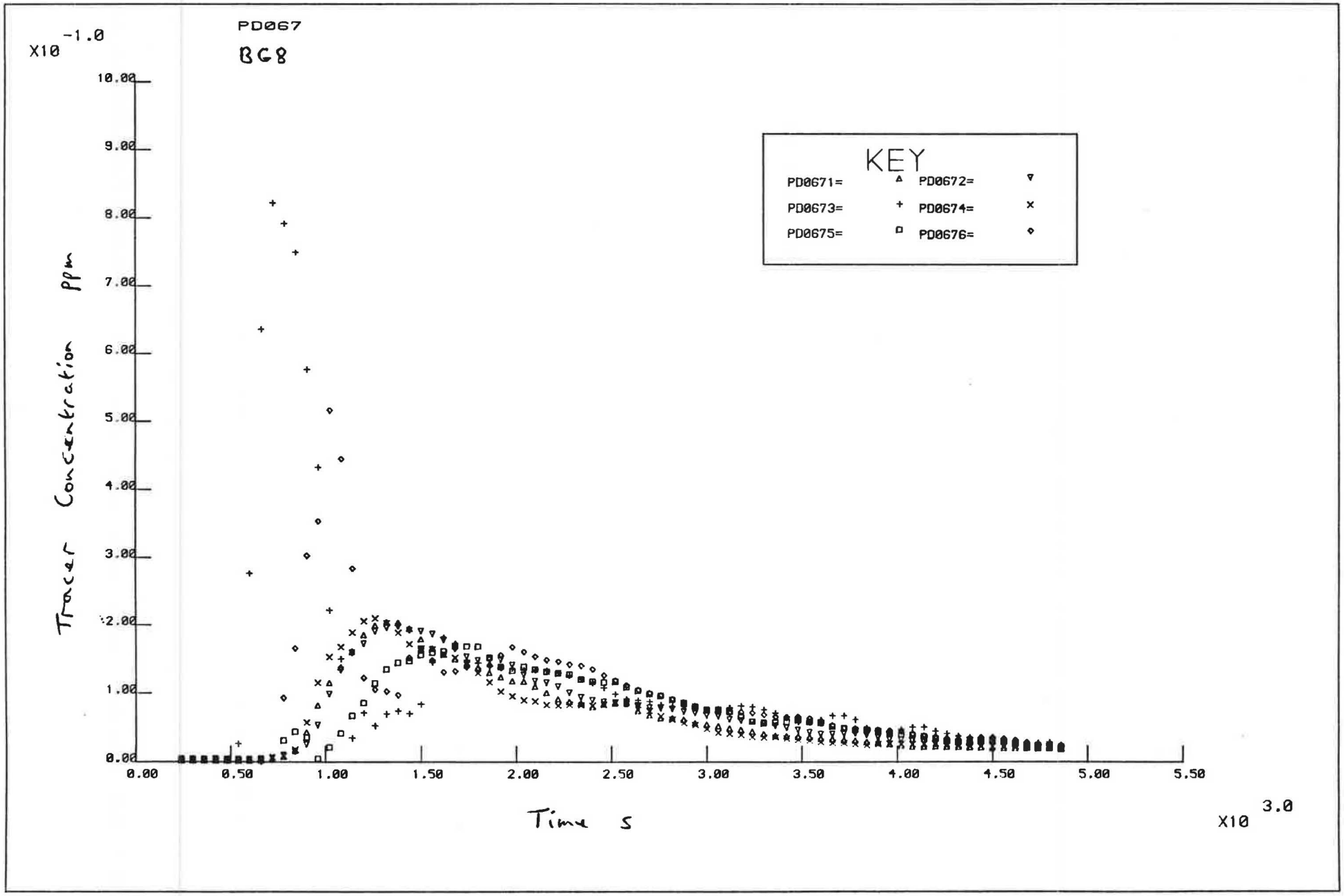
PD067
BG8
X10 -1.0
Tracer Concentration ppm
10.00
9.00
8.00
7.00
6.00
5.00
4.00
3.00
2.00
1.00
0.00
0.00
0.50
1.00
1.50
2.00
2.50
3.00
3.50
4.00
4.50
5.00
5.50
Time s
X10 3.0
KEY
PD0671=
PD0672=
PD0673=
PD0674=
PD0675=
PD0676=

Ventilation and Air Movement Measurement System

Coventry (Lanchester) Polytechnic
Dept Civil Engineering and Building
G.V.Lawrance B.Sc.

Date: 17.9.86 Time: 13.30 Run: BG8

Location: British Gas Duddestone Mill Matainance Depot

Program: VAMMS6 Data Number PD 067

Comments:

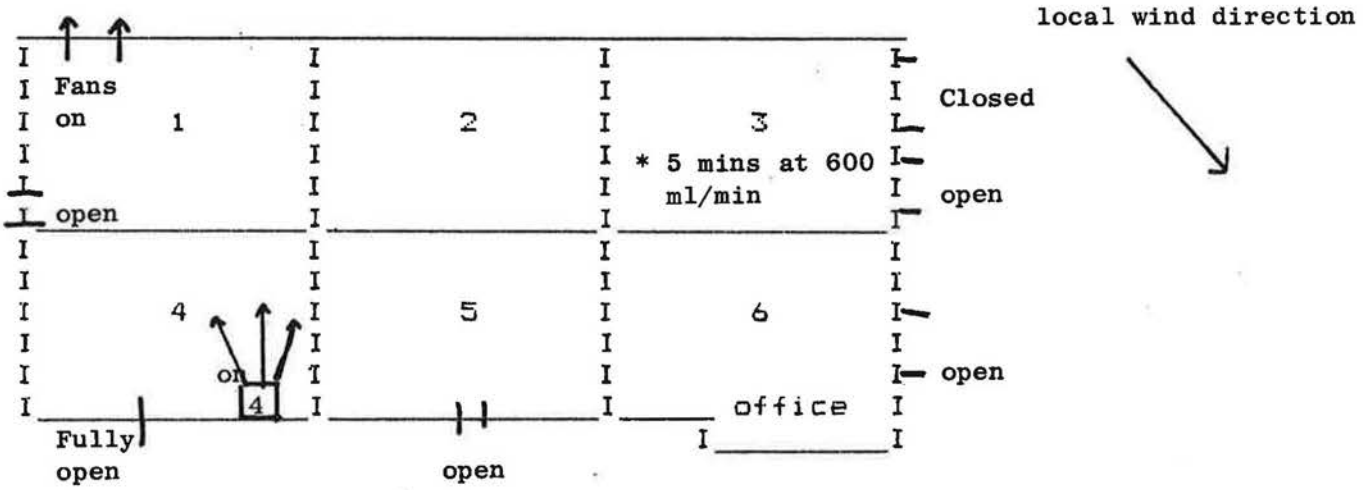

Air Handling System Off. BA Wind Data : 360°, 5 knots (9)

Constraints = i) $F_{32} \leq 6.4$, $14.2 \leq F_{03} + F_{23} + F_{63} \leq 54.6$, $F_{36} \leq 12.2$

ii) All $F \geq 0$

Data Used	Flow ACH	Graph ACH	Constraints
1st 1/3	1.395	4.29	i & ii
2nd 1/3	4.043	3.26	"
3rd 1/3	4.332	2.96	"
1st 2/3	2.979	3.50	"
last 2/3	4.939	3.06	"
All	3.763	3.17	"
All	3.023		ii only
All	0.297		none

Coventry Polytechnic
Department of Civil Engineering and Building
G.V.Lawrance B.Sc.

British Gas , Duddestone Mill Depot

BG8/PD067 17/09/86 1330hrs

Flow Map from All of Data Set , Fully Constrained

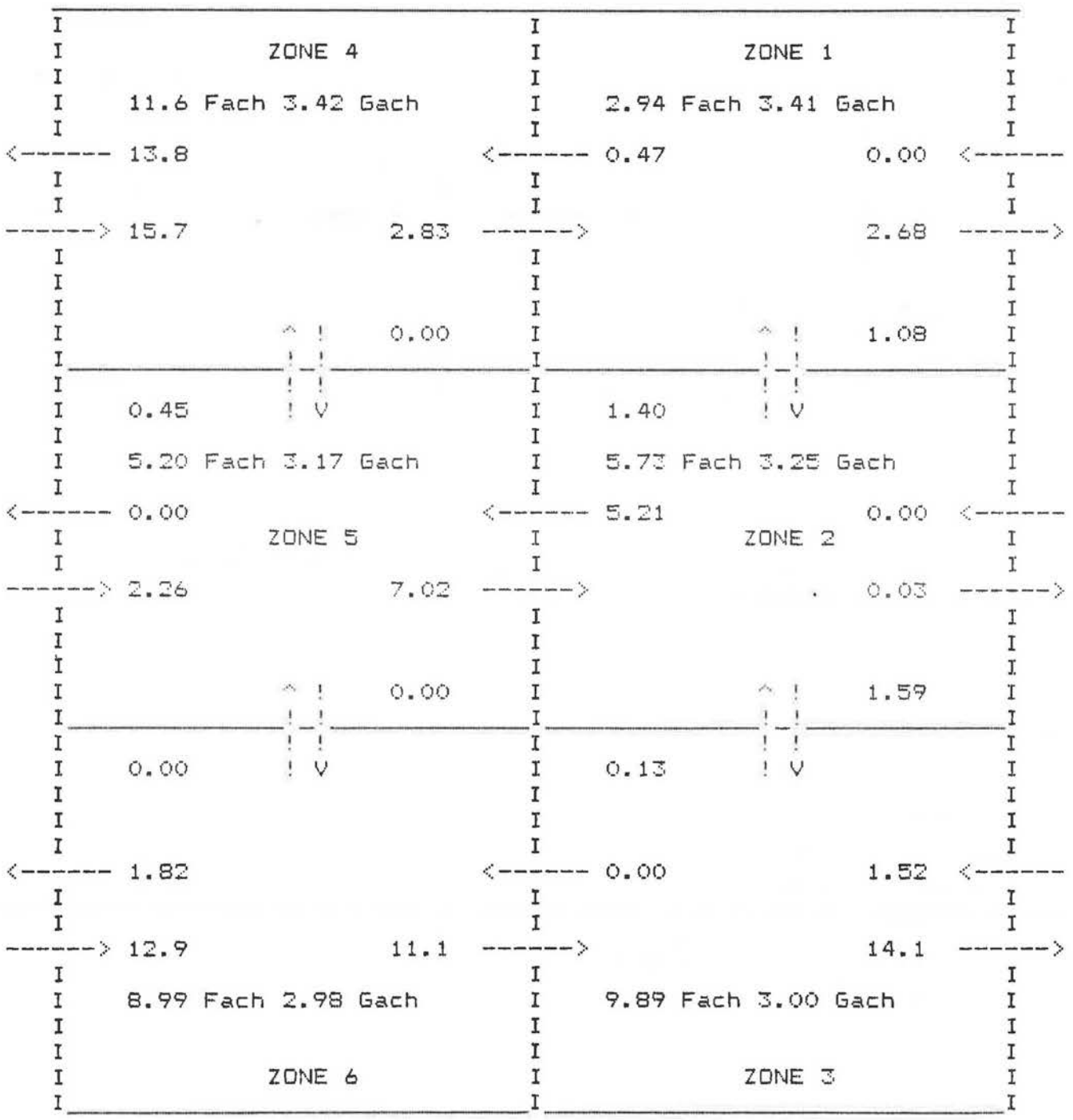

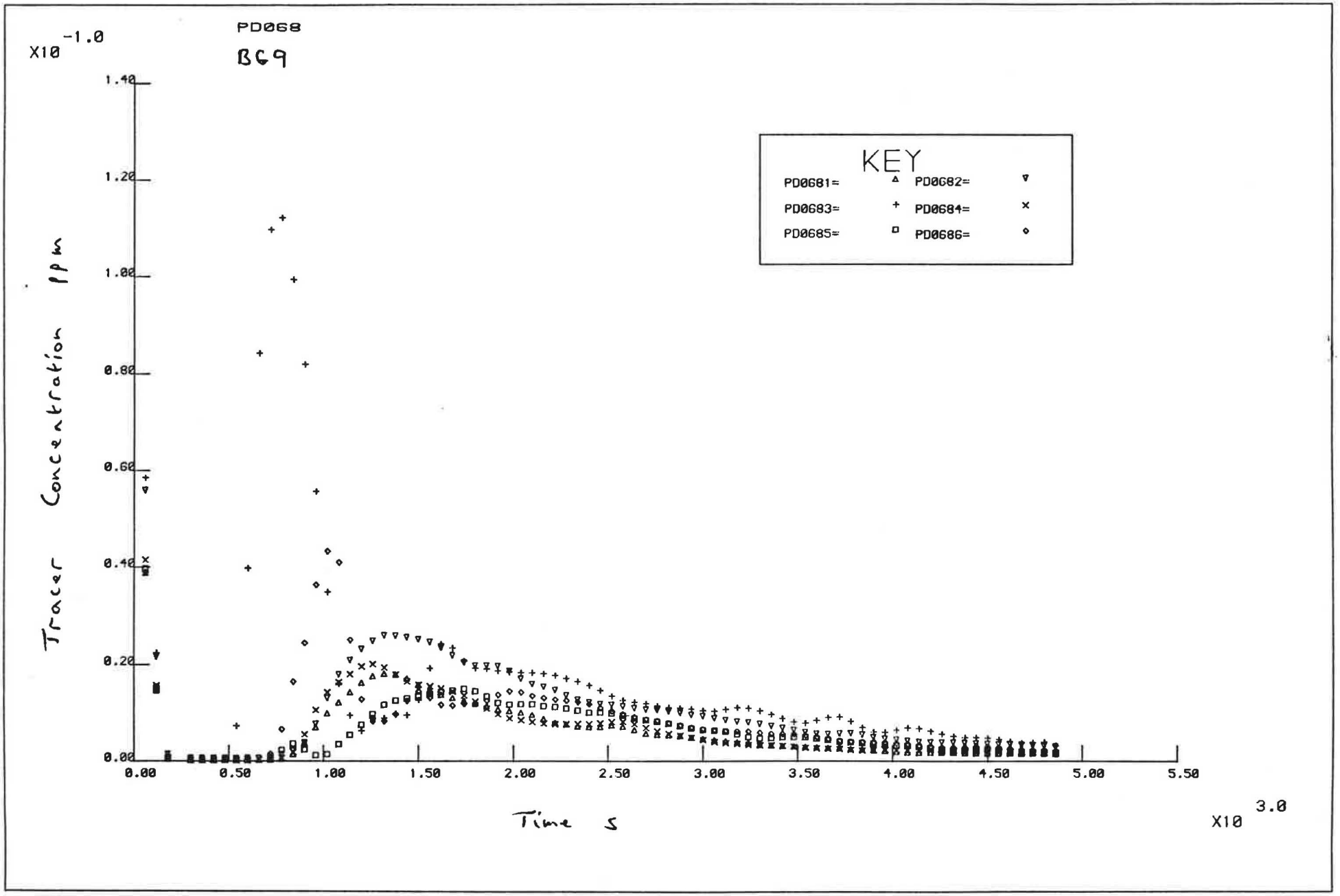
PD068
BG9
X10 -1.0
1.40
1.20
1.00
0.80
0.60
0.40
0.20
0.00
Tracer Concentration ppm
KEY
PD0681=
PD0682=
PD0683=
PD0684=
PD0685=
PD0686=
0.00
0.50
1.00
1.50
2.00
2.50
3.00
3.50
4.00
4.50
5.00
5.50
Time s
X10 3.0

Ventilation and Air Movement Measurement System

Coventry (Lanchester) Polytechnic
Dept Civil Engineering and Building
G.V.Lawrance B.Sc.

Date: 17.9.86 Time: 15.30 Run: B69

Location: British Gas Duddestone Mill Matainance Depot

Program: VAMMS6 Data Number PD 068

Comments:

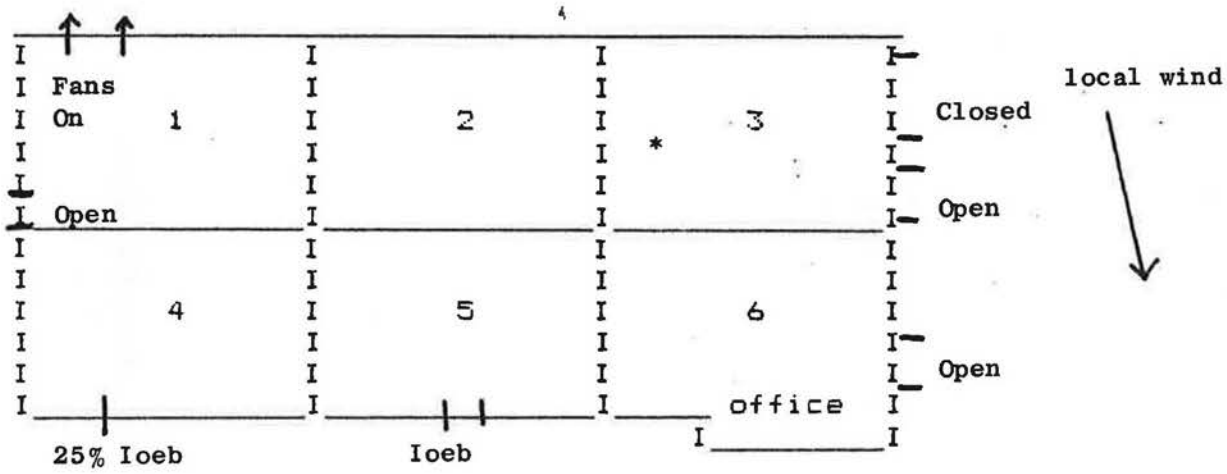

Air Handling System Off. BA Wind Data : 340°, 7 knots (12)

Constraints i) $F_{32} \leq 11.2$, $11.8 \leq F_{03} + F_{23} + F_{63} \leq 46.3$, $F_{36} \leq 10.1$

ii) All $F \geq \emptyset$

Air change rates for whole building

Data Used	Flow ACH	Graph ACH	Constraints Applied
1st 1/3	6.551	9.29	i & ii
2nd 1/3	2.894	6.07	"
3rd 1/3	5.143	4.91	"
1st 2/3	2.327	6.82	"
last 2/3	4.943	5.28	"
All	4.356	5.63	"
All	6.127		ii only
All	4.373		none

Coventry Polytechnic
Department of Civil Engineering and Building
G.V.Lawrance B.Sc.

British Gas , Duddestone Mill Depot

BG9/PD068 17/09/86 1530hrs

Flow Map from First Third of Data Set , Fully Constrained

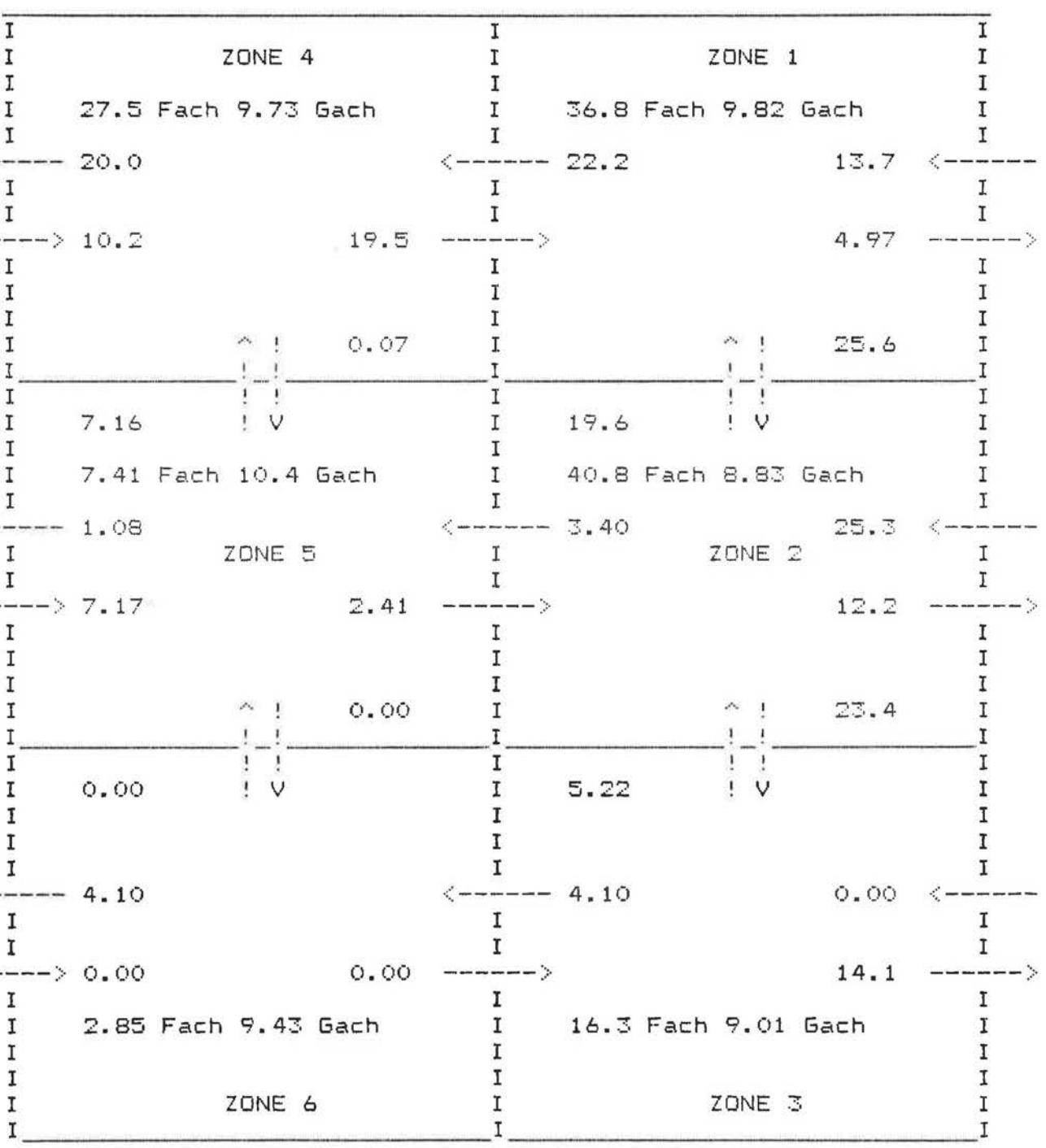

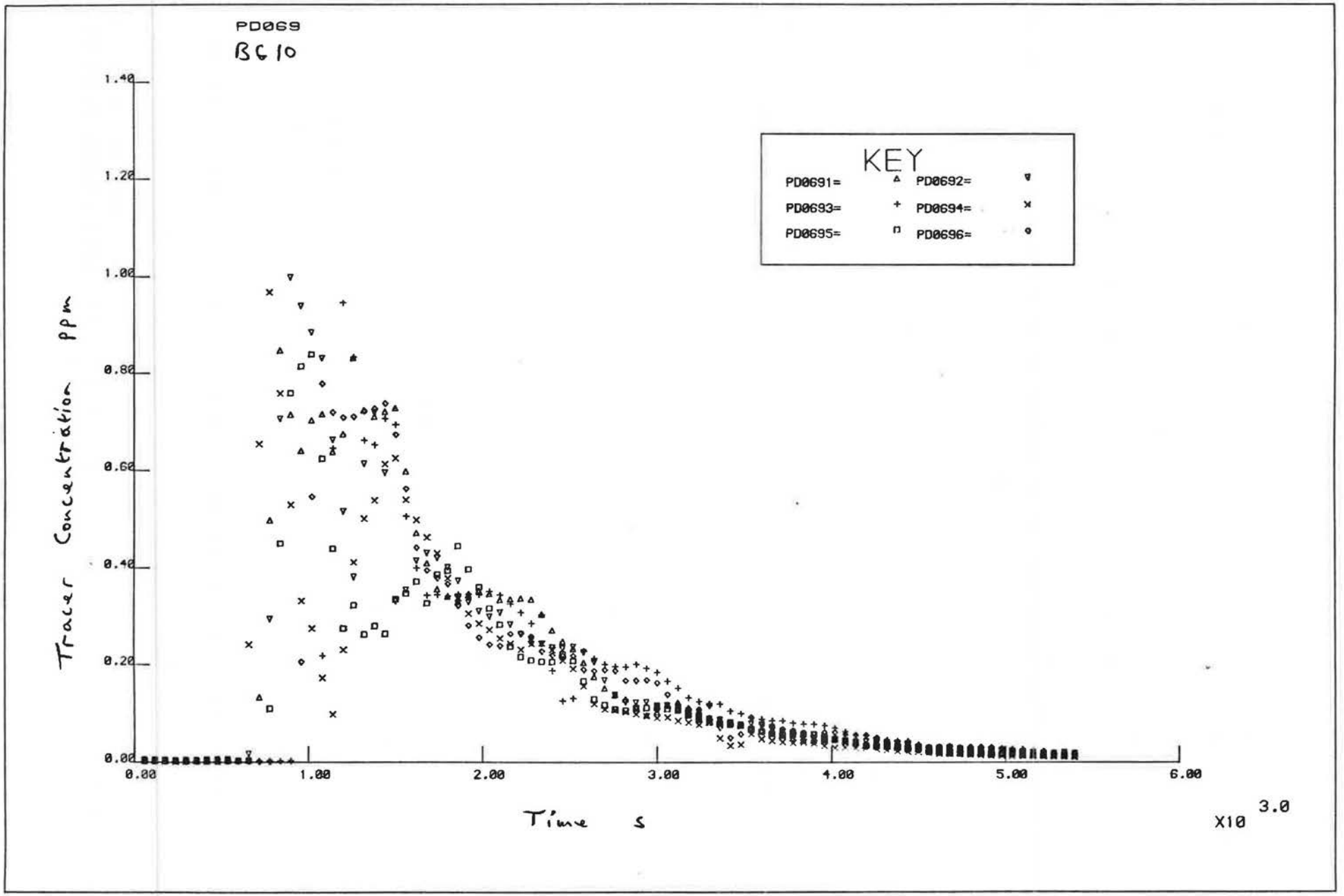
PD069
BG 10
KEY
PD0691=
PD0692=
PD0693=
PD0694=
PD0695=
PD0696=
Tracer Concentration ppm
1.40
1.20
1.00
0.80
0.60
0.40
0.20
0.00
0.00
1.00
2.00
3.00
4.00
5.00
6.00
Time s
X10 3.0

Ventilation and Air Movement Measurement System

Coventry (Lanchester) Polytechnic
Dept Civil Engineering and Building
G.V.Lawrance B.Sc.

Date: 18.9.86 Time: 10.15 Run: BG10

Location: British Gas Duddestone Mill Matainance Depot

Program: VAMMS6 Data Number PD 069

Comments:

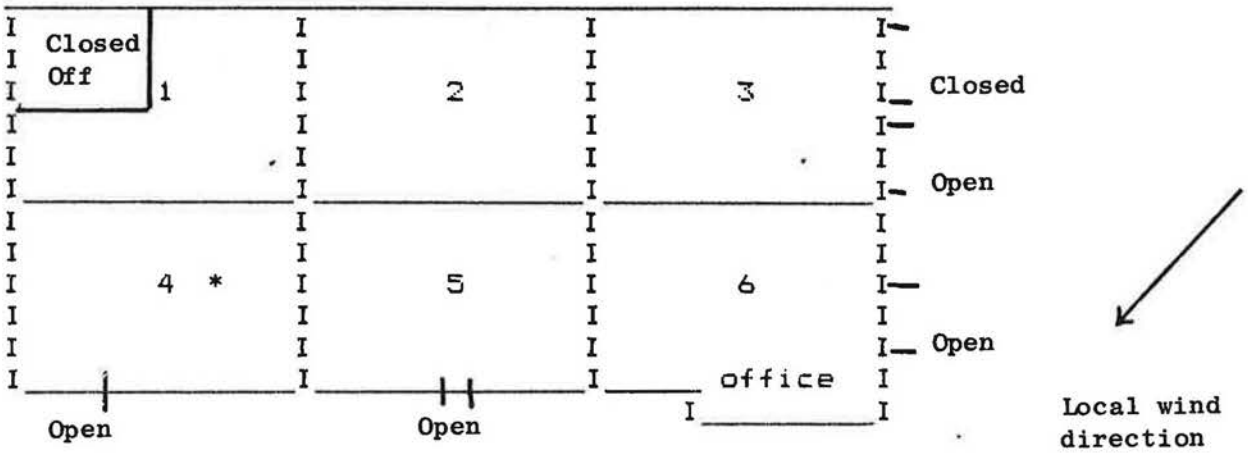

Air Handling System Off: BA Wind Data: 20^{o}, 9 knots (13)

Constraints: i) $F_{41} \leq 22.0$, $16.4 \leq F_{09} + F_{14} + F_{34} \leq 39.3$, $F_{45} \leq 26.7$

ii) All $F \geq 0$

Air change Rates for Whole Building

Data Used	Flow ACH	Graph ACH	Constraints Applied
1st 1/3	0.883	1.97	i & ii
2nd 1/3	1.967	2.59	"
3rd 1/3	1.275	2.83	"
1st 2/3	0.613	2.46	"
last 2/3	2.309	2.76	"
All	1.166	2.69	"
All	2.172		ii only
All	2.793		none

Coventry Polytechnic
Department of Civil Engineering and Building
G.V.Lawrance B.Sc.

British Gas , Duddestone Mill Depot

BG10/PD069 18/09/86 1015hrs

Flow Map from All of Data Set , Fully Constrained

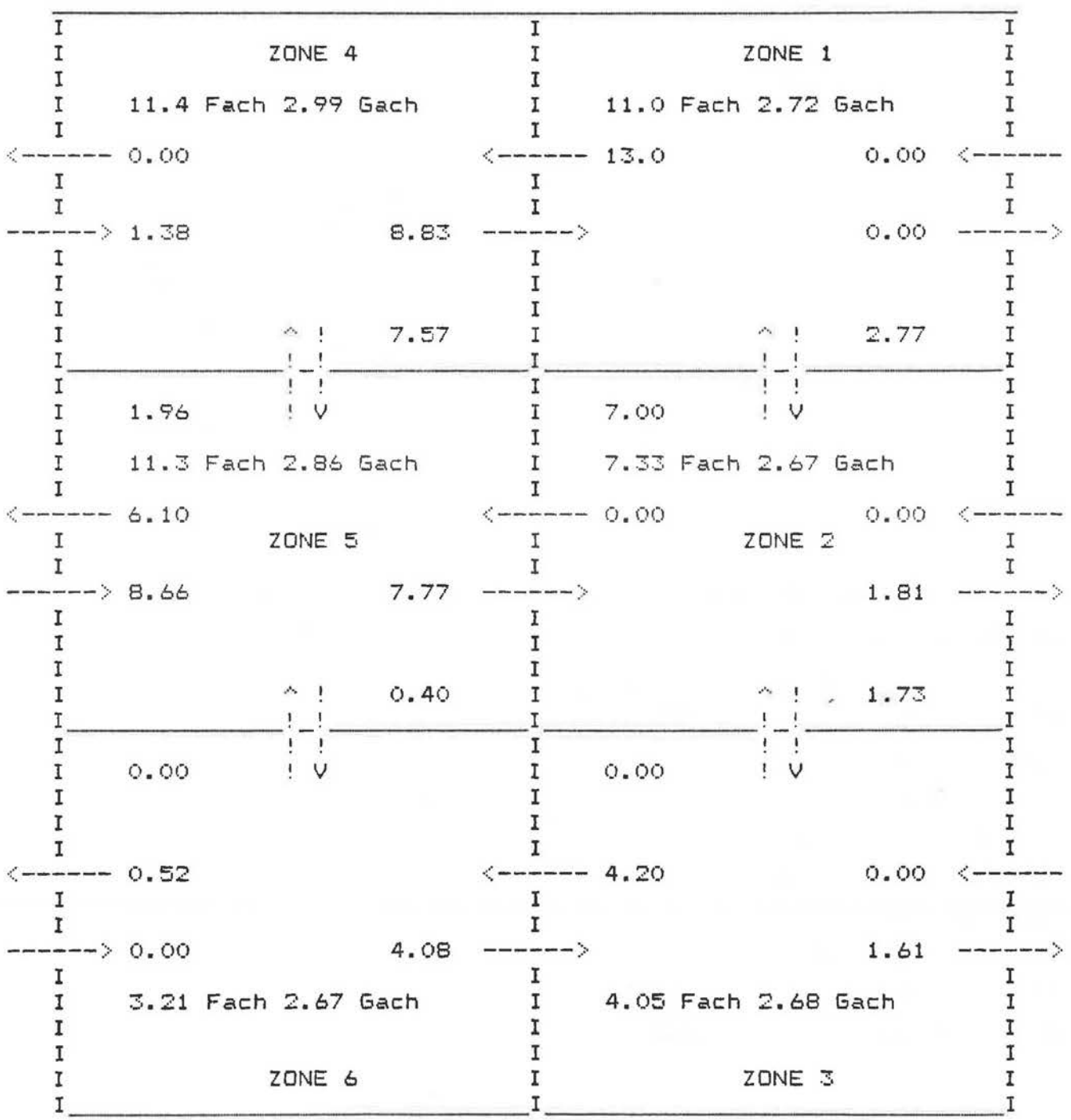

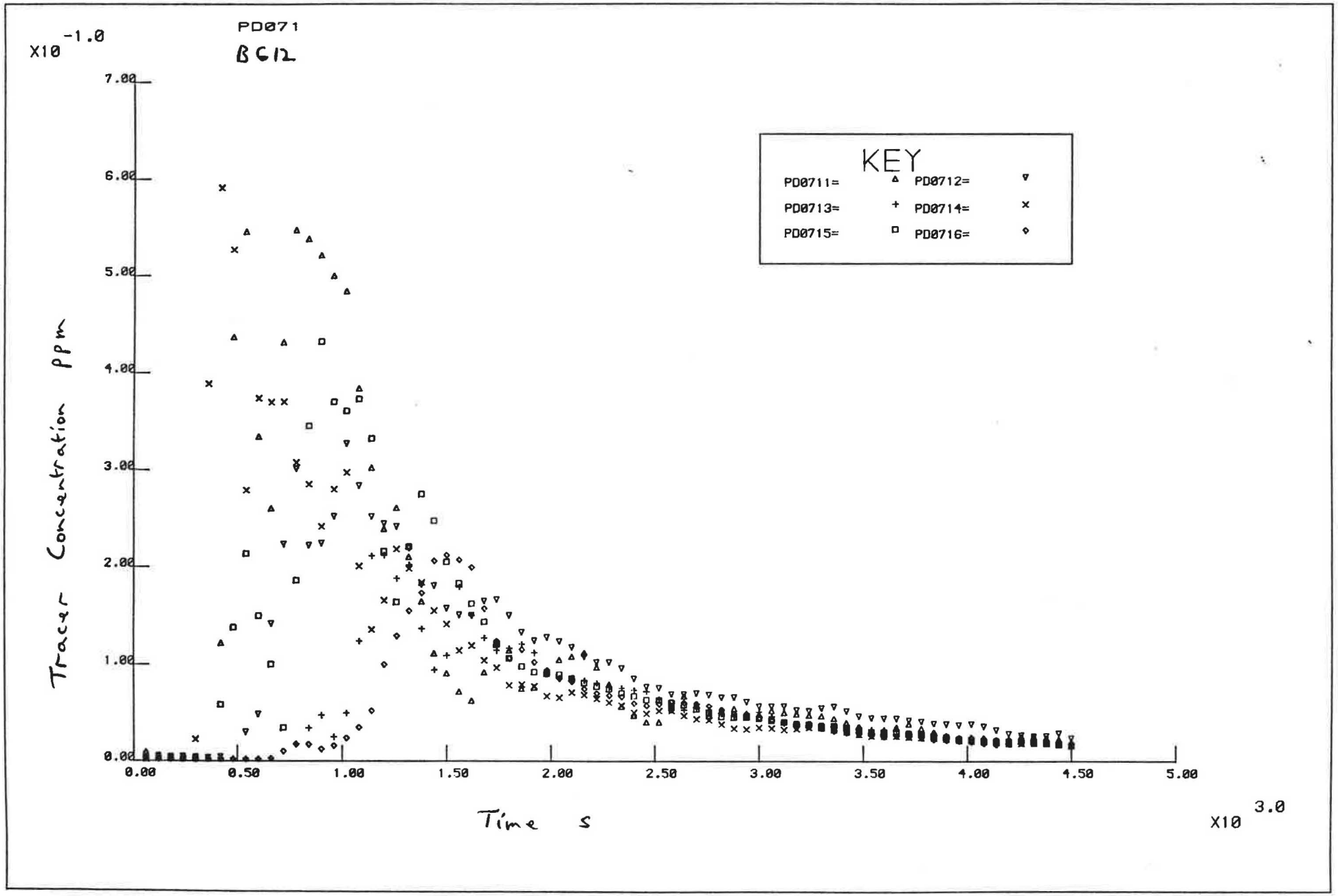
PD071
BC12
X10 -1.0
7.00
6.00
5.00
4.00
3.00
2.00
1.00
0.00
Tracer Concentration ppm
KEY
PD0711=
PD0712=
PD0713=
PD0714=
PD0715=
PD0716=
0.00
0.50
1.00
1.50
2.00
2.50
3.00
3.50
4.00
4.50
5.00
Time s
X10 3.0

Ventilation and Air Movement Measurement System

Coventry (Lanchester) Polytechnic
Dept Civil Engineering and Building
G.V.Lawrance B.Sc.

Date: 22.9.86 Time: 10.40 Run: BG12

Location: British Gas Duddestone Mill Matainance Depot

Program: VAMMS6 Data Number PD 071

Comments:

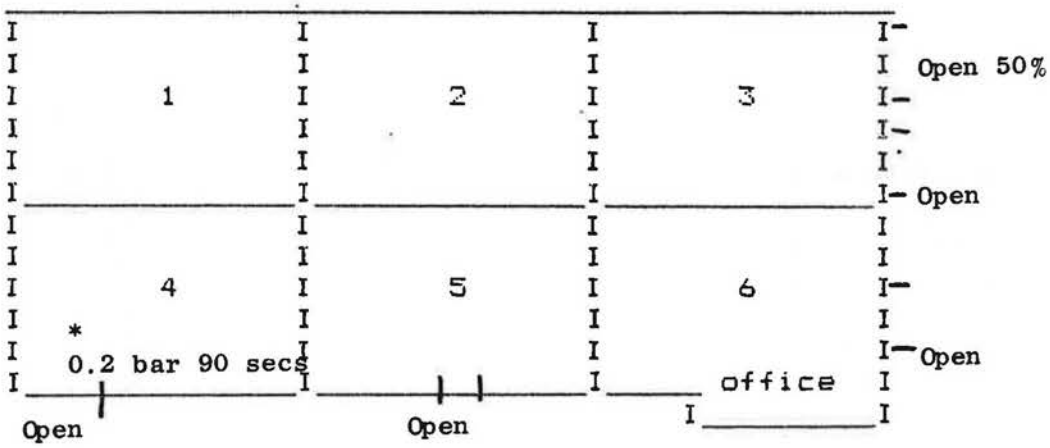

Air Handling System On (10-15% Fresh Air)
BA Wind Data 260°, 5 knots (10)
Constraints i) $F_{41} \leq 25.4$, $6.6 \leq F_{04} + F_{14} + F_{54} \leq 24.7$, $F_{45} \leq 26.7$

ii) All $F \geq \emptyset$

Air Change Rates for Whole Building

Data Used	Flow ACH	Graph ACH	Constraints Applied
1st 1/3	0.542	4.47	i & ii
2nd 1/3	2.159	3.85	"
3rd 1/3	3.713	3.36	"
1st 2/3	0.991	4.00	"
Last 2/3	2.147	3.52	"
All	0.748	3.61	"
All	0.748		ii only
All	2.510		none

Note Full Match ie. constraints (i) had no bearing on these results.

NB: with the air handling system on the normal connections between zones are added tog this is because the AHS extracts in zone 2 and intracts in all zones.

Coventry Polytechnic
Department of Civil Engineering and Building
G.V.Lawrance B.Sc.

British Gas , Duddestone Mill Depot

BG12/PD071 22/09/86 1040hrs

Flow Map from All of Data Set , Initial Condition Constraints had no effect

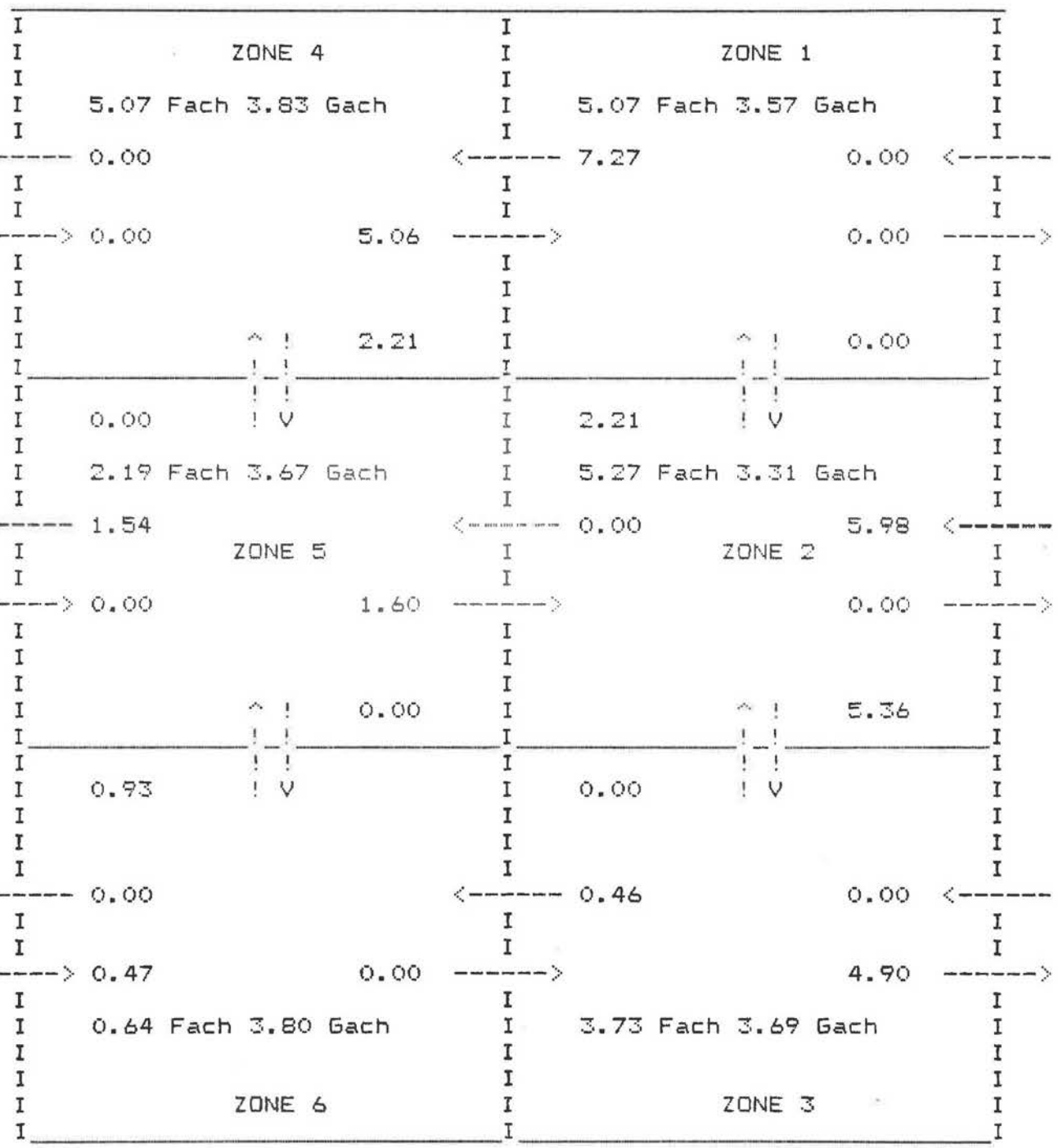

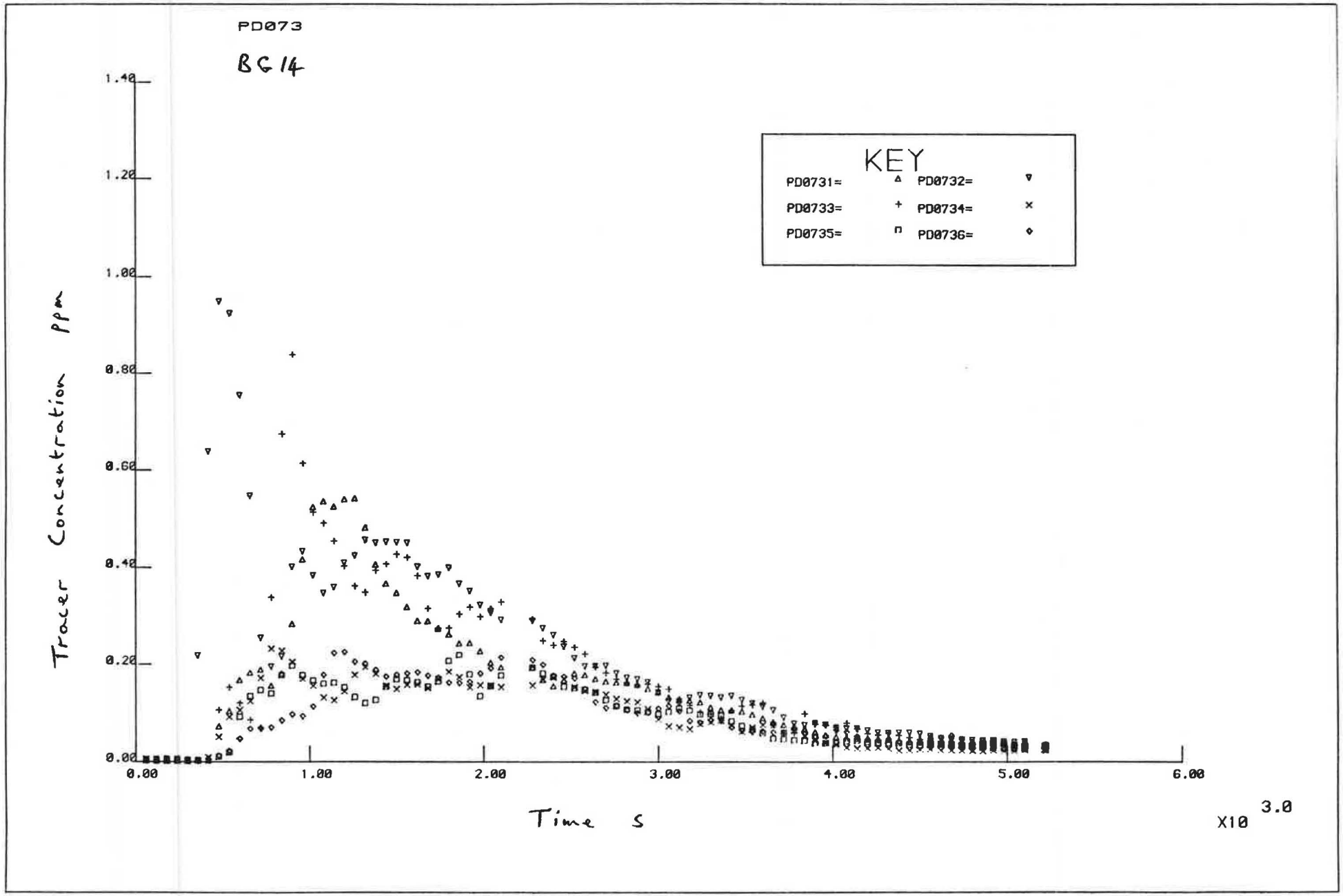
PD073
BG14
KEY
PD0731=
PD0732=
PD0733=
PD0734=
PD0735=
PD0736=
Tracer Concentration ppm
1.40
1.20
1.00
0.80
0.60
0.40
0.20
0.00
0.00
1.00
2.00
3.00
4.00
5.00
6.00
Time s
X10 3.0

Ventilation and Air Movement Measurement System

Coventry (Lanchester) Polytechnic
Dept Civil Engineering and Building
G.V.Lawrance B.Sc.

Date: 23.9.86 Time: 10.15 Run: BG 14

Location: British Gas Duddestone Mill Matainance Depot

Program: VAMMS6 Data Number PD 073

Comments:

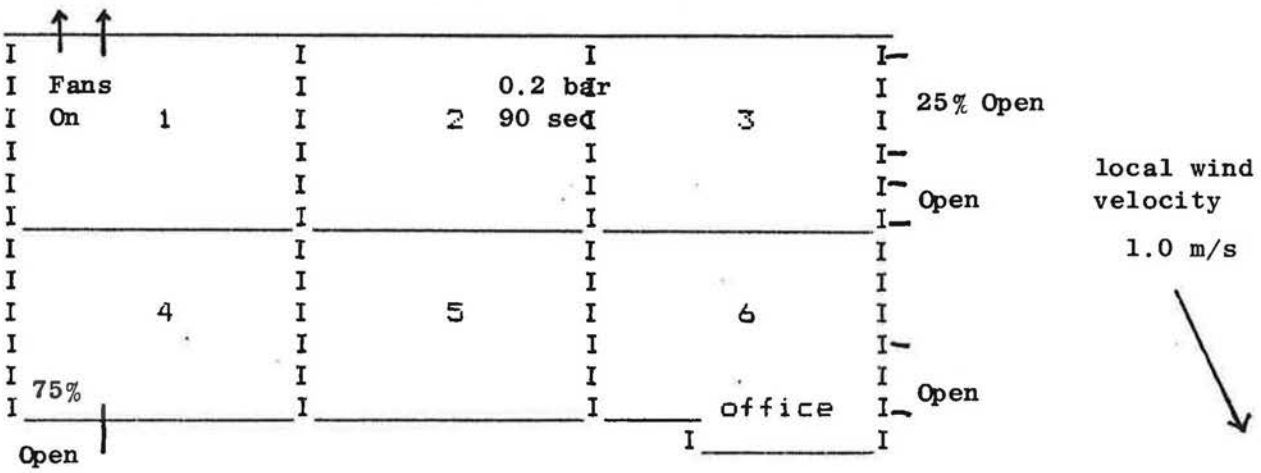

Air Handling System On at 10% Fresh Air
BA Wind Data : 320°, 5 knots (9)
Constraints: i) $F_{21} \leq 5.0$, $8.3 \leq F_{10} + F_{12} + F_{32} + F_{52} \leq 51.6$, $F_{23} \leq 7.9$, $F_{25} \leq 3.9$

ii) All $F \geq 0$

Air Change Rates for Whole Building

Data Used	Flow ACH	Graph ACH	Constraints Applied
1st 1/3	0.962	2.92	i & ii
2nd 1/3	2.849	2.52	"
3rd 1/3	1.140	2.56	"
1st 2/3	0.538	2.61	"
Last 2/3	1.645	2.55	"
All	1.205	2.58	"
All	1.220		ii only
All	2.599		none

Coventry Polytechnic
Department of Civil Engineering and Building
G.V.Lawrance B.Sc.

British Gas , Duddestone Mill Depot

BG14/PD073 23/09/86 1015hrs

Flow Map from First Third of Data Set , Fully Constrained

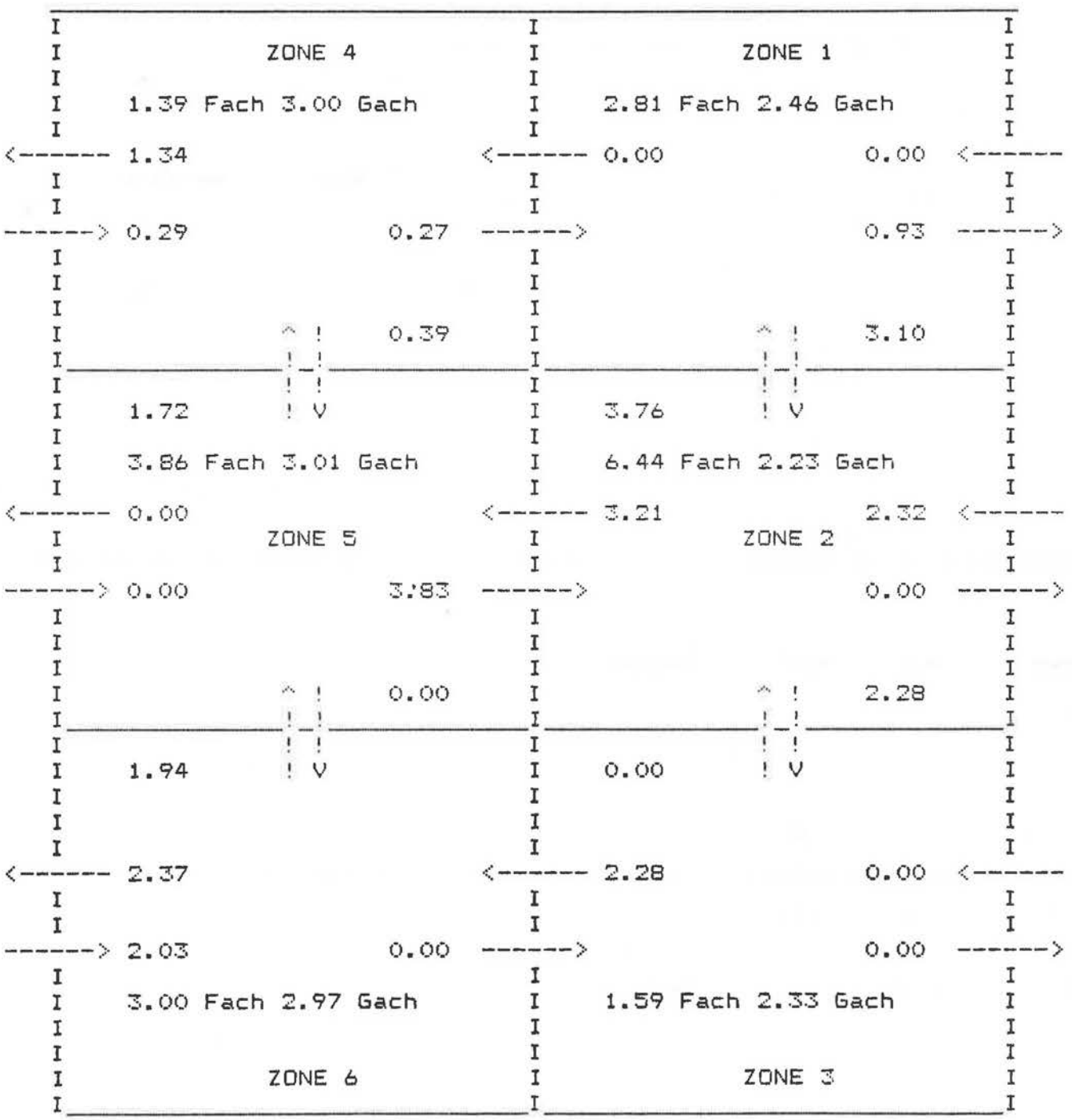

THE MEASUREMENT OF VENTILATION AND AIR MOVEMENT IN FACTORY BUILDINGS

M.W. SIMONS and J.R. WATERS

International Congress on Building Energy Management
ICBEM '87
Lausanne
September/October 1987

THE MEASUREMENT OF VENTILATION AND AIR MOVEMENT IN FACTORY BUILDINGS

M.W. SIMONS and J.R. WATERS
Department of Civil Engineering and Building
Coventry Lanchester Polytechnic
Coventry CV1 5FB, U.K.

1. Introduction

The majority of factory buildings may be considered as large single-cell structures. In order to measure the air infiltration characteristics of such buildings, it has been found necessary to consider air movement patterns within them. The simultaneous consideration of both air infiltration and internal air movement has the added advantage that the dispersal of air-borne contaminants within the factory can also be studied. Using multi-zone air movement theory, in which one zone represents the outside air, air exchange between the inside and the outside and between internal zones may be measured and evaluated.

The equations governing flows in the multi-zone model are well known (1,2). Application of these equations to multi-zone tracer decay measurements (3) has shown how it is possible to:

1. determine the best initial distribution of the tracer gas, i.e. the most advantageous seeding strategy,

2. avoid inaccurate results due to ill conditioning or linear dependence,

3. maximise the information that can be obtained from a set of measured data.

An automated tracer gas monitoring system has been designed and built. The system is being used to measure air infiltration and air movement in a range of large single cell buildings, most of which are factories. The objective is to gain experience of the operation of the equipment, to refine data analysis techniques, and to provide a data bank as a basis for further developments of the theory.

2. Instrumentation

An automated six channel tracer decay system, using sulphur hexafluoride as the tracer gas, has been specially designed and constructed (4). The design is based on the experience of a pilot study (5), and a review of similar work in large single cell buildings (e.g. 6). The

principal features of the system are:

1. Tracer gas concentration is measured by six independent gas chromatographs, one per channel. This allows fast sampling on each channel, so that rapid changes in tracer gas concentration may be followed.

2. Each chromatograph uses a pulse modulated electron capture detector. This gives a combination of high sensitivity and a wide linear operating range, so that large changes of tracer gas concentration can be measured without loss of accuracy.

3. The chromatograph parameters have been optimised for sulphur hexafluoride, thereby minimising interference due to other electrophilic compounds which may be present in industrial atmospheres.

To avoid cross contamination, the tracer injection system is separate from the measuring system. It consists of a gas cylinder, flow meter, and nozzle, the nozzle being attached to a small fan to provide mixing of the tracer at the point of injection.

3. Theory and Data Analysis

Accepted methods of measuring infiltration rates by tracer gas methods require that the air is uniformly mixed. Whilst this is easily achieved in small buildings, in large single cell buildings it is rarely possible. Also, the position of openings such as industrial doors, and the existence of internal air movement patterns, create variations in the effective infiltration rate throughout the building. Artificial stirring would destroy these variations.

An alternative approach is to divide the space into a number of hypothetical zones and, assuming the air in each zone is fully mixed, sample the concentration in each zone. This enables multizone theory to be used, from which may be derived the inter-zone flow rates. Summing the individual flows into each zone from the outside gives the infiltration rate for the whole building. Figure 1 illustrates the essentials of the multizone model, and defines the essential terms.

Initially, each zone contains a known concentration of tracer gas, and there is no injection of tracer gas after time zero. A volumetric balance on tracer gas gives

$$V_j \dot{c}_j(t) = \sum_{\substack{i=o \\ i \neq j}}^{n} F_{ij}\, c_i(t) - c_j(t)\, S_j \qquad 1.$$

where n is the number of zones within the building, and S_j is the summation of the flows into or out of zone j. Conservation of total flow into any zone gives

$$S_j = \sum_{\substack{i=o \\ i \neq j}}^{n} F_{ij} = \sum_{\substack{i=o \\ i \neq j}} F_{ji} \qquad 2.$$

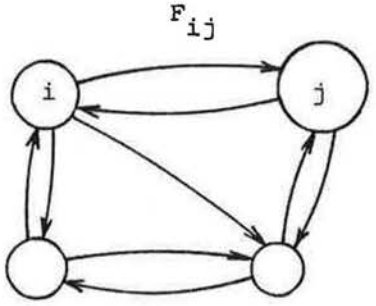

F_{ij} = flow from i to j

V_i = volume of i

c_i = tracer concentration in i

Figure 1. The multizone model

This is a system of first order equations with the general solution

$$\underline{c}(t) = \sum_{k=o}^{n} a_k \underline{x}_k e^{\lambda_k t} \qquad 3.$$

where the n + 1 values of λ_k and $\underline{x}_k$ are the eigenvalues and eigenvectors of

$$\lambda V \underline{x} = F \underline{x} \qquad 4.$$

The coefficients a_k are determined by the initial tracer gas distribution.

In a system of n zones, each connecting with the outside, there are $n^2 + n$ flows, F_{ij}. The necessary $n^2 + n$ equations to find the F_{ij} may be formed from n of the conservation equations 2, and measurement of the concentrations $c_1(t)$, ... $c_n(t)$ and their derivatives $\dot{c}_1(t)$, ... $\dot{c}_n(t)$ at n different points in time, since at each point in time equation 1 yields n tracer equations. Assuming $c_i(t)$ and $\dot{c}_i(t)$ can be measured, and providing the data set is error free, there is no difficulty in solving for the F_{ij}, provided the following dangers are avoided:

1. Irrespective of initial conditions, zonal concentrations tend to relative magnitudes equivalent to the components of the dominant eigenvector of equation 4. If more than one set of

$c_i(t)$ and $c_i(t)$ are taken as this condition is approached, an ill conditioned set of equations yielding an inaccurate solution will result. Therefore adequate time must be available for n significantly different sets of measurements to be made before this condition is approached. It can be shown (3) that this is best achieved by seeding only that zone which will have the lowest equilibrium concentration. This is the seeding strategy which is normally used.

2. Care must be taken when seeding buildings with symmetric zone layout and symmetry in the flow patterns, because, if the ratio of the concentrations in two zones remains constant with time, linear dependence in the equations will occur. In practice, this type of linear dependence is usually masked by experimental scatter, and is therefore observed as ill-conditioning (3), which again leads to an inaccurate solution.

Real experimental data is subject to scatter from a variety of sources, and since the solution technique relies on measurement of gradient as well as magnitude, the resulting errors in the F_{ij} may be substantial . The effects of errors are reduced by the following analysis procedure:

1. The data for each channel is smoothed using a standard fourth difference technique (7). This is preferred to the time-wise integration method used by Penman and Rashid (8).

2. Because of building geometry, not all F_{ij} exist, and so the number of unknowns is reduced by setting non-existent F_{ij} to zero.

3. Using the smoothed data, a constrained least squares technique is used to obtain the non-zero F_{ij} from equations 1 and 2. Constraints are necessary to avoid the appearance of negative values of F_{ij} in the solution. Penman and Rashid (8) used the constraint $F_{ij} \geqslant 0$. Additional upper and lower bounds may be obtained for some of the F_{ij} by examining the tracer concentrations at the start of the process (4); these additional constraints are also used here.

In addition to the multizone analysis, the readings from all six channels are combined to give a volume weighted average, which is fitted to a simple exponential decay curve. The decay constant is expressed as an infiltration rate for the whole building.

For both methods of analysis, each data set is split into six blocks (first third, second third, last third, first two-thirds, last two-thirds, whole set) and results computed for each block. For the multizone solution, the F_{ij} should be approximately the same whichever block is used. Large differences, therefore, indicate poor consistency in the data or possibly ill-conditioning in the solution. For the volume weighted average solution, the decay constant taken from the first third of the data will over estimate the infiltration rate, whereas that taken from the final third will underestimate it (3). Thus, the infiltration

rate may be found within limits.

4. Results

Measurements have been carried out in five buildings, ranging in internal volume from 4220 m^3 to 31300 m^3. A similar pattern of results has been obtained in all these buildings. Some of the results for one of them (9) have been selected to illustrate the main points. This is a vehicle maintenance depot, a simple rectangular building approximately 81m x 48m x 8m high, as shown in figure 2.

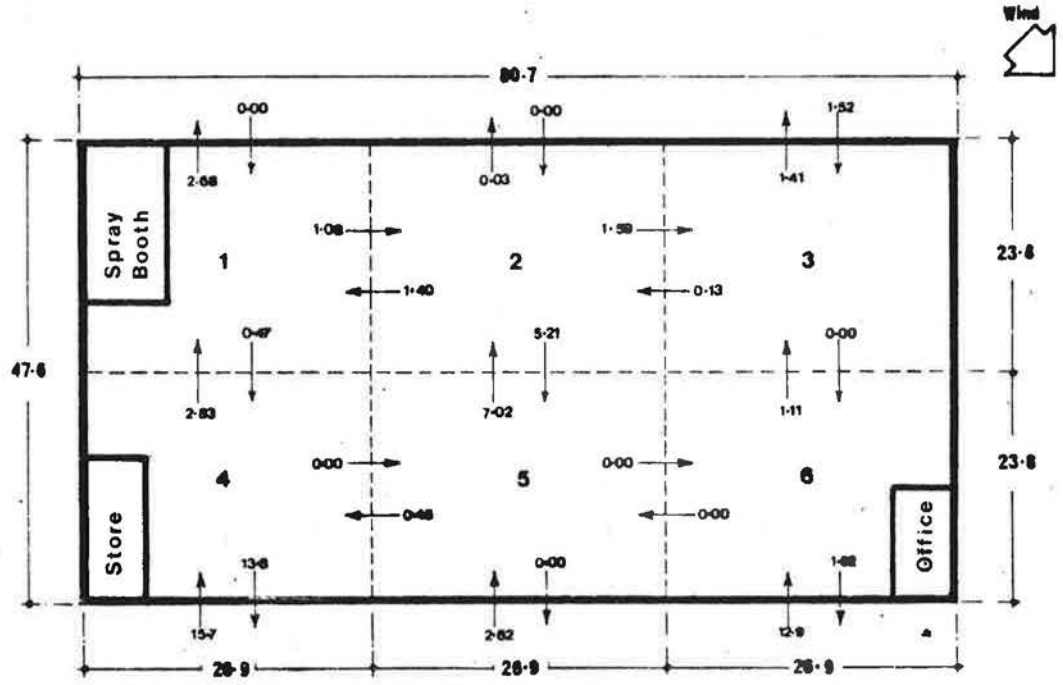

Figure 2. Vehicle maintenance depot, showing interzone flow rates in m s^{-1}.

Apart from the office, store and spray booth, the interior is obstructed only by vehicles and their repair equipment. For measurement purposes, the building was imagined to be divided into zones of approximately equal volume, with sampling points placed at the plan centre of each zone and at a height of about 5.7m (to allow clearance for vehicles). The building is naturally ventilated, but over each vehicle repair bay there is an extract nozzle for clipping to the exhaust pipe of the vehicles to remove engine fumes. Table 1 shows the whole building infiltration rate computed from 9 measured data sets by the methods described in Section 3. The infiltration rates obtained from the averaged data behave in the manner expected, with few exceptions. That is, the highest rate is obtained from the first third of the data set, and the lowest from the last third. Where this occurs, i.e. in the majority of the

measurements, it is therefore reasonable to take the value from the whole data set as the best estimate, and the other two values as limits. Thus, for example, the result for run number 4 may be expressed as:

$$\text{Infiltration rate} = 3.17 \begin{matrix} +\ 1.12 \\ -\ 0.21 \end{matrix} \text{ air changes per hours.}$$

Table 1. Measured infiltration rate, Duddeston vehicle maintenance depot.

Run No.	Infiltration rate in air changes per hour											
	From interzone flows						From averaged data					
	a	b	c	d	e	f	a	b	c	d	e	f
1	3.65	4.05	6.08	2.01	4.65	2.20	3.54	2.54	2.83	2.77	2.74	2.81
2	0.53	1.00	2.12	2.26	1.66	0.91	3.14	2.47	2.46	2.60	2.46	2.51
3	1.75	1.38	0.81	0.46	1.78	0.80	6.42	4.29	3.65	4.79	3.86	4.09
4	1.40	4.04	4.33	2.98	4.94	3.76	4.29	3.26	2.96	3.50	3.06	3.17
5	6.55	2.89	5.14	2.33	4.94	4.36	9.29	6.07	4.91	6.81	5.28	5.63
6	0.88	1.97	1.27	0.61	2.31	1.17	1.97	2.59	2.83	2.46	2.76	2.69
7	0.54	2.16	3.71	0.99	2.15	0.75	4.47	3.85	3.36	4.00	3.52	3.61
8	0.96	2.85	1.14	0.54	1.05	1.20	2.92	2.52	2.56	2.61	2.55	2.58
9	6.05	3.07	4.33	3.42	5.75	4.19	3.44	2.73	2.81	2.94	2.78	2.87

Key: columns a to f give results for blocks of data as follows:

a	first third	d	first two thirds
b	second third	e	last two thirds
c	last third	f	whole data set

The infiltration rates obtained from the multizone analysis of flow rates are sometimes consistent with expectation. Runs 1, 4 and 5 show a measure of consistency between results from different portions of the data set, and the result in column f for the whole data set is reasonably close to the corresponding value from the averaged data. In these cases, the individual interzone flows are probably a good indication of air movement patterns within the building. The flows shown in figure 2 were obtained from run 4. However, some of the runs show marked inconsistencies. For run 7 for example the infiltration rate computed from interzone flows varies between 0.54 and 3.71 air changes per hour, depending on which portion of the data set is analysed. In such cases there is little agreement with the infiltration rate obtained from the averaged data. Also, where there is inconsistency in the overall infiltration rate, it is found that the individual interzone flows computed from different portions of the data set also show lack of consistency.

5. Discussion and Conclusions

The fact that the results for some data sets are not only plausible but exhibit an internal consistency gives grounds for some degree of optimism. It suggests that dividing a large building into only six hypothetical zones is sometimes sufficient to give a reasonable description of the air infiltration and air movement patterns. However, the lack of consistency in many of the results has lead to several possible avenues

of improvement. Experimentally, the next stage of the measurement program will examine the effect of multiplexing the channels in order to increase the number of zones and sample points. Also, the effect of sampling the air over a greater part of each zone will be investigated (currently each sample head draws air over a 2m radius). Both these measures, however, will increase the level of disruption to the building occupants. Theoretically, the effect of time lags on the decay curves will be examined. For a two zone model, Waters (10) has shown that time lags in the flow between zones produces an oscillation in the decay curves. Similar oscillations have been observed in many of the measured results, where it appears as a high frequency ripple. Figure 3 is part of the measured tracer concentrations for run 7. The ripple, which is clearly visible, cannot be explained, on the basis of normal multizone theory.

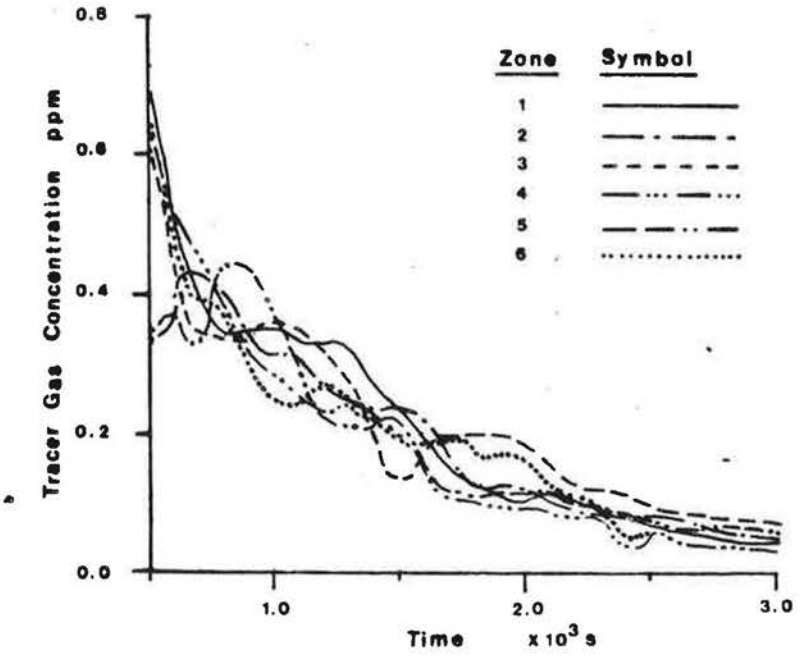

Figure 3. Tracer gas decay curve showing ripple effect.

References

(1) Sinden F.W., Multi-chamber theory of air infiltration. Building and Environment, 1978, 13, 21-28.

(2) Sandberg M., The multi-chamber theory reconsidered from the viewpoint of air quality studies. Building and Environment, 1984, 19, 221-233.

(3) Waters J.R. and Simons M.W., The evaluation of contaminant concentrations and air flows in a multizone model of a building. To be published.

(4) Waters J.R., Lawrance G.V., and Jones N., A tracer gas decay system for monitoring air infiltration and air movement in large single cell buildings. In Proceedings, Symposium on Design and Protocol for Monitoring Indoor Air Quality, ASTM, Cincinnati, April 1987.

(5) Waters J.R. and Simons M.W., The measurement of air infiltration in large single cell industrial buildings. In H.R. Trechsel and P.L. Lagus (Eds), Measured Air Leakage of Buildings, ASTM STP 904, American Society for Testing and Materials, Philadelphia, 1986, pp. 106-119.

(6) Potter I.N., Dewsbury J., and Jones T.J., The measurement of air infiltration rates in large enclosures and buildings. In Proceedings, 4th AIC Conference, Elm, Switzerland, September 1983, Air Infiltration and Ventilation Centre, Bracknell, U.K.

(7) Lanczos C., Applied Analysis. Pitman, London, 1957.

(8) Penman J.M. and Rashid A.A.M., Experimental determination of airflow in a naturally ventilated room using metabolic carbon dioxide. Building and Environment, 1982, 17, 253-256

(9) Waters J.R., and Lawrance G.V., Ventilation and air movement measurements at Duddeston Mill Maintenance Depot, Birmingham. Report No.CB/85/0002, Department of Civil Engineering and Building, Coventry Lanchester Polytechnic, January 1987.

(10) Waters J.R., The effect of time lags in a two zone air movement model. To be published.

Coventry Polytechnic
Department of Civil Engineering and Building
G.V.Lawrance B.Sc.

British Gas , Duddestone Mill Depot

BG15/PD074 23/09/86 1200hrs

Flow Map from Full Data Set , Fully Constrained

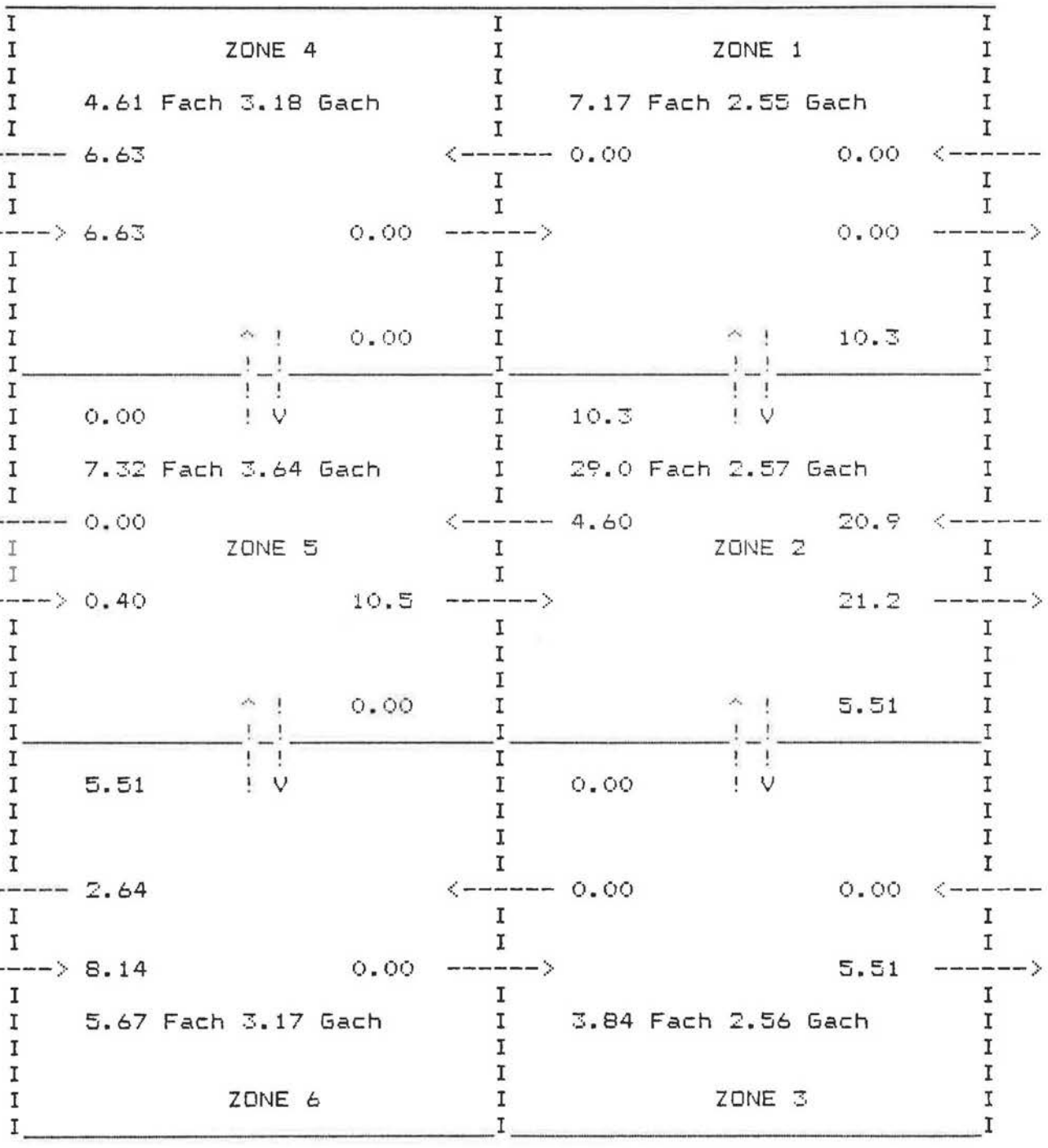

THE EFFECT OF TIME LAGS IN A TWO ZONE AIR MOVEMENT MODEL

J. R. WATERS

Building Services Engineering Research
and Technology

Building Serv. Eng. Res. Technol. 8 (1987) 43–46 Printed in Great Britain

Technical Note

Summary Multi-zone models of air movement in buildings usually assume that there is no time lag in the flows between zones. Nevertheless, such time lags could have a significant effect on the pattern of contaminant distribution throughout a building. This note shows how such effects can be evaluated by examining theoretically a two-zone model with time lags. The results have implications for the interpretation of tracer decay measurements.

Time lags in a two-zone air movement model

J R WATERS BSc MPhil PhD MCIBSE
Department of Civil Engineering and Building, Coventry Lanchester Polytechnic, Priory Street, Coventry CV1 5FB, UK

Received 22 December 1986, in final form 1 April 1987

1 Introduction

In multi-zone air movement models it is assumed that a building can be represented by an assembly of zones with the air in each zone perfectly mixed. The flows between zones are usually assumed to occur without time lags, that is, a particle of air in the flow from zone 1 to zone 2 will, on leaving zone 1, reappear instantaneously in zone 2. This assumption is implicit in the multi-zone air movement model of Sinden[1], and is perpetuated by authors such as Sandberg[2], Perera[3] and Waters and Simons[4] who have used Sinden's model. In practice, zones may be remote enough from one another for time lag effects to become important, especially if the principal connecting path is a corridor or duct. The effect of time lags will be most significant in a transient process, such as the spread of a contaminant following its release in one part of the system, or the decay of a tracer gas in a tracer decay experiment. The introduction of time lags into the model renders the mathematics cumbersome. This note is therefore confined to an analysis of a two-zone model.

2 Theory and analysis

Consider a two-zone model as shown in Figure 1. The zones have volumes V_1 and V_2, and the contaminant concentrations at time t are $x_1(t)$ and $x_2(t)$. The flow, F, from 1 to 2 must, in this simple model, be the same as the flow from 2 to 1, but the time delay on the flow paths may be different. Let the time delay be g_1 for the flow from 1 to 2 and g_2 for the flow from 2 to 1. Assume that at time zero the contaminant concentration in zone 1 is suddenly raised to unity, and everywhere else in the system (including connecting ducts) it is zero. To determine the subsequent pattern of contaminant concentrations in zones 1 and 2, we may write the following equations:

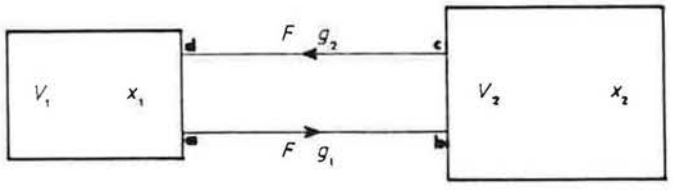

Figure 1 Two-zone air movement model with time lags

For $t < g_2$

$$V_1\dot{x}_1(t) = -Fx_1(t) + Fx_2(0)$$

For $t \geqslant g_2$

$$V_1\dot{x}_1(t) = -Fx_1(t) + Fx_2(t - g_2)$$

For $t < g_1$

$$V_2\dot{x}_2(t) = Fx_1(-0) - Fx_2(t)$$

For $t \geqslant g_1$

$$V_2\dot{x}_2(t) = Fx_1(t - g_1) - Fx_2(t)$$

The notation $x_1(-0)$ indicates the contaminant concentration in zone 1 before time zero, and is therefore the concentration in the connecting duct ab. Introducing, H, the Heaviside unit step function, and writing $v_1 = V_1/F$, $v_2 = V_2/F$, allows the equations to be written more concisely in the form

$$v_1\dot{x}_1(t) = -x_1(t) + H(t - g_2)x_2(t - g_2) - H(t - g_2)x_2(0) + x_2(0)$$

$$v_2\dot{x}_2(t) = H(t - g_1)x_1(t - g_1) - H(t - g_1)x_1(-0) + x_1(-0) - x_2(t)$$

These equations may be solved by routine application of the Laplace transform. The transformed equations are

$$v_1(s\bar{x}_1 - x_1(0)) = -\bar{x}_1 + e^{-g_2 s}\bar{x}_2 - \frac{1}{s}e^{-g_2 s}x_2(0) + \frac{1}{s}x_2(0)$$

$$v_2(s\bar{x}_2 - x_2(0)) = e^{-g_1 s}\bar{x}_1 - \frac{1}{s}e^{-g_1 s}x_1(-0) + \frac{1}{s}x_1(-0) - \bar{x}_2$$

The initial condition is that at $t = 0$, $x_1(0) = 1$, $x_2(0) = 0$, $x_1(-0) = 0$. The equations therefore simplify to

$$v_1 s\bar{x}_1 - v_1 = -\bar{x}_1 + e^{-g_2 s}\bar{x}_2$$

$$v_2 s\bar{x}_2 = e^{-g_2 s}\bar{x}_1 - \bar{x}_2$$

The solution for $\bar{x}_1$ and $\bar{x}_2$ may be written, with $k = g_1 + g_2$,

in the form

$$\bar{x}_1 = \frac{v_1(v_2 s + 1)}{(v_1 s + 1)(v_2 s + 1) - e^{-(g_1 + g_2)s}}$$

$$= \frac{v_1}{(v_1 s + 1)}\left(1 - \frac{e^{-ks}}{(v_1 s + 1)(v_2 s + 1)}\right)^{-1} \quad (1)$$

$$\bar{x}_2 = \frac{v_1 e^{-g_1 s}}{(v_1 s + 1)(v_2 s + 1) - e^{-(g_1 + g_2)s}}$$

$$= \frac{v_1 e^{-g_1 s}}{(v_1 s + 1)(v_2 s + 1)}\left(1 - \frac{e^{-ks}}{(v_1 s + 1)(v_2 s + 1)}\right)^{-1} \quad (2)$$

Using $(1 - a)^{-1} = 1 + a + a^2 + \ldots$, the solutions may be expressed as a series expansion. For example, for $\bar{x}_1$,

$$\bar{x}_1 = \frac{v_1}{(v_1 s + 1)}\left(1 + \frac{e^{-ks}}{(v_1 s + 1)(v_2 s + 1)} + \frac{e^{-2ks}}{(v_1 s + 1)^2 (v_2 s + 1)^2} + \ldots\right)$$

Similarly for $\bar{x}_2$. To obtain the Laplace inverse for the general case, each term in the series must be split into partial fractions. For instance, provided $v_1 \neq v_2$, the denominator of the second term in $\bar{x}_1$ is

$$\frac{1}{(v_1 s + 1)} \frac{1}{(v_1 s + 1)(v_2 s + 1)} = \frac{v_1/(v_1 - v_2)}{(v_1 s + 1)^2} - \frac{v_1 v_2/(v_1 - v_2)^2}{v_1 s + 1} + \frac{v_2^2/(v_1 - v_2)^2}{v_2 s + 1}$$

Hence, taking the Laplace inverse term by term,

$$x_1(t) = e^{-t/v_1} + H(t - k)\left(\frac{t - k}{v_1 - v_2} e^{-(t-k)/v_1} - \frac{v_1 v_2}{(v_1 - v_2)^2} e^{-(t-k)/v_1} + \frac{v_1 v_2}{(v_1 - v_2)^2} e^{-(t-k)/v_2}\right)$$

+ terms in $H(t - 2k), H(t - 3k)$ etc.

Similarly for $x_2(t)$.

When $v_1 = v_2 = v$, the series expansions for $\bar{x}_1$ and $\bar{x}_2$ may be written as

$$\bar{x}_1 = \frac{1}{(s + v^{-1})} + \frac{e^{-ks}}{v^2(s + v^{-1})^3} + \frac{e^{-2ks}}{v^4(s + v^{-1})^5} + \ldots$$

$$\bar{x}_2 = \frac{e^{-g_1 s}}{v(s + v^{-1})^2} + \frac{e^{-(k+g_1)s}}{v^3(s + v^{-1})^4} + \frac{e^{-(2k+g_1)s}}{v^5(s + v^{-1})^6} + \ldots$$

The Laplace inverse may be obtained directly to give

$$x_1(t) = e^{-t/v}\left(1 + H(t - k)\frac{(t - k)^2}{2!v^2} e^{k/v} + H(t - 2k)\frac{(t - 2k)^4}{4!v^4} e^{2k/v} + \ldots\right) \quad (3)$$

$$x_2(t) = e^{-(t-g_1)/v}\left(H(t - g_1)\frac{(t - g_1)}{v} + H(t - \overline{k + g_1})\frac{(t - \overline{k + g_1})^3}{3!v^3} e^{k/v} + H(t - \overline{2k + g_1})\frac{(t - \overline{2k + g_1})^5}{5!v^5} e^{2k/v} + \ldots\right) \quad (4)$$

It is interesting to note that when $g_1 = k = 0$, the solution reduces to

$$x_1(t) = \tfrac{1}{2}(1 + e^{-2t/v})$$

$$x_2(t) = \tfrac{1}{2}(1 - e^{-2t/v})$$

which is obviously the solution for the zero time lag case.

The equilibrium value of x_1 and x_2 may be found by means of the final value theorem,

$$\lim_{t \to \infty}[x(t)] = \lim_{s \to 0}[s\bar{x}(s)]$$

Applying this to equations 1 and 2 (with $v_1 = v_2$) gives

$$x_1 = x_2 = \frac{v}{2v + k} \quad \text{at } t = \infty \quad (5)$$

When $k = 0$, the zero time lag case, the equilibrium value is clearly $\frac{1}{2}$.

Since v is the time constant of the process, it is convenient to normalise the time dimension with respect to v, i.e.

$$t' = \frac{t}{v}, g_1' = \frac{g_1}{v}, g_2' = \frac{g_2}{v} \text{ and } k' = \frac{k}{v}$$

Assuming plug flow in the connecting ducts, it can then be seen that the volumes of these ducts are given by

$$V_{ab} = g_1 F = g_1' V \text{ and } V_{cd} = g_2 F = g_2' V$$

3 Examples and discussion

Equations 3 and 4 have been evaluated for five examples, with values of k' ranging from zero to 1.2. The zero time lag case, with $k' = 0$, is plotted in Figure 2, and shows the concentrations $x_1(t)$ and $x_2(t)$ smoothly approaching the expected equilibrium value of 0.5. Figures 3 to 6 show the effect of increasing the time lag. For small time lags ($k' = 0.3$ and $k' = 0.6$) the effect is not only to reduce the equilibrium value given by equation 5, but also to cause the concentrations to approach equilibrium more rapidly. For larger time lags ($k' = 0.9$ and $k' = 1.2$), the concentration curves show instability, with an oscillation of half period

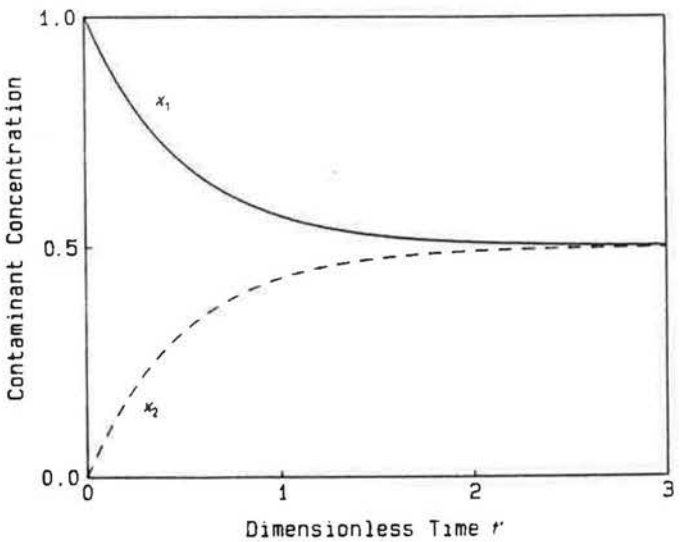

Figure 2 Two-zone decay, zero time lag case. $g_1 = g_2 = 0$

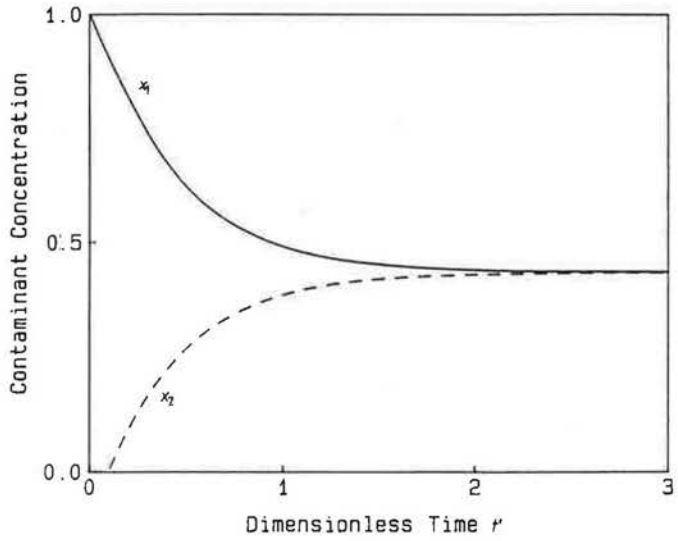

Figure 3 Two-zone decay, $k' = 0.3$, $g_1 = 0.1$, $g_2 = 0.2$

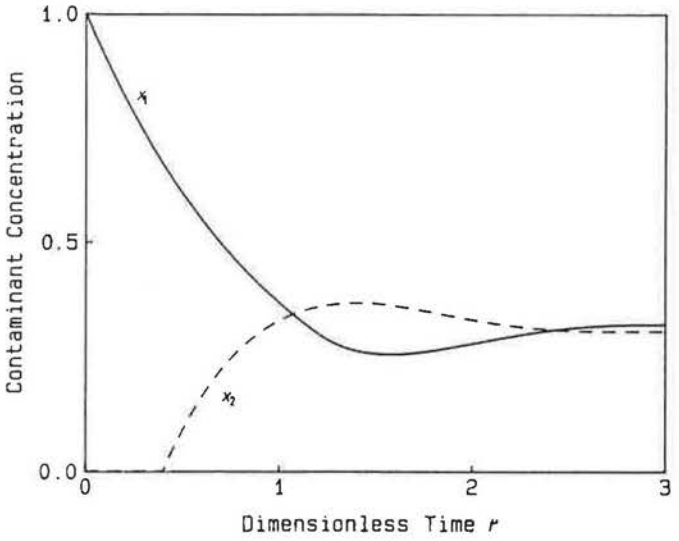

Figure 6 Two-zone decay, $k' = 1.2$, $g_1 = 0.4$, $g_2 = 0.8$

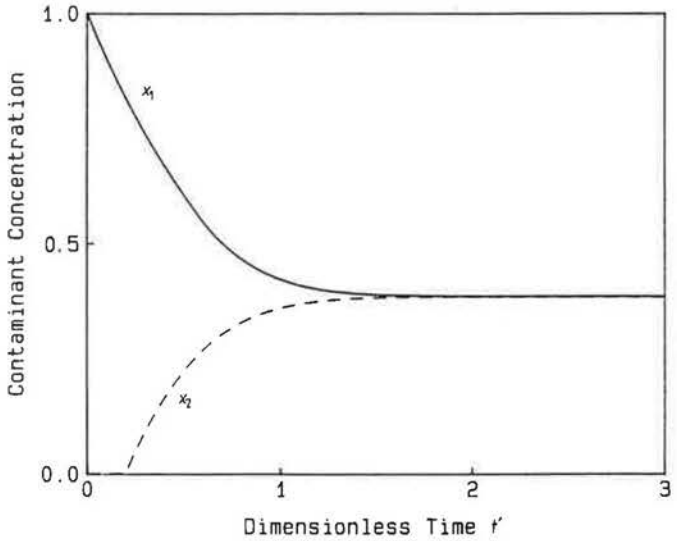

Figure 4 Two-zone decay, $k' = 0.6$, $g_1 = 0.2$, $g_2 = 0.4$

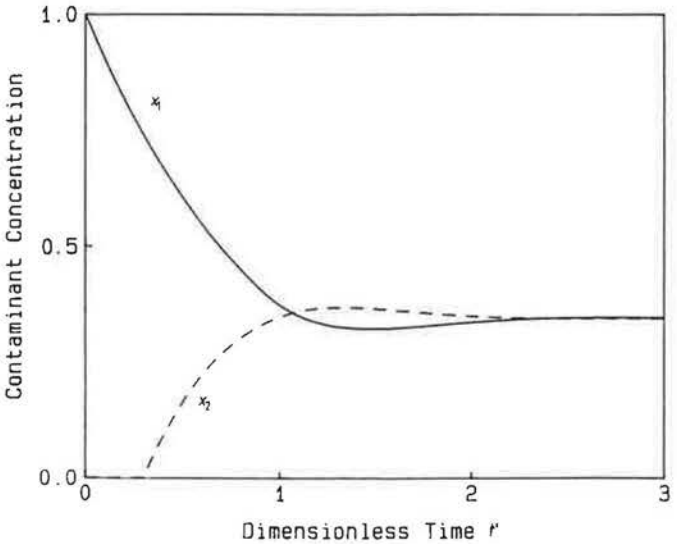

Figure 5 Two-zone decay, $k' = 0.9$, $g_1 = 0.3$, $g_2 = 0.6$

roughly equal to k' and amplitude increasing with k'. The value of k' at which instability begins may be found by looking for a minimum in the $x_1(t)$ curve between $t = k'$ and $t = 2k'$. Taking the first two terms only in equation 3, differentiating, and solving for $(t' - k')$ when $\dot{x}_1(t) = 0$, shows that the required minimum exists when $k' \geq \ln 2$, i.e. $k' \geq 0.69$. Thus, instability exists when the total volume of the connecting ducts is given by

$$V_{ab} + V_{cd} = (g_1' + g_2')V \geq 0.69\,V$$

Inspection of equations 3 and 4 shows that the pattern of the $x_1(t)$ and $x_2(t)$ curves depends only on the total time lag, k', and that the effect of g_1' is to offset the curve for $x_2(t)$ on the time axis. Thus the pattern of the curves, the equilibrium values, and the condition for instability all depend only on k'.

The effect of allowing additional flows between each zone and the outside has not been included in this analysis. Nevertheless it is obvious that if there is no contaminant in the outside air, the effect will be to make $x_1(t)$ and $x_2(t)$ asymptote to zero instead of $1/(2 + k')$, without affecting the periodicity and offset of the decay curves. However, the value of k' at which instability commences may not be the same.

4 Applications

An important application is in the measurement of infiltration rates and air movement by the tracer decay technique. The presence in the measured decay curves of oscillations of the type shown in Figures 5 and 6 would be an indication of the possible existence of time lags. Such oscillatory behaviour has been observed in measurements in industrial buildings, and Figure 7 due to Simons and Waters[5] is an example of measured decay curves in a six-zone building. Clearly, time lags, if present, will affect both the values of the tracer gas concentration and the gradient of the decay curves throughout the decay process.

Estimates of fresh air infiltration based on decay curve gradients may be in error, because compared with normal single-zone and multi-zone theory, gradients will be steeper

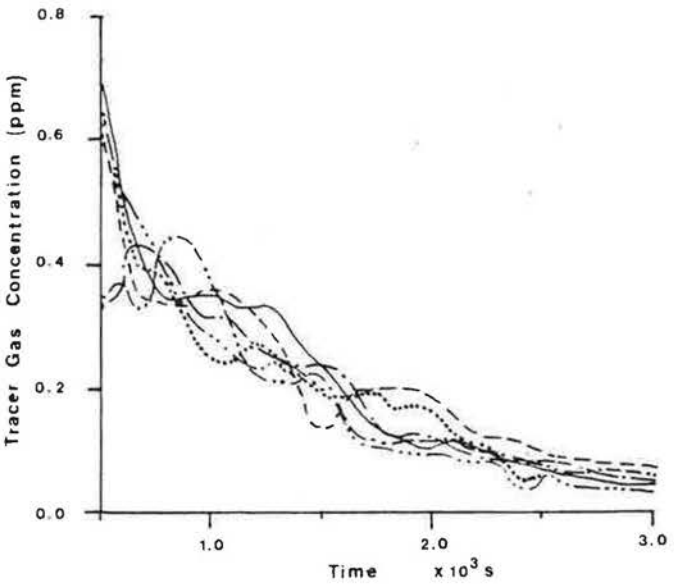

Figure 7 Measured decay curves in a factory building. Zones: 1 ——, 2 —·—·-, 3 ----, 4 —···—···, 5 ——··—, 6 ·····

during the early part of the decay process and shallower during the later stages.

5 Conclusion

The simple two-zone model examined in this paper is sufficient to demonstrate that the existence of time delays in the flow paths between zones has a considerable effect on the contaminant versus time curves. The method described here could in principle be extended to predict contaminant concentrations in models with more than two zones. The reverse process, of establishing flow rates from measured tracer decay curves, is clearly more difficult than in the absence of time lags, as there will be additional unknowns to evaluate.

References

1 Sinden F W Multi-chamber theory of air infiltration *Building Env.* **13**(1) 21–28 (1978)
2 Sandberg M The multi-chamber theory reconsidered from the viewpoint of air quality studies *Building Env.* **19**(1) 221–233 (1984)
3 Perera M D A E S Review of techniques for measuring ventilation rates in multicelled buildings *Energy Conservation in Buildings—Heating Ventilation and Insulation* (ed. Ehringer, Hoyaux and Ziegers) (Dordrecht: Reidl) (1982)
4 Waters J R and Simons M W The evaluation of contaminant concentrations and air flows in a multizone model of a building *Building Env.* To be published
5 Simons M W and Waters J R The measurement of ventilation and air movement in factory buildings. *Proc. Int. Cong. Building Energy Management ICBEM '87, Lausanne* (Sept–Oct 1987)